NASA Contractor Report 185262
Aerojet 2459-56-1

Orbital Transfer Vehicle Oxygen Turbopump Technology

Final Report, Volume II—Nitrogen and Ambient Oxygen Testing

R.J. Brannam, P.S. Buckmann, B.H. Chen,
S.J. Church, and R.L. Sabiers

GENCORP Aerojet TechSystems
Sacramento, California

December 1990

Prepared for
Lewis Research Center
Under Contract NAS3-23772

NASA
National Aeronautics and
Space Administration

TABLE OF CONTENTS

TABLE OF CONTENTS (cont.)

LIST OF TABLES

LIST OF FIGURES

LIST OF FIGURES (CONTINUED)

LIST OF FIGURES (CONTINUED)

FOREWORD

This document represents a final report to the National Aeronautics and Space Administration for work performed under Test Task Order B.7 to Contract NAS 3-23772. The task work span was from 21 September 1987 to 30 August 1989.

The tests reported herein are Series "C," "D," and "E," of a planned series of six tests that will verify the operation of a gaseous oxygen driven turbine powering a liquid oxygen pump. No interpropellant seals or purge gas are required for this concept.

The extended test schedule was the result of a need to convert the test unit from a bearing test configuration to a complete turbopump between the Series "B" and Series "C" tests.

Volume I, Reference 1 of this report covered the turbopump design, fabrication, and Series A and B testing. Volume III will report on the testing with 400°F oxygen turbine drive gas which will duplicate the expected engine operating conditions. The site of the 400°F oxygen testing (Series F and G) is the NASA-JSC White Sands Test Facility in New Mexico.

ORBITAL TRANSFER VEHICLE OXYGEN TURBOPUMP TECHNOLOGY

FINAL REPORT, VOLUME II
NITROGEN AND AMBIENT OXYGEN TESTING

R.J. Brannam, P.S. Buckmann, B.H. Chen,
S.J. Church, and R.L. Sabiers
GENCORP Aerojet TechSystems
Aerojet Propulsion Division
Sacramento, California 95813-6000

SUMMARY

This report documents the continuation of testing of a rocket engine turbopump (TPA) designed to supply high pressure liquid oxygen propellant to the engine. This TPA is unique in that it uses hot (400°F) gaseous oxygen as the turbine drive fluid. It is a critical technology for the dual propellant expander cycle, a cycle using both hydrogen and oxygen as the working fluids for a maximum performance cryogenic propellant rocket engine.

The first volume of this report (Reference 1) documents the results of earlier NASA LeRC funded work to determine the structural materials most compatible with liquid and 400°F oxygen and the detailed design of the turbopump using these materials. It also has a discussion of the TPA fabrication and the Series A and B tests which verified the hydrostatic bearing concept in a bearing tester using many common parts from the TPA. These tests successfully demonstrated the hydrostatic bearing system at speeds up to 72,000 rpm in liquid nitrogen. Following these tests, the housing and rotating assembly turbine impellers were finish machined to form a complete oxygen TPA. Difficulties in finding a competent machine shop willing to bid on this finish machining caused the start of the next series of tests to be delayed well over a year. The test series documented herein, Series C, D, and E, started on 15 February 1989 and were concluded on 21 March 1989.

Series C1 used liquid nitrogen in the pump and gaseous nitrogen as the turbine drive gas. Series C2 used liquid oxygen as the pumped fluid with gaseous nitrogen driving the turbine. The TPA performed as expected with limitations on the turbine speed due to the use of nitrogen as the turbine drive fluid which has a lower density than that of oxygen. In addition, the drive gas temperature was lower than design temperature and the flow passage resistance was higher than expected.

Series D also used gaseous nitrogen drive while pumping liquid oxygen, but the starts were made without any prepressurization of the hydrostatic bearings using the separate bearing assist supply. This is a realistic condition for actual engine operation, and results in a rubbing start. When the drive pressure exceeded the "breakaway" force the rotating assembly accelerated normally.

Test Series E1 demonstrated the pure gaseous oxygen turbine drive with LOX in the pump. This was done with the bearing assist system on. Series E2 again used an ambient oxygen turbine drive but the bearing assist system was off, and the hydrostatic bearing system provided its own pressurization after a rubbing start.

Total operating time during the testing was 2268 seconds. The test article had 14 starts without bearing assist pressurization. Operating speeds of up to 80,000 rpm were logged (Test 135) with a steady state speed of 70,000 rpm (Test 165) demonstrated.

The hydrostatic bearing system performed satisfactorily exhibiting no bearing load or stability problems. Post test examinations of the journal and thrust bearing surfaces showed minor evidence of operating wear. The silver plated bearing surfaces showed some smearing from rubbing and one gouged area apparently due to a particle passing through the bearing. No monel surfaces were exposed by the silver plate wear. There was no evidence of any melting or oxidation due to the oxygen exposure. There was one minor anomaly encountered that was not traced to a particular cause. This was a slow axial motion, sinusoidal at 10,000 cpm, (≈167 Hz) of ± 0.0005 inch amplitude. It caused no problems during the testing but was plainly evident in the distance readings from the axial probe.

The conclusion of Series C, D, and E testing made the turbopump hardware available for refurbishment prior to continued testing. Testing as an operational turbopump, pumping liquid oxygen and powered by hot gaseous oxygen to the turbine, is scheduled in 1990 at the NASA White Sands Test Facility, New Mexico.

1.0 INTRODUCTION

1.1 BACKGROUND

This oxygen turbopump test program supports the NASA-OAST plans for development of a new orbit transfer vehicle (OTV) to be operational in the late 1990s. Critical to the economical operation of a space based OTV is a new O_2/H_2 rocket engine with capabilities superior to existing engines. Table 1.1-1 presents the technology goals for the new OTV engine. It summarizes the characteristics of the production RL-10 reference engine and those desired in a new engine. In total, these requirements represent a substantial advance in the state-of-the-art, and a considerable challenge to rocket engine designers. Aerojet Propulsion Division has selected a unique engine cycle and turbopump designs in response to those requirements. The result is an advancement in the state of the art that combines a heated oxygen driven turbine with a long life hydrostatic bearing system to yield an advanced, high performance oxygen turbopump.

1.1.1 Aerojet Dual Expander Cycle

In a conventional (single) expander cycle engine hydrogen is routed through passages in the combustion chamber where it cools the wall and acquires thermal energy to power the turbine of both hydrogen and oxygen pumps. It is then routed to the injector for combustion. This cycle is fairly simple, and it offers good performance potential as all propellant is burned in the combustion chamber. It does not have the losses associated with open cycles. Its limitations are related to dependence on only one propellant as a turbine drive fluid which, in turn, requires interpropellant seals and purge gas for the oxygen turbopump. To obtain the needed power the hydrogen must be heated to a temperature very near to the design limit for the copper based alloys employed for the chamber liner. With the added limits imposed by the high number of starts, long operating times without maintenance, and a 10:1 or greater engine thrust throttling requirement, the hydrogen expander cycle is capable of only modest performance and life improvements over the production RL-10 engine.

The Aerojet dual expander cycle alleviates these limitations by using oxygen as a working fluid as well as hydrogen. This reduces the demands on the hydrogen

TABLE 1.1-1

TECHNOLOGY GOALS FOR THE NEW OTV ENGINE

Parameters	Reference Engine System Characteristics	October 1986 NASA Goals and/or Requirements	1988 Updated Goals or Requirements
Basing	Earth	Not Specified	Space
Human-rating	No	Not Specified	Yes
Safety Criteria	Not Specified	Not Specified	Fail Operational, Fail Safe
Propellants - Fuel	Hydrogen	Hydrogen	Hydrogen
- Oxidizer	Oxygen	Oxygen	Oxygen
Vacuum Thrust (Design Point)	15,000 lbf	10,000 - 25,000 lbf*	7500 lbf (per engine)
Number of Engines per Vehicle		Not Specified	2 Minimum
Engine Mixture Ratio, O/F (Design Point)	5.0	6.0	6.0
Engine Mixture Ratio Range, O/F	4.4 to 5.6	5 - 7	5 - 7
Propellant Inlet Temperature -			
Hydrogen	38.3°R	37.8°R	37.8°
Oxygen	175.3°R	162.7°R	162.7°R
Gimbal	±4.0 Degrees	±6.0 Degrees (Sq. Pattern)	±20 degrees Pitch & Yaw
Aerobraking Design Criteria	The engine must be compatible with aeroassist return of the vehicle to low-earth orbit.		
Vacuum Specific Impulse	444 lbf-sec/lbm	520 lbf-sec/lbm	490 lbf-sec/lbm
Vacuum Thrust Throttling Ratio	No Throttling	30:1	10:1
Net Positive Suction Head (NPSH) -			
Hydrogen	133.0 ft-lbf/lbm	0	15 ft-lbf/lbm
Oxygen	16.7 ft-lbf/lbm	0	2 ft-lbf/lbm
Weight	290 lbm	360 lbm	360 lbm (2 engines)
Length	70.1 in.	40	TBD (Assume 60", Stowed)
Reliability (90% Confidence Level)	0.9982	1.0	.9975 Single engine, .99958 Dual engine**
Operational Life	3 Starts, 4000 sec	500 Starts, 20 Hours	500 Starts, 20 Hours
Service Free-Life		100 Starts, 4 Hours	100 Starts, 4 Hours
Start Cycle		Chilldown with propulsive dumping of propellants, tankhead start, pumped idle operation, autogenous tank pressuration required	

Updated 1 March 1990

*Vehicle engine set total thrust must be in this range
**MSFC/Boeing Vehicle Studies

circuit as the oxygen turbopump is driven by heated oxygen. It also eliminates the need for an interpropellant seal and the associated helium purge system weight penalty. The oxygen is heated to approximately 400°F by flowing through a LOX/GH_2 heat exchanger and then through the regeneratively cooled nozzle extension. The flow schematic is shown in Figure 1.1-1. The hydrogen used to heat the cold oxygen in the heat exchanger is the effluent from the hydrogen TPA turbine. It provides the thermal energy to the oxygen at a thermodynamic cost to the hydrogen circuit of the pressure drop across the heat exchanger. Also, both propellants are delivered to the thrust chamber injector as superheated gases; an important aid to combustion stability over a wide throttling range.

1.1.2 Oxygen Turbopump

Key to this turbopump design is the use of a hot oxygen turbine drive. Many turbopumps have been successfully used to pump liquid oxygen, but hot oxygen has been considered too reactive to use as a turbine drive fluid. The NASA LeRC has sponsored an extensive program in oxygen compatibility experiments with various materials and under various conditions of pressure, temperature, and mechanical stress. A number of materials have been identified that can be used in an oxygen turbopump with high confidence that the materials will not ignite under either particle impact or minor rubbing at temperatures in the 400°F range. Despite the experimental data, verification of an oxygen turbopump requires successful completion of an extensive test program with a TPA in oxygen service. At the completion of this program the TPA will have demonstrated compatibility of the selected materials with cryogenic oxygen, ambient oxygen, and 400°F oxygen in conditions closely approximating actual service.

The oxygen TPA also uses a number of design innovations other than materials selection. The most critical is the self aligning hydrostatic bearing system. The long life requirements of the OTV engine are incompatible with conventional ball bearing systems that require rolling and sliding contact in liquid oxygen at high speeds. A hydrostatic bearing was chosen for this TPA as it had the potential for very long service life free of wear or fatigue life limits.

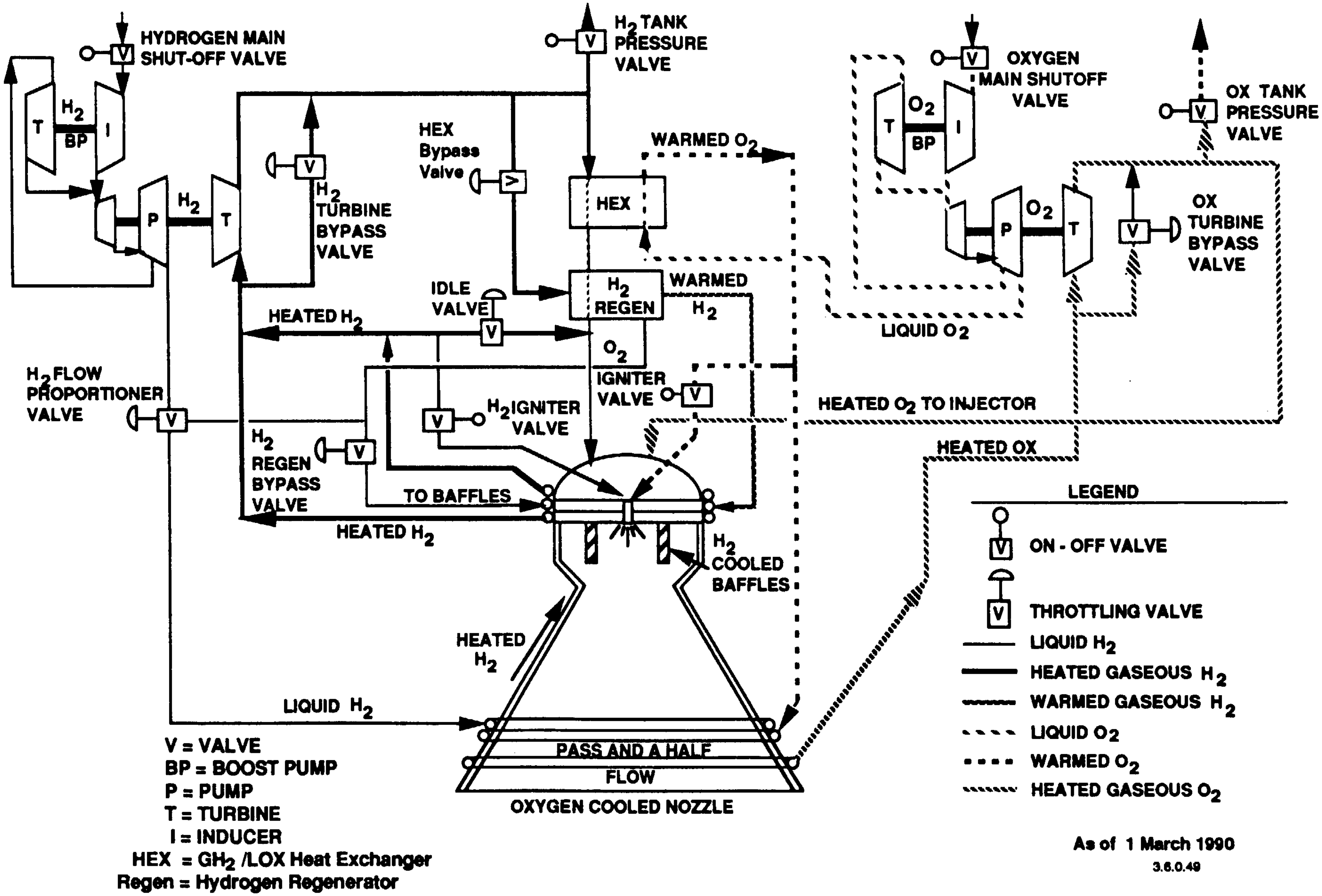

Figure 1.1-1 Dual Expander Cycle Schematic

The oxygen turbopump consists of a single stage full admission axial flow turbine that drives an inducer and a two stage centrifugal pump, Figure 1.1-2. The centrifugal pump impellers face in opposite directions utilizing the back of their hubs as part of the axial thrust bearing. A journal bearing is integral with the second stage thrust bearing and is located between the thrust faces. A second journal bearing, located between the pump and turbine, carries radial load only. Both bearings are hydrostatically supported to permit self-alignment. Maximum bearing capacity is achieved with parallel alignment. The inducer permits full speed operation down to a minimum Net Positive Suction Head of 80 ft-lbf/lbm of liquid oxygen. An additional 17.3 gpm capacity is designed into the inducer. This flow is turned radially before the first stage centrifugal impeller and is collected in an annulus to then be conveyed to a boost pump hydraulic turbine.

A boost pump, not part of this contract, will be required to meet the 2 ft. lbf/lbm minimum Net Positive Suction Head at 162.7°R when flowing liquid oxygen, Table 1.1-1. The 156 hp turbine powers the pumps to 75,000 rpm which deliver 34 gpm of liquid oxygen at 4600 psi pressure rise. Complete design specifications are discussed in Reference 1.

The design of this bearing system as well as the turbopump design, materials selection, fabrication, and Test Series "A" and "B" are covered in detail in Volume I of this report (Reference 1).

1.2 OBJECTIVES

The fundamental objective of the OTV oxygen turbopump test program is to identify and develop the pertinent technology for operating a high pressure LOX pumping/GOX driven turbopump for extended duration with multiple start/stop cycles. The main technology issue is the ignition potential from a metal rub or particle impingement in pure oxygen service. The overall goal is to provide extended life and restart capability. The main thrust of the test program is to demonstrate the viability of this design approach for high-speed LOX/GOX turbopumps, and to develop a data base in this area.

Specific test objectives for series testing are outlined below.

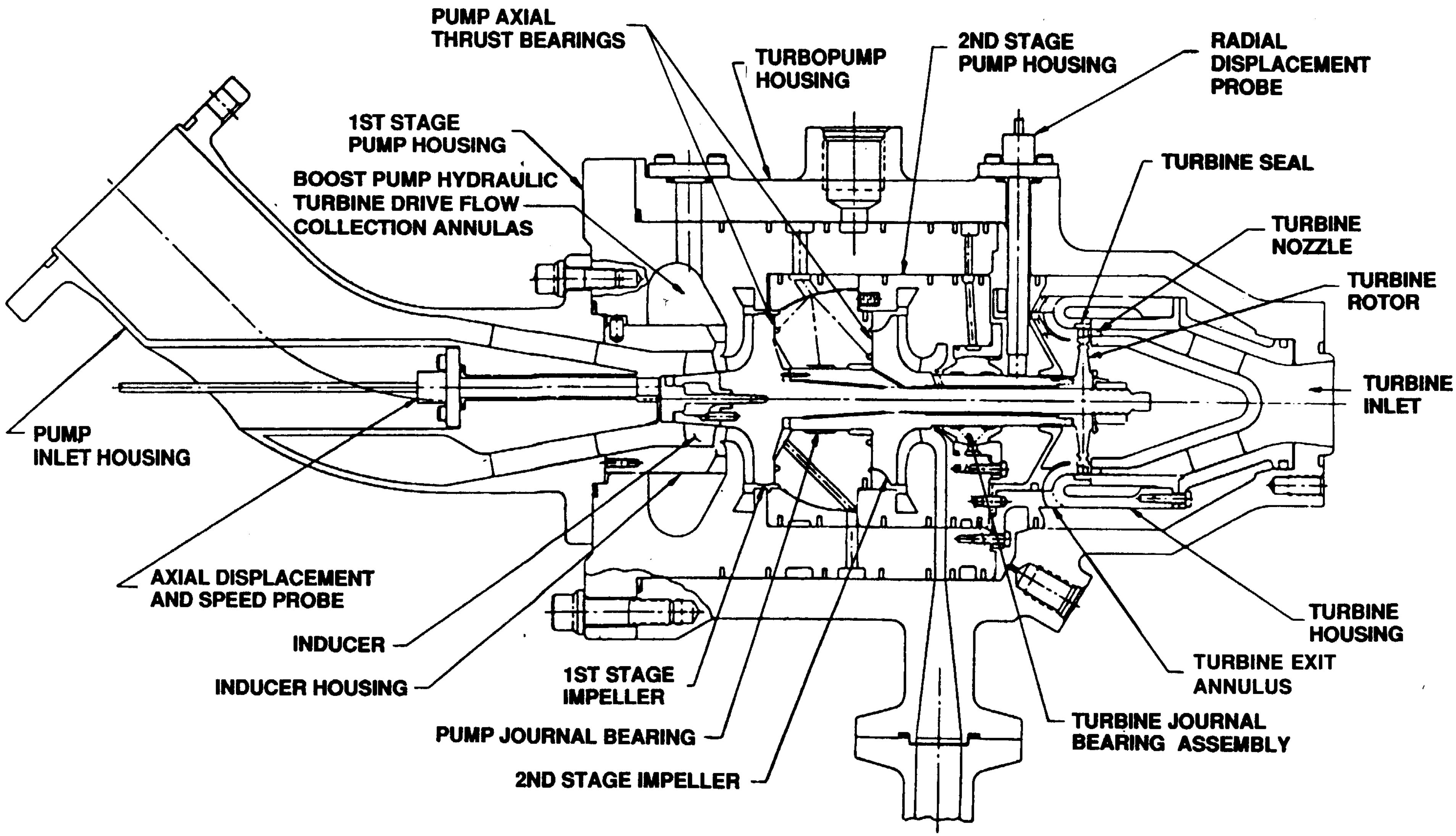

Figure 1.1-2. OTV Oxygen Turbopump Assembly

1.2.1 Test Series "O"

The objective of Series "O" was to checkout all systems prior to shaft rotation. This included a helium leak and moisture content check of the turbopump and all associated plumbing. The system was then chilled with liquid nitrogen and all instrumentation was checked for function without shaft rotation. At this time, the bearings were pressurized with liquid nitrogen to ensure proper shaft/bearing alignment.

1.2.2 Test Series "C"

The objective of Test Series "C" was to obtain turbopump performance data of the OTV oxygen turbopump with minimum risk to the hardware. Risk was minimized by powering the turbine with ambient temperature gaseous nitrogen and by using a high pressure bearing assist to support the shaft prior to and during low speed rotation. Performance was measured over a range of 40 to 120 percent design pump flowrate to speed ratios, Q/N, at intervals of 20%. Test Series C1 used LN_2 in the pump and bearings. These tests were followed by Test Series C2 which used LO_2 in the pump and bearings.

1.2.3 Test Series "E1"

The objective of Test Series "E1," was to demonstrate the pure oxygen driven gas turbine for the first time. The turbine was plumbed to the ambient GOX supply and it powered the pump, pumping LOX from zero to the maximum operating speed with ambient GOX. Approximately five minutes of run time was to be accumulated with the bearing assist system on.

1.2.4 Test Series "D"

The objective of Test Series "D" was to demonstrate a start of the turbopump shaft system without the external bearing assist system. In this configuration (unassisted bearing start) the bearings are initially supplied with suction line pressure only. A discussion of the bearing assist system is given in Section 2.1.2.3. Bearings were fed from the pump discharge so that shaft rotation would start with bearing hydrostatic lift limited to pump discharge pressure. Series "D" testing was run using GN_2 as the turbine drive gas and LOX as the pumped fluid.

1.2.5 Test Series "E2"

The objective of Test Series "E2" was to demonstrate six unassisted bearing starts as in Series "D," using an ambient oxygen driven turbine while pumping liquid oxygen. Bearing lift-off was achieved with oxygen tapped from the pump second stage discharge line.

1.3 SCOPE OF WORK

1.3.1 General

Aerojet Propulsion Division shall conduct a test program to determine the performance and operating characteristics of the oxygen turbopump for the Aerojet Orbit Transfer Vehicle engine design concept.

1.3.2 Specific Subtasks

1.3.2.1 Subtask I - Testing

Aerojet Propulsion Division shall conduct test evaluations to determine the design and off-design performance and operating characteristics of the oxygen turbopump previously designed, fabricated, and tested as a bearing tester. Testing shall be conducted in accordance with the detailed test plan and shall consist of the following series:

Series C: The turbopump configuration shall consist of bladed pump and turbine stages but shall utilize external pressurization of the hydrostatic bearings. The pump fluid shall be liquid oxygen and the turbine drive fluid shall be gaseous nitrogen. Tests shall be conducted to verify overall turbopump performance and to demonstrate the ignition-resistance of the pump circuit.

Series D: The same configuration shall be tested with internal (pump discharge) pressurization of the bearings. The same fluids shall be used. Tests shall be conducted to demonstrate the bearing start transient with internal pressurization and the ignition-resistance of materials in the pump circuit.

Series E: The same configuration as used in Series D shall be tested with liquid oxygen as the pump fluid and gaseous oxygen as the turbine drive fluid. Turbopump performance at nominal and off-nominal operation shall be characterized. The ignition-resistance of the turbine circuit shall be demonstrated.

1.3.2.2 Subtask II - Reporting

The reports shall be prepared and distributed in accordance with contract requirements. In addition, a final formal report will be submitted and will cover the design, fabrication and testing.

1.4 RELEVANCE TO CURRENT ROCKET ENGINE TURBOPUMP DESIGN

The intent of this technology program is to demonstrate and reduce to practice several key design innovations that, taken together, significantly advance the design base for rocket engine turbopumps. These design innovations are:

1) Use of hot (400°F) oxygen as a turbine drive fluid.

2) Use of the monel family of alloys along with various platings for material's compatibility with both liquid and hot oxygen.

3) Use of a hydrostatic bearing system in LOX to meet performance goals and operating life goals well beyond current rocket engine requirements.

4) Use of an articulating, self adjusting spherical bearing system to hold close running clearances by accommodating minor shaft motion and misalignment.

5) Demonstration of a rotating assembly design that will operate subcritically over the operating range for a deep throttling engine.

6) Incorporation of unshrouded impellers to achieve a more stable head versus flow operating characteristic (negative slope) over a 20:1 thrust throttling range.

7) Elimination of the need for an interpropellant seal and a purge gas system by using an oxygen turbine driving an oxygen pump.

1.5 FACILITY DESCRIPTION

The oxygen TPA testing was conducted at the Aerojet 'A Zone' test facility. This test complex includes a central control room adjoining a laboratory experimental facility. An earth embankment separates the control room from the complex of test bays. The oxygen TPA testing was done in Bay 7.

The facility is set up such that all valves are actuated from the control room. Propellant tanks used in Series "C," "D," and "E" testing are located outside Bay 7, either in other Bays or on the other side of the earth embankment. The propellants used in Series "C," "D," and "E" testing, nitrogen, helium, and oxygen, were vented directly to atmosphere after passing through the TPA. Testing was conducted remotely from the control room and monitored by video, sound, and other electronic instrumentation.

Figure 1.5-1 shows the TPA early in the installation period, mounted on the test stand. Figure 1.5-2 shows the TPA, obscured by wires and lines, after the intallation was completed.

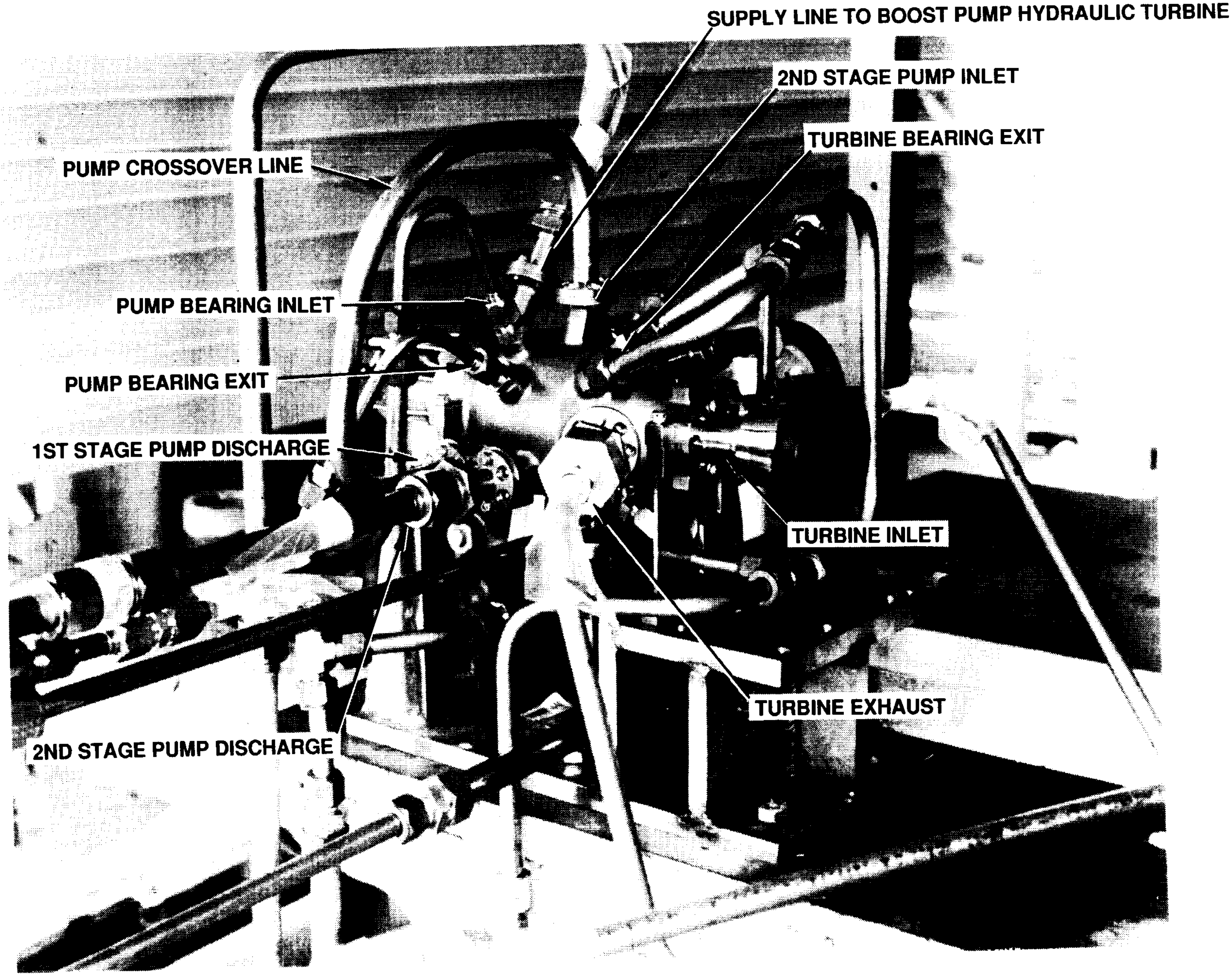

Figure 1.5-1. Oxygen Turbopump on Stand Early in Installation

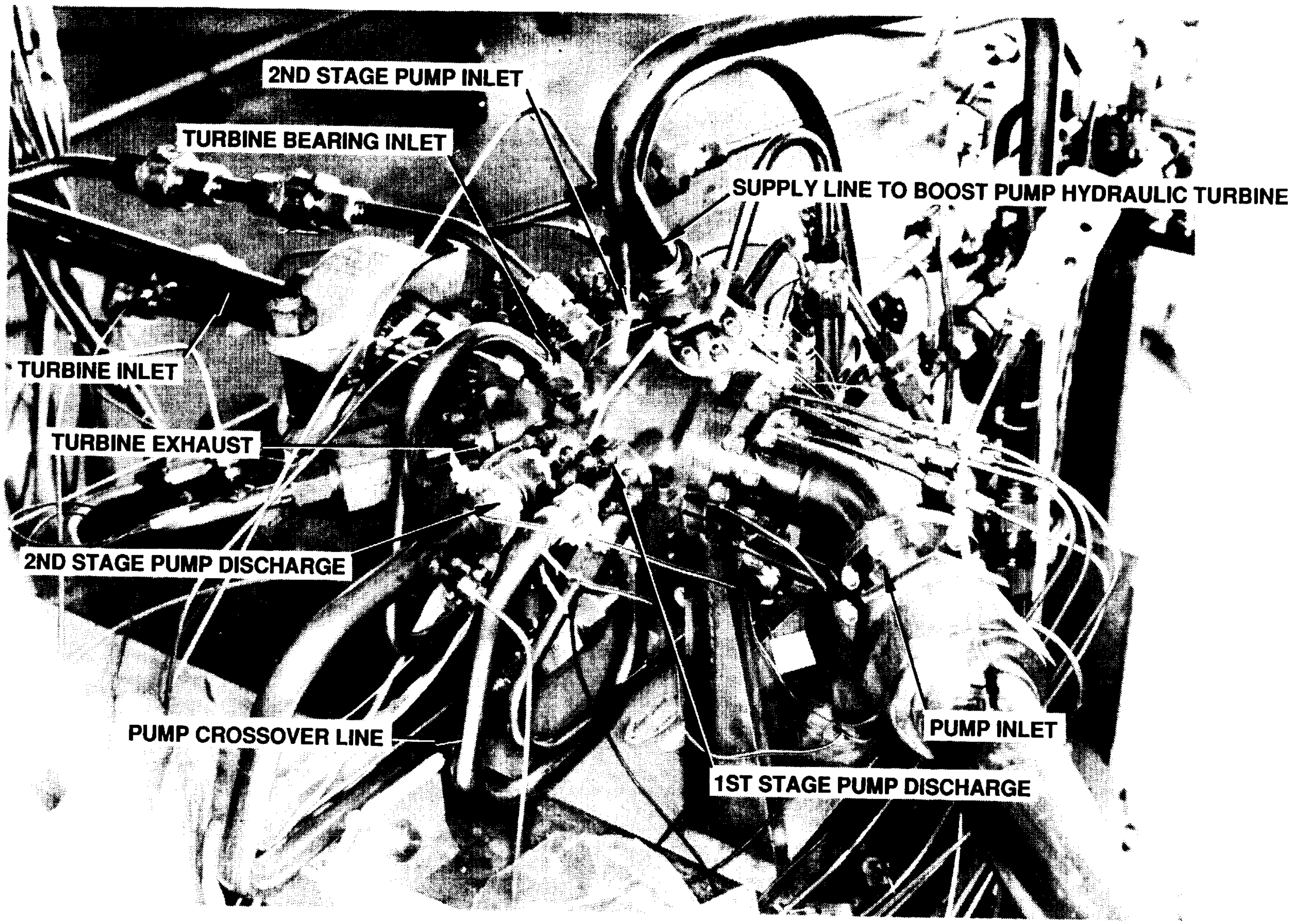

Figure 1.5-2. Oxygen Turbopump on Stand – Installation Completed

ORIGINAL PAGE
BLACK AND WHITE PHOTOGRAPH

2.0 OXYGEN TURBOPUMP TESTING

2.1 TEST PREPARATION

2.1.1 Test Approach

The test program consisted of taking a fully operational turbopump through a series of tests, Table 2.1-1, progressively obtaining performance, operational and life experience. Test Series "C" and "E1" were setup with the bearing inlet ports pressurized by a separate supply tank before power was supplied to the turbine in order to ensure the bearings would lift-off the shaft assembly prior to rotation (refer to the schematic in Figure 2.1-1). Test Series "C" and "D" used gaseous nitrogen to drive the turbine, and Test Series "E1" and "E2" used gaseous oxygen for turbine operation. Test Series "D" and "E2" were run without the high pressure assist to the bearings in order to demonstrate tank-head start conditions.

2.1.2 Facility Buildup

2.1.2.1 Facility Requirements

The turbopump predicted performance tabulation shown in Table 2.1-2 was provided to assist in determination of storage vessel capacities, line sizes, test run durations, pressure capabilities, and other parameters impacting the test facility design.

2.1.2.2 Facility Schematic

Figure 2.1-1 is a schematic diagram depicting the turbopump along with major test stand components and lines.

2.1.2.3 Hardware Description

The OTV LOX turbopump consists basically of a two-stage centrifugal pump directly driven by a single-stage axial flow turbine (Figure 1.1-2). The first pump stage incorporates an inducer section to meet Suction Specific Speed requirements and to provide pressurization for the low speed boost pump which would be used in a flight system. The interstage pump flow (Stage 1 to Stage 2) is routed external to the main housing through two ducts connecting first-stage

TABLE 2.1-1
OTV Oxygen Turbopump Testing Conditions

TEST SEQUENCE	TEST SERIES	OBJECTIVE	(1) TURBINE FLUID	PUMP FLUID	MAXIMUM SHAFT SPEED (RPM)	(2) MINIMUM RUN TIME (MIN)	BEARING ASSIST SYSTEM	Q/N
1	O	SYSTEM LEAK CHECK	GHe	GHe	0	- - - -	- - - -	
2		INSTRUMENTATION CHECK	GN2	LN2				
3	C1.1	ROTATING CHECKOUT	GN2	LN2	40,000	1	ON	100%
	.2				70,500	1		100%
	.3				70,500	1		120%
	.4				50,000	1		60%
	.5				30,000	1		40%
4	C2.1	PERFORMANCE VERIFICATION	GN2	LO2	40,000	1	ON	100%
	.2				75,000	4		100%
	.3				60,000	1		80%
	.4				70,500	1		120%
	.5				50,000	1		60%
	.6				30,000	1		40%
	.7				70,500	1		90%
5	E1.1	GO2 DRIVEN TURBINE	GO2	LO2	40,000	5	ON	100%
	.2				60,000			100%
6	D	UNASSISTED BEARING START	GN2	LO2	40,000	(3) 1	OFF	100%
7	E2	GO2 DRIVE WITHOUT BEARING ASSIST	GO2	LO2	60,000	(4) 6	OFF	100%

NOTES:
(1) ALL TURBINE DRIVE GAS AT AMBIENT TEMPERATURE
(2) GN2/GO2 SUPPLY TANK VOLUME WILL LIMIT RUN TIME TO APPROXIMATELY ONE MINUTE PER START/STOP CYCLE
(3) 1 START/STOP CYCLE
(4) 6 START/STOP CYCLES

3/18/89

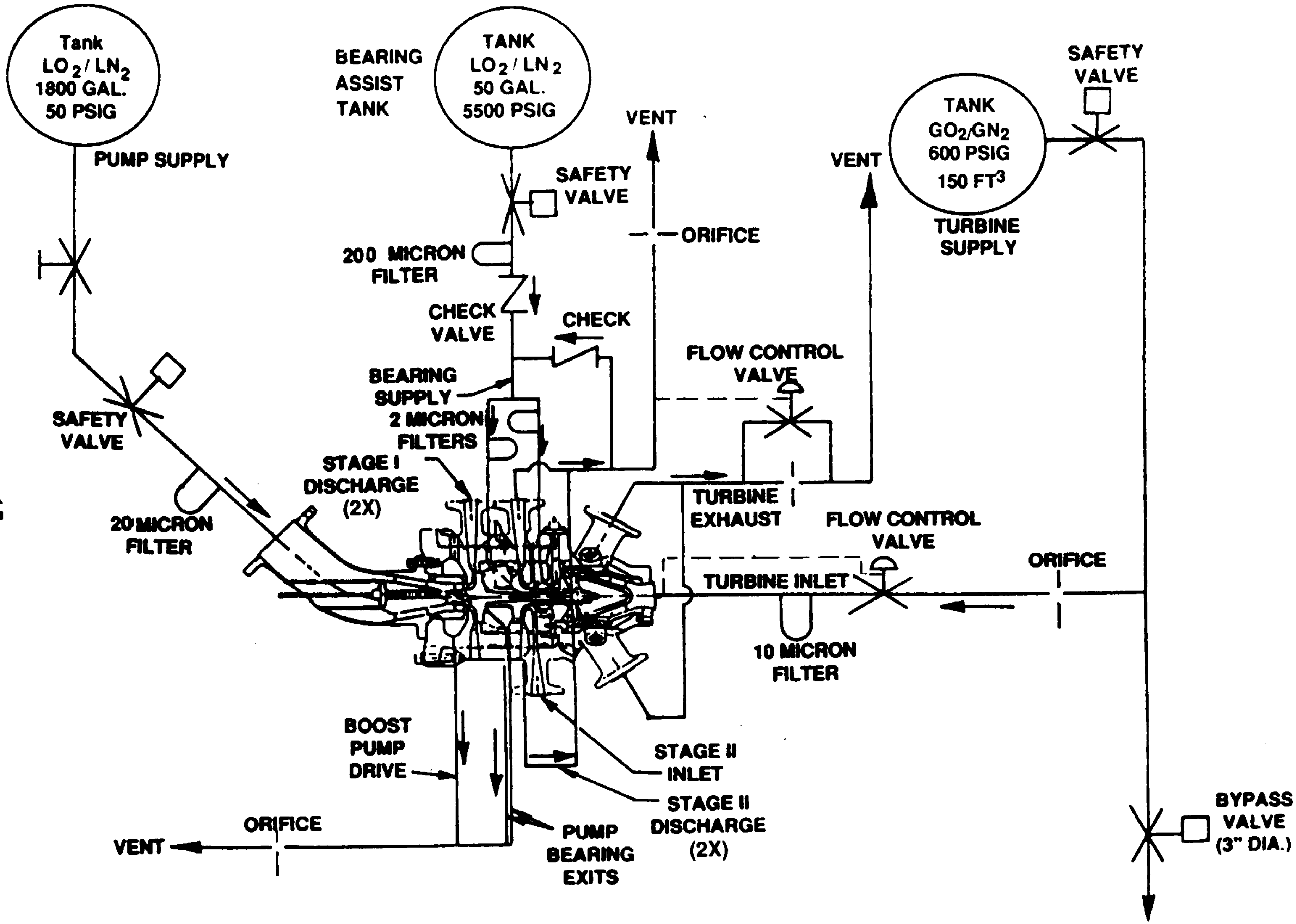

Figure 2.1-1. Test Schematic: Series C, D, and E

TABLE 2.1-2

TEST SERIES "C," "D," AND "E" OPERATING CONDITIONS

Maximum Speed Operating Conditions - Predicted Performance

Conditions	Design Nominal	Test Series "C1"	Test Series "C2" & "D"	Test Series "E1" & "E2"
Pump				
Pumped Fluid	LO_2	LN_2	LO_2	LO_2
Number of Stages	2	2	2	2
Weight Flow Rate -lb/sec	5.4	4.3	5.4	5.4
Volume Flow Rate - Inducer - GPM	51.4	58.0	51.4	51.4
Volume Flow Rate - Impellers - GPM	34.1	38.5	34.1	34.1
Net Postive Suction Head - ft.	80	97.1	71.3	71.3
Suction Pressure - psia	54.6	50	50	50
Discharge Pressure - psia	4,655	2,500	4,580	4,580
Head Rise, Inducer - ft	525	459	520	520
Head Rise per Stage - ft.	4,575	3,504	4,575	4,575
Speed - RPM	75,000	70,500	75,000	75,000
Pump Shaft Power - HP	158	102	155	155
Turbine				
Drive Gas	GO_2	GN_2	GN_2	GO_2
Tubine Shaft Power - HP	163	105	163	163
Inlet Temperature - °R	860	510	510	510
Inlet Pressure - psia	4,170	2,200	3,780	4,130
Exit Pressure - psia	2,327	1,250	2,290	2,290
Pressure Ratio	1.79	1.76	1.65	1.80
Flow Rate - lb/sec	4.91	3.32	5.58	6.31

discharge to second-stage inlet. Double discharges are utilized on both pump stages to reduce flow induced hydraulic radial loading. The shaft system is supported by two hydrostatic bearings each supplied with high pressure propellant (LOX or LN_2) from the second stage pump discharge after pump discharge pressure exceeds bearing assist pressure. Both bearings articulate on spherical seats, providing a measure of compensation for misalignment and/or transient thermal distortion. The hydrostatic bearings provide a very stiff radial and axial support for the rotor system. This facilitates sub-critical operation with ample margin, and very small shaft displacements at all speeds. The result is high efficiency in the turbo-machinery by virtue of the close running clearances at which impellers and turbines can be operated.

Provision is made for future addition of a hydraulic boost pump, with an internal extraction point at the inducer discharge and delivered via a flanged port in the outer housing. Although the boost pump was not incorporated for this test, the flow for boost pump drive was tapped off, orificed and measured.

A separate high pressure liquid oxygen (or nitrogen) supply system is used for bearing pressurization. Without this bearing assist pressurization there will always be a brief period at low speed where the rotating assembly contacts the bearing surfaces. As the speed increases and pump output rises the rotating assembly is stabilized within high pressure fluid films without any mechanical contact. The rotating pump bearing journal and thrust faces have a thin dense chromium surface treatment at potential contact points for a hard, low friction, wear resistant surface. The turbine bearing journal was left with the untreated monel K500 surface in an attempt to verify the prediction that the K500 has adequate wear resistance without surface treatment. Post test inspection showed both the treated and untreated surfaces in good condition. The corresponding bearing surfaces are silver plated to give a low friction, highly ignition resistant surface whose mechanical wear products will not add combustible particles to a high speed stream of oxygen. These surfaces then, are designed to accept the repeated rubbing starts from actual engine operation.

2.1, Test Preparation (cont.)

For the initial testing the bearing assist system reduces potential hazards and the wear attendant in over a hundred starts by prepressurizing the bearings prior to rotation. Transition from bearing assist to pump provided pressurization is done with a check valve that opens when the pump discharge pressure is greater than the bearing assist pressure. In a flight system there would be no special bearing assist; all pressurization would be from the pump discharge.

The test configuration of this turbopump is shown in Figure 2.1-2 and is further defined in Aerojet drawing No. 1197585-9 and sub-tier drawings. The test unit incorporates special instrumentation which is detailed in Section 2.1.2.4. The instrumentation provided with the turbopump assembly also includes axial and radial shaft displacement sensors.

2.1.2.4 Instrumentation

The scheme for identification and location of instrument ports on the test unit is presented in Section 2.1.2.4.1. The instrumentation list in Section 2.1.2.4.2 includes units, ranges, and type of instrument for all parameters that were recorded. The accompanying sketches relate the symbols in the instrumentation list to approximate locations on the test unit.

2.1.2.4.1 Port Location Scheme

The instrumentation list gives nomenclature and locations for ports located on the test unit. The nomenclature refers to the symbol etched or tagged on the test unit. The approximate location of each port is designated by a distance and an angle as described in Figure 2.1-3.

2.1.2.4.2 Instrumentation List

The instrumentation list is divided into the three functional types of wiring used to transmit the electrical output of the instruments: (1) a two-wire system, (2) a transducer system and (3) a high frequency system.

The two-wire system is outlined in Table 2.1-3. The location of the sensor is number coded, (n), on the flow diagram Figure 2.1-4.

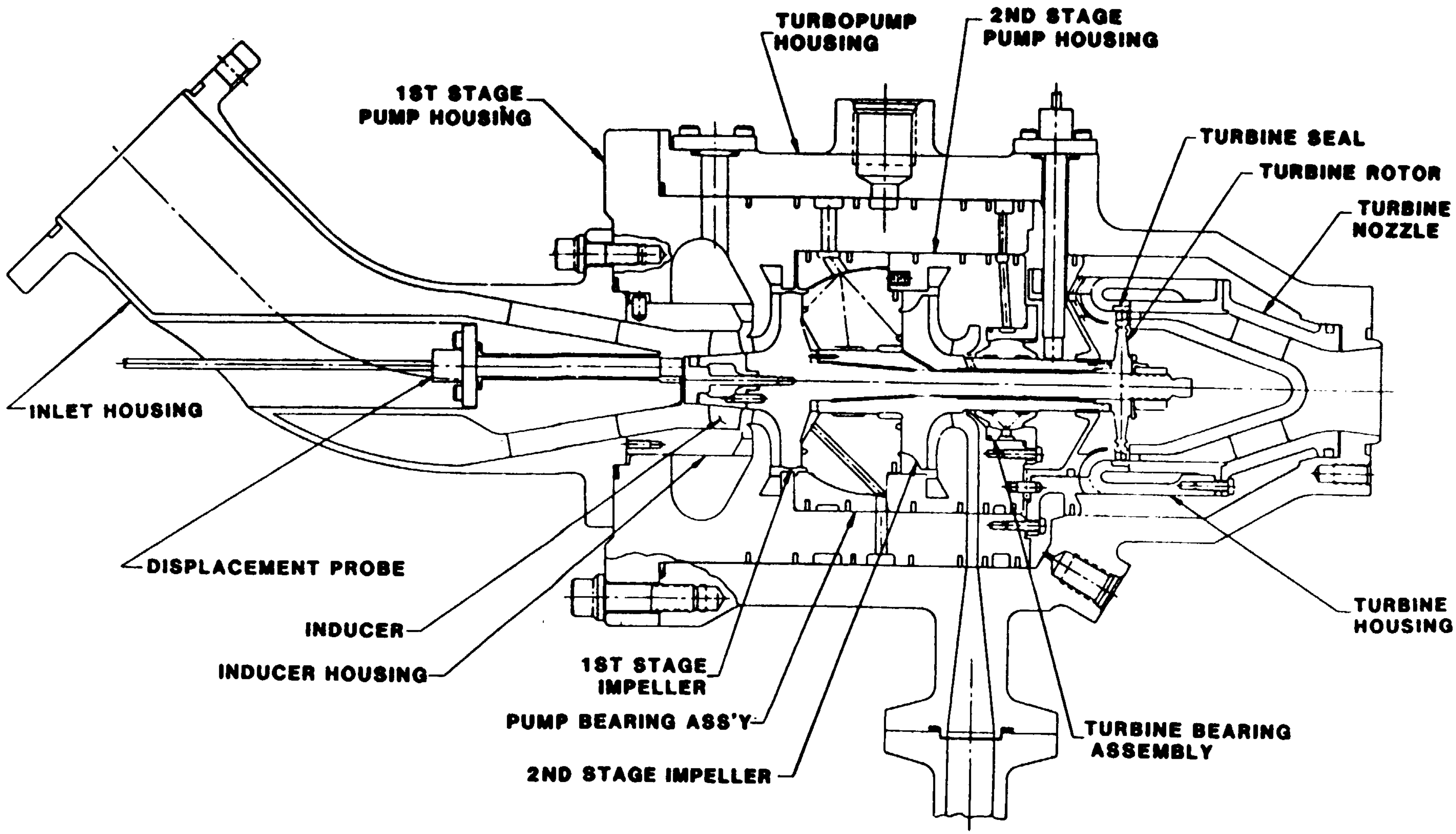

Figure 2.1-2. OTV Oxygen Turbopump Assembly

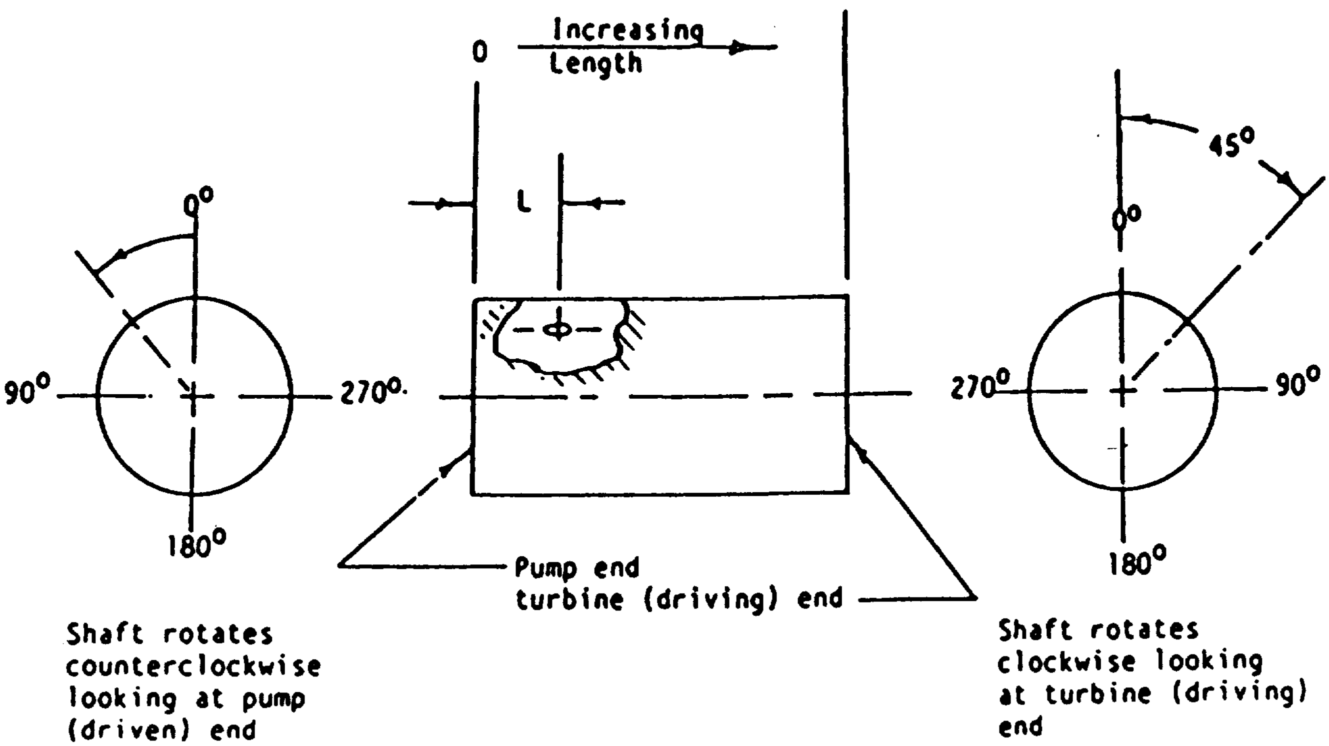

EXAMPLE:
Port location illustrated on cylinder outside diameter is noted as (L,45) for "L" distance from outside surface of the pump end in a plane 45 degrees from the vertical center line in a clockwise direction when looking from the turbine end. Location designator ignores radial distance.

Figure 2.1-3. Instrument Port Location Scheme

TABLE 2.1-3.
Instrumentation List — 2-Wire Channels

SYMBOL AND NO.	FUNCTION	TPA PORT NOMENCLATURE & LOCATION (INCH,DEGREES)	TEST LAB INSTRUMENT NOMENCLATURE	TYPE	UNITS & RANGE
1	HSG EXTERIOR TEMP @ TURB	(4.82,0)	TTH7	C/A (K)	+100F TO -350F
2	TURB BRG INLET FLUID TEMP	TBI	TBI	C/A (K)	+100F TO -350F
3	PUMP BRG FLOW RATE	PBI	FMPBI	TURBINE	0.5 GPM TO 15 GPM
4	PUMP DISCHARGE FLOW RATE	2SD1	FMPD-E	TURBINE	0.5 GPM T0 25 GPM
5	PUMP DISCHARGE FLOW RATE	2SD2	FMPD-W	TURBINE	0.5 GPM TO 25 GPM
6	TURB BRG FLOW RATE	TBI	FMTBI	TURBINE	0.5 GPM TO 15 GPM
7	PUMP 1ST STAGE DISCH TEMP	TSD1(3.03,70)	TPD1	RTD	+100F TO -350F
8	PUMP 1ST STAGE DISCH TEMP	TSD2(3.03,250)	TPD2	RTD	+100F TO -350F
9	PUMP SUCTION FLOW RATE		FMSI	TURBINE	4 GPM TO 55 GPM
10	HSG EXTERIOR TEMP @ TURB BRG	(3.79,0)	TTBH8	C/A (K)	+100F TO -350F
11	HSG EXTERIOR TEMP @ PUMP INLET	(0.25,0)	TTIPH10	C/A (K)	+100F TO -350F
12	PUMP BRG EXIT TEMP	PBE1	TPBE	C/A (K)	+100F TO -350F
13	BOOST PUMP DRIVE TURB FLUID TEMP		TBPD	RTD	+100F TO -350F
14	BOOST PUMP DRIVE TURBINE FLOW		FMBPD	TURBINE	0.5 GPM TO 15 GPM
15	HSG EXTERIOR TEMP @ PUMP BRG	(1.78,0)	THX9	C/A (K)	+100F TO -350F
16	DISTANCE DETECTOR, TURB	(4.08,120)	DDTX	PROBE	0 TO 40 VOLTS
17	DISTANCE DETECTOR, TURB	(4.08,210)	DDTY	PROBE	0 TO 40 VOLTS
18	DISTANCE DETECTOR, PUMP AXIAL	(-1.23,C'LINE)	DDPZ	PROBE	0 TO 40 VOLTS
19	SHAFT SPEED, RADIAL	(4.08,120)	NT-X	PROBE	0 TO 80,000 RPM
20	SHAFT SPEED, RADIAL	(4.08,210)	NT-Y	PROBE	0 TO 80,000 RPM
21	SHAFT SPEED, AXIAL	(-1.23,C'LINE)	NT-Z	PROBE	0 TO 80,000 RPM
22	PUMP SUCTION TEMP		TS	RTD	+100F TO -350F
23	2ND STAGE DISCHARGE TEMP		TPD2-E	RTD	+100F TO -350F
24	2ND STAGE DISCHARGE TEMP		TPD2-W	RTD	+100F TO -350F
25	PUMP BEARING INLET FLUID TEMP	PBI	TPBI	C/A (K)	+100F TO -350F
26	TURBINE INLET TEMP		TTI	C/A (K)	+100F TO -350F
27	TURBINE DISCH HOUSING TEMP	TET (5.0,225)	TTDH	C/A (K)	+100F TO -350F
28	PUMP BEARING EXIT FLOW RATE	PBE1 (2.54,120)	FMPBE	TURBINE	0.5 GPM TO 15 GPM
29	TURB INLET ORIFICE UPSTREAM TEMP		TTIOU	C/A (K)	+100F TO -350F
30	TURB EX ORIFICE DOWNSTREAM TEMP		TTEOD	C/A (K)	+100F TO -350F

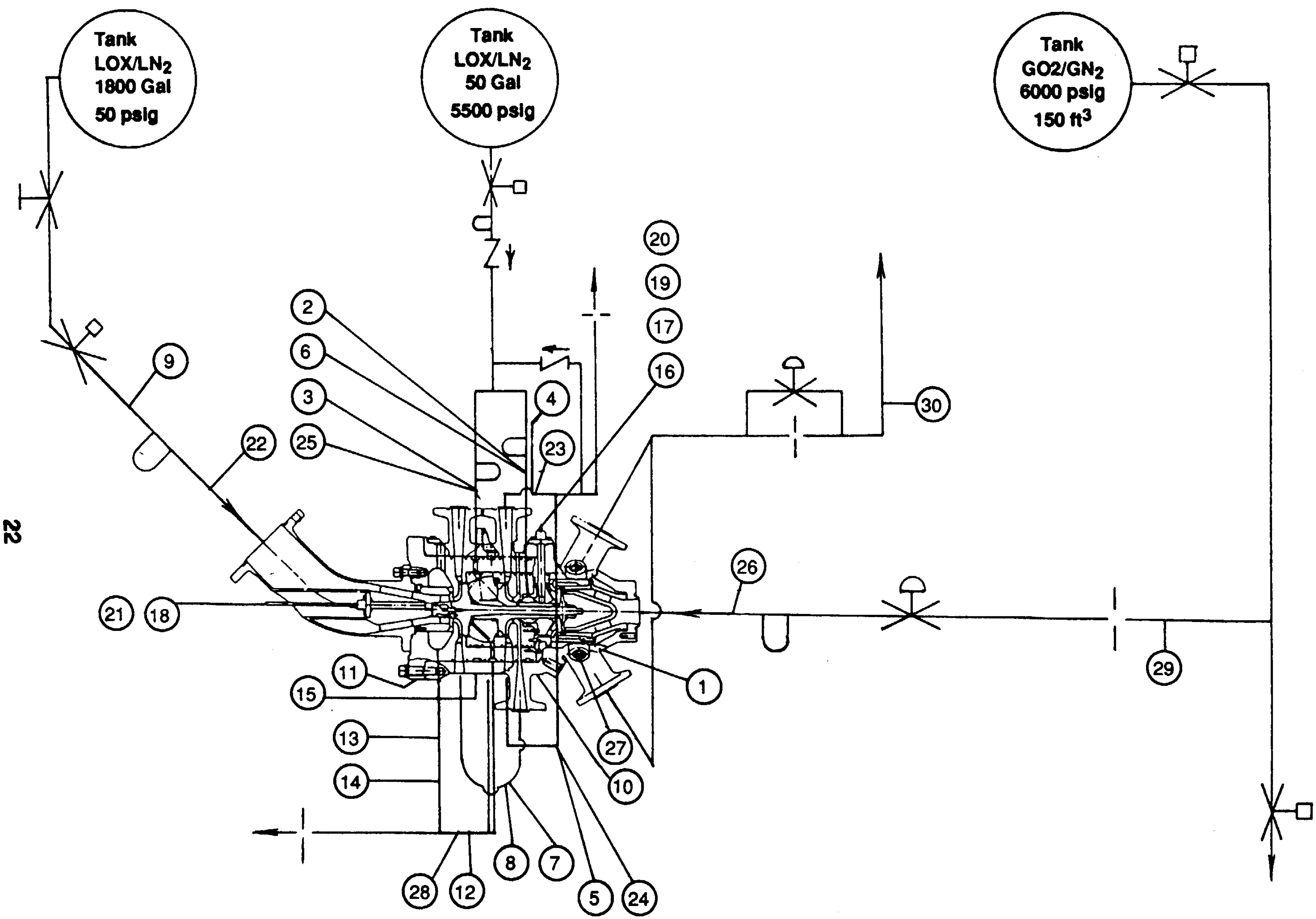

Figure 2.1-4. Instrumentation Locations – 2 Wire Channels

2.1, Test Preparation (cont.)

The transducer system is outlined in Table 2.1-4. The location of the sensor is number coded, n, on the flow diagram Figure 2.1-5.

The high frequency system is outlined in Table 2.1-5. The location of the sensor is number coded, $\boxed{n}$, on the flow diagram Figure 2.1-6.

2.1.3 <u>Test Procedure</u>

2.1.3.1 Test Descriptions

<u>Test Series "O"</u> - Checkout

After plumbing was completed in Bay A7, the system was leak checked by pressurizing with 50 psig dry (less than 50 ppm water) helium. After leaks were sealed, a helium purge at 50 psig was applied to the turbopump, and maintained at all times when testing was not in progress.

An instrumentation checkout was performed next, followed by a moisture content check of the helium discharged from the TPA. When the moisture content was found to be less than 50 ppm water, liquid nitrogen was introduced in the pump circuit and bearing feed lines. The pressure in the bearing feed was cycled from zero to 2800-3800 psia five times in order to align the bearing/shaft system.

<u>Test Series "C1"</u> - Pump, Bearing and Turbine Performance

The complete turbopump was operated with the inducer and centrifugal pumps pumping liquid nitrogen and the turbine flowing ambient temperature gaseous nitrogen plumbed per Figure 2.1-1. The turbopump was powered by increasing turbine inlet pressure to 3000 psia maximum with a speed limit of 68,000 rpm. Speed changes were limited to a rate of 4000 rpm/second. Flows, pressures, speed and temperatures were recorded per Section 2.1.2.4. Bearing assist pressure was initially set at 1200 psia minimum for this Series. Dual check valves were employed to ensure the bearings were fed by the bearing assist system pressure before shaft rotation. Sufficient runs were conducted at approximately 20%

TABLE 2.1-4.
Instrumentation List – Transducer Channels

SYMBOL AND NO.	FUNCTION	TPA PORT NOMENCLATURE & LOCATION (INCH,DEGREES)	TEST LAB INSTRUMENT NOMENCLATURE	TYPE	UNITS & RANGE
1	PUMP BRG INLET PRESSURE	PBI (2.06,330)	PPBI	TRANSDUCER	0 TO 6000 PSIG
2	TURB BRG INLET PRESSURE	TBI (3.63,45)	PTBI	TRANSDUCER	0 TO 6000 PSIG
3	TURB EXH PRESSURE	TD1 (5.81,90)	PTD-W	TRANSDUCER	0 TO 3000 PSIG
4	TURB HOUSING EXH PRESSURE	TEP (5.03,225)	PTDH	TRANSDUCER	0 TO 3000 PSIG
5	TURB EXH PRESSURE	TD2 (5.81,270)	PTD-E	TRANSDUCER	0 TO 3000 PSIG
6	PUMP PRESSURE, MID	PP1 (0.0,330)	PIM1	TRANSDUCER	0 TO 3000 PSIG
7	PUMP BRG EXIT PRESSURE, PBE 2 (2.54, 300)	PBE1 (2.54,120)	PPBE (1)	TRANSDUCER	0 TO 3000 PSIG
8	PUMP PRESSURE, TIP	PP2 (0.0,300)	PIT2	TRANSDUCER	0 TO 3000 PSIG
9	TURBINE BRG CAVITY PRESSURE	TBCP (4.64,45)	PTBC	TRANSDUCER	0 TO 3000 PSIG
10	SUCTION LINE PRESSURE		PS	TRANSDUCER	0 TO 400 PSIG
11	2ND STAGE DISCHARGE PRESSURE	2SD1 (3.03,70)	PD2-W	TRANSDUCER	0 TO 6000 PSIG
12	2ND STAGE DISCHARGE PRESSURE	2SD2 (3.03,250)	PD2-E	TRANSDUCER	0 TO 6000 PSIG
13	PUMP PERIPHERAL PRESSURE	PPP1 (0.0,0)	PPP1	TRANSDUCER	0 TO 3000 PSIG
14	PUMP PERIPHERAL PRESSURE	PPP2 (0.0,270)	PPP2	TRANSDUCER	0 TO 3000 PSIG
15	PUMP PERIPHERAL PRESSURE	PPP3 (0.0,180)	PPP3	TRANSDUCER	0 TO 3000 PSIG
16	PUMP PERIPHERAL PRESSURE	PPP4 (0.0,90)	PPP4	TRANSDUCER	0 TO 3000 PSIG
17	BOOST PUMP DRIVE LINE PRESSURE	BPP (0.86,15)	PBPD	TRANSDUCER	0 TO 500 PSIG
18	TURB INLET PRESSURE	(6.96,C'LINE)	PTI	TRANSDUCER	0 TO 5000 PSIG
19	BOOST PUMP SUPPLY, HOUSING PRESSURE	BPDP	PBPH	TRANSDUCER	0 TO 3000 PSIG
20	TURB INLET ORIFICE UPSTREAM		PTIO	TRANSDUCER	0 TO 6000 PSIG
21	TURB INLET ORIFICE DELTA-P		DPTIO	TRANSDUCER	0 TO 100 PSID

(1) PORTS PBE 1 AND PBG 2 COMBINED

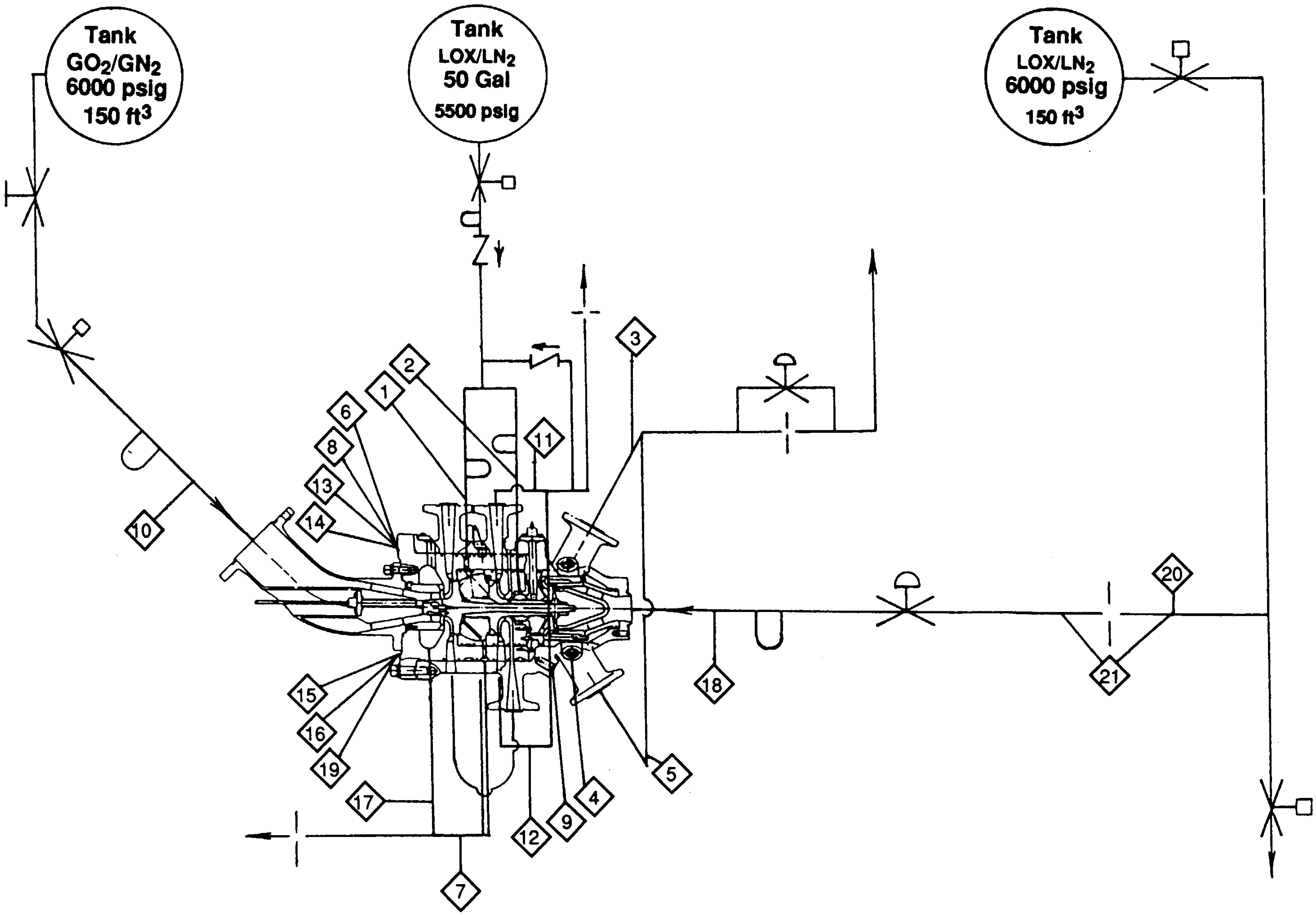

Figure 2.1-5. Instrumentation Locations – Transducer Channels

TABLE 2.1-5. Instrumentation List — High Frequency Channels

SYMBOL AND NO.	FUNCTION	TPA PORT NOMENCLATURE & LOCATION (INCH,DEGREES)	TEST LAB INSTRUMENT NOMENCLATURE	TYPE	UNITS & RANGE
1	TURB END ACCELERATION, VERTICAL	(6.86,0)	GTX	ENDEVCO 2272	0 TO 15G, 10 TO 15KHZ
2	TURB END ACCELERATION, HORIZONTAL	(6.86,270)	GTY	ENDEVCO 2272	0 TO 15G, 10 TO 15KHZ
3	PUMP END ACCELERATION, AXIAL	(-0.56,180)	GPZ	ENDEVCO 2272	0 TO 15G, 10 TO 15KHZ
4	PUMP END ACCELERATION, VERTICAL	(0.81,0)	GPX	ENDEVCO 2272	0 TO 15G, 10 TO 15KHZ
5	PUMP END ACCELERATION, HORIZONTAL	(0.81,270)	GPY	ENDEVCO 2272	0 TO 15G, 10 TO 15KHZ

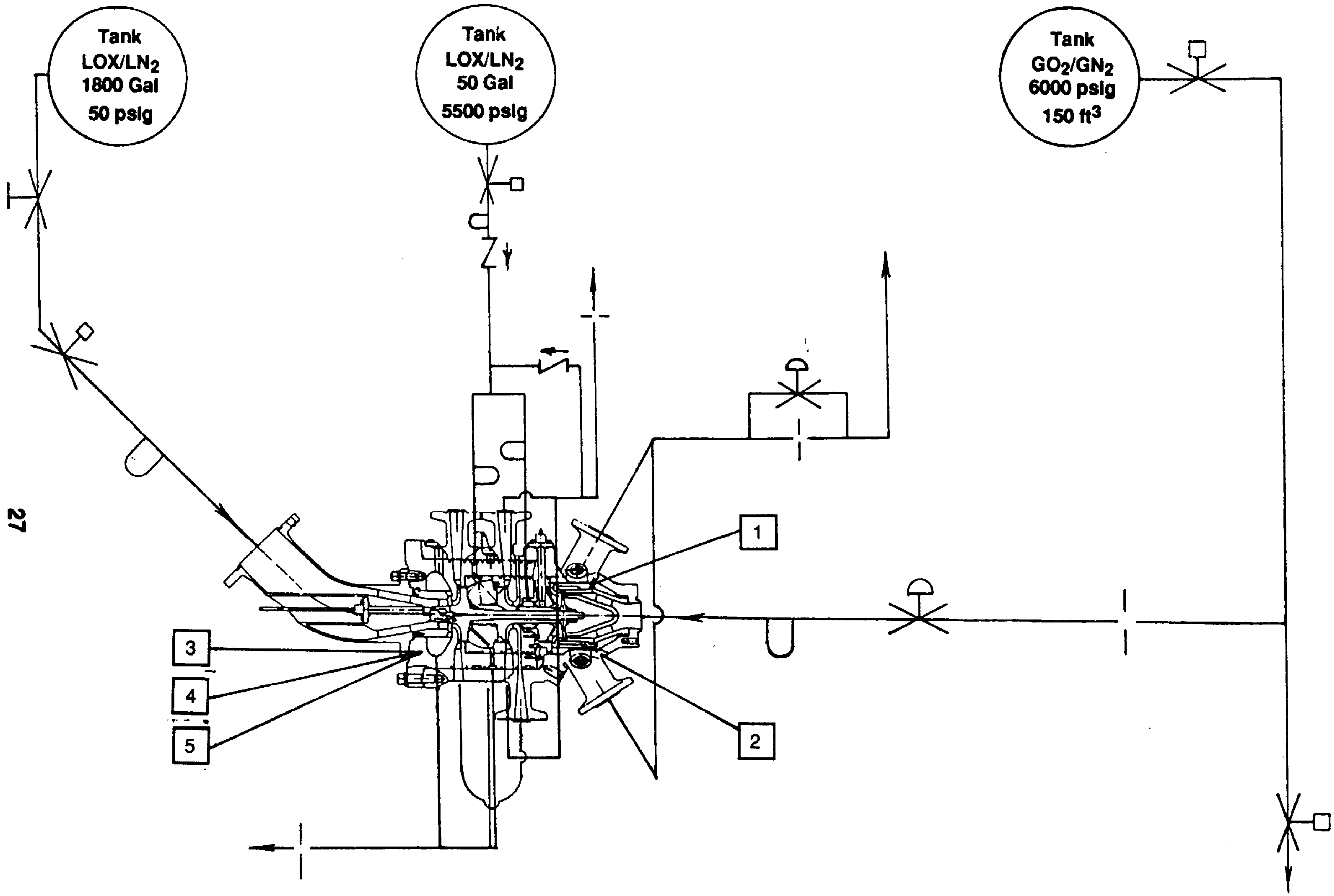

Figure 2.1-6. Instrumentation Locations – High Frequency Channels

intervals of design flow/speed ratio from 40% to 120% Q/N until the goals of Table 2.1-1 were met for this series.

Test Series "C2" - Pump, Bearing and Turbine Performance

The complete turbopump was operated with the inducer and centrifugal pumps pumping liquid oxygen and turbine flowing ambient temperature gaseous nitrogen. The turbopump was powered by increasing turbine inlet pressure to 4,850 psia max with a speed limit of 70,000 rpm. Flows, pressures, speed and temperatures were recorded per Section 2.1.2.4. Bearing assist pressure was 500 ± 50 psia for this Series. Sufficient runs were conducted until the goals outlined in Table 2.1-1 were achieved.

Test Series "E1" - Demonstrate Oxygen Driven Turbine

The turbopump was operated with the inducer and centrifugal pumps pumping liquid oxygen and turbine powered by ambient temperature gaseous oxygen during this series. The turbopump was powered by increasing turbine inlet pressure to 4000 psia with a speed limit of 63,000 rpm. Bearing assist pressure was 500 ± 50 psia for this series. Eight runs were necessary to achieve the goals outlined for Series E1 in Table 2.1-1.

Test Series "D" - Demonstrate Unassisted Start of Bearings

The turbopump was operated with the inducer and centrifugal pumps flowing liquid oxygen and the turbine flowing ambient temperature gaseous nitrogen. Bearing assist pressure was reduced to 55 ± 5 psia (pump suction pressure) to simulate a tank-head start. Turbine inlet pressure was increased to 1600 psia with a speed limit of 42,000 rpm. Six unassisted starts were necessary to achieve the 60 second run time goal of Table 2.1-1.

Test Series "E2" - Demonstrate Unassisted Start with Oxygen Driven Turbine

The turbopump was operated with the inducer and centrifugal pumps pumping liquid oxygen and the turbine powered by ambient temperature gaseous oxygen. The turbopump was powered by increasing turbine inlet pressure to 4000 psia with a speed limit of 63,000 rpm. Bearing assist and pump inlet pressures were 55 ± 5 psia for this series. Eight unassisted starts were necessary to achieve the minimum run time requirement of this Series.

2.1.3.1.2 Special Requirements

Aerojet Propulsion Division Test Laboratory furnished alternate sized pump discharge orifices in addition to the one for nominal Q/N for off-design Q/N operating points. Data points were recorded over the full speed range. Turbine inlet pressure was not increased until saturated liquid was present at the pump inlet for all runs.

2.1.3.1.3 Starts with Bearings Assisted

In Series "C" and "E" the hydrostatic bearings were pressurized directly from a high pressure 50 gallon run tank to assure lift-off in the bearings before rotation. During LN_2 pump tests, Series C1, the bearing assist pressure was maintained well above pump discharge pressure to assure adequate critical speed margin. Check valves were placed in the tank fed bearing supply line and a second valve in the pump discharge fed bearing supply line, Figures 2.1-4 and 1.2-6. When pump discharge pressure exceeded bearing assist pressure the pump then supplied the high pressure to the hydrostatic bearings.

2.1.3.1.4 Starts with Bearings Unassisted

The bearing assist system pressure was reduced to pump inlet Pressure (55 psia) for Series "D" and "E2" so that bearing lift-off occurred as a result of pump discharge pressure alone as discharge pressure increased with pump speed. A speed kill was set at 80,000 rpm for this test.

The shaft experienced auto rotation during chill-in. This made it a necessary to supply the bearings with 200 psia minimum assist pressure until 5 seconds before an unassisted start.

2.1, Test Preparation (cont.)

2.1.3.2 Data Requirements

The data furnished by the Test Laboratory for each test performed falls into five general categories. These are digital data, plots, floppy diskettes, magnetic tape and calculated performance. The requirements are described in the following sections. The Test Laboratory shall retain archive copies of all test data for a minimum of 3 years.

2.1.3.2.1 Digital Data

Digital printed data was provided for all test runs for quick look purposes, in absolute engineering units. This data was in the form of a time history for the test. An "edit ratio" was used in printing the data scans, for selected tests, to reduce the volume of printed data. The digital data is in the form of computer printouts. One copy of all digital data was furnished to the TPA Lead Engineer.

2.1.3.2.2 Plotted Data

Plots were provided of all pertinent parameters versus time for selected test runs. One copy of all plots were provided to the TPA Lead Engineer.

2.1.3.2.3 Floppy Diskettes

Raw data from selected tests was furnished to Engineering on floppy diskettes in spread sheet format. These data were calibrated but not screened or reduced.

2.1.3.2.4 Magnetic Tape

Output signals from accelerometers and distance detector probes were continuously recorded on magnetic tape. One copy of all magnetic tape data will be stored at Aerojet Propulsion Division Test Area Archives for three years.

2.1.3.2.5 Calculated Parameters

Performance calculations were performed for selected test runs. Equations for these parameters (using variable names and channel numbers) are provided in Appendix A.

2.1.3.3 Photographic Records

The Test Laboratory has provided 8" x 10" color photographs documenting the test stand with the test unit installed. These include both overall views and close-up views. The photographs are sufficient in quantity and detail to identify plumbing and instrumentation line connections. Figures 2.1-7 and 2.1-8 are examples of such photos. Additional photographs were taken of the stand during the test program. The test stand was videotaped during all testing, as was the oscilloscope when a shaft orbit was visible.

2.2 TESTING

Testing of the OTV oxygen turbopump was performed at Aerojet Propulsion Division from 9 February through 21 March of 1989. Testing was divided into three main test series, "C," "D," and "E," and performed in the order of increasing risk.

2.2.1 Facility Checkout and TPA Chilldown

Before beginning high-speed turbopump testing, a facility checkout and TPA chilldown tests were performed. Minor facility and TPA leaks were sealed on 9 February, and time was spent determining the most efficient method of chilling the TPA to saturated LN_2 temperature. A circuit bypass chill-in flow around the highly restrictive pump discharge orifice had to be installed.

It was also during this phase that instrumentation problems were addressed. The main problem was the nonfunction of displacement/speed probes. The displacement probes used are quite sensitive to operating temperature and produce out-of-range readings when either the operating temperature or gap between

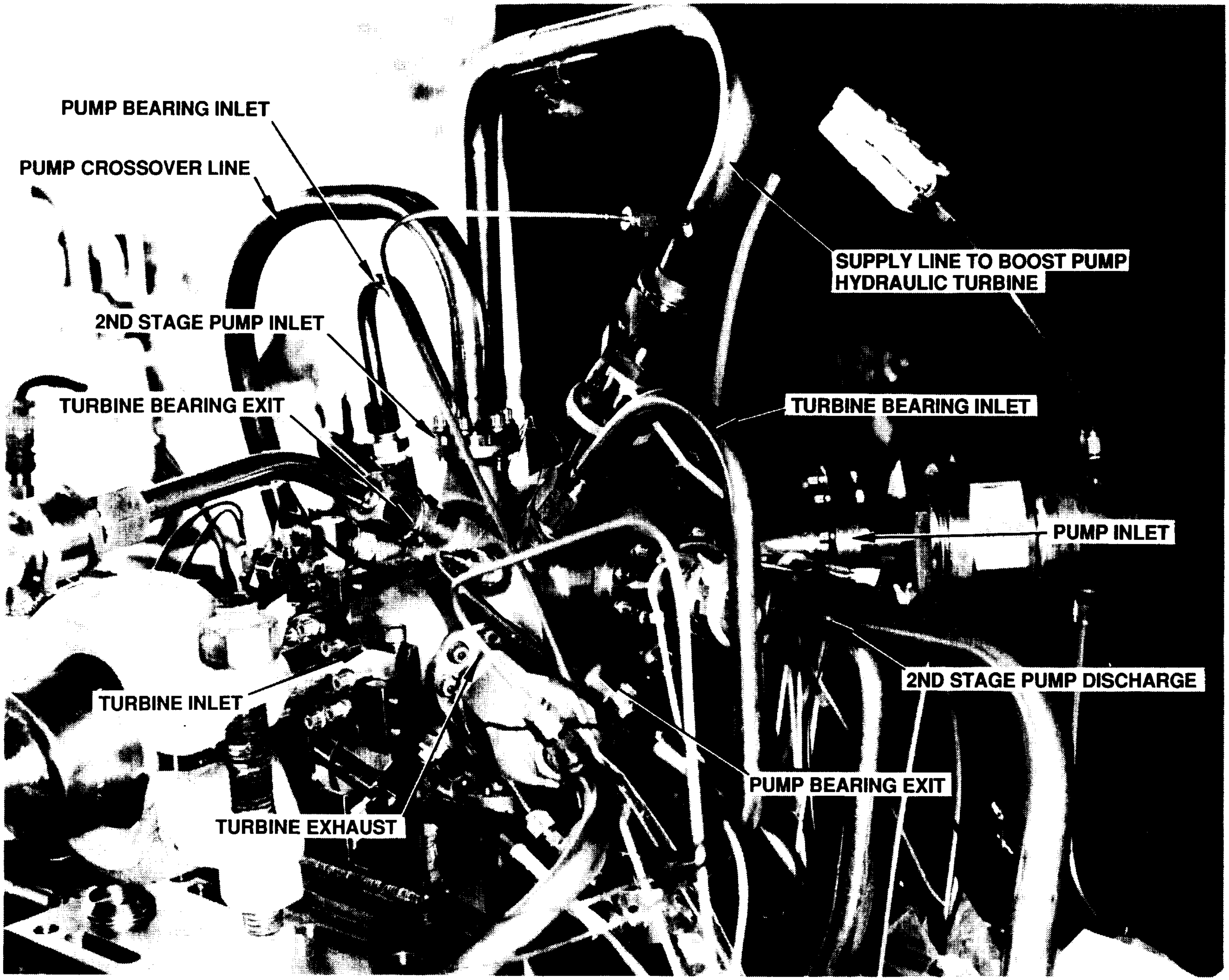

AT Photo #C0289 0699

Figure 2.1-7. Oxygen Turbopump on Test Stand

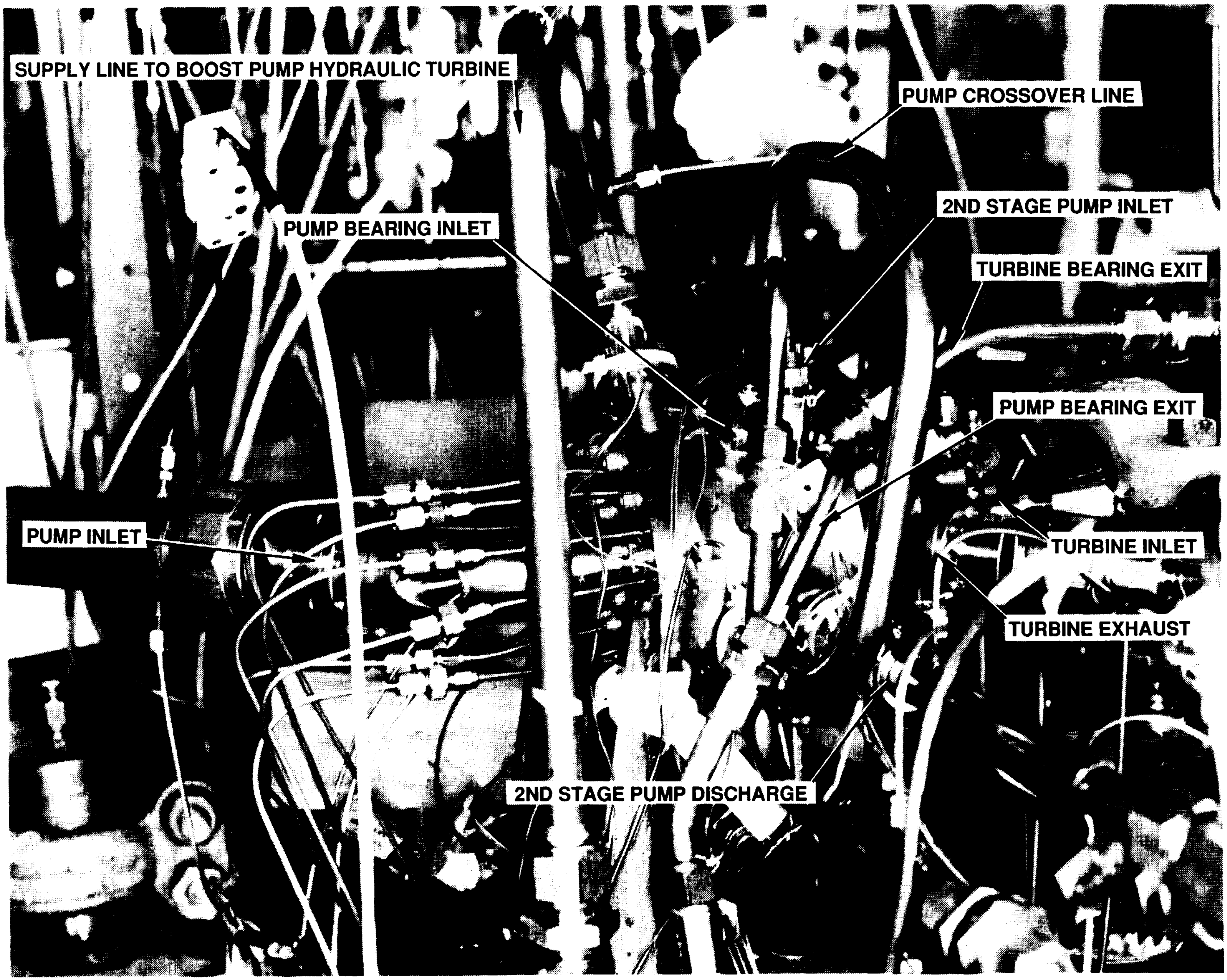

AT Photo #C0289 0700

Figure 2.1-8. Oxygen Turbopump on Test Stand the probe and target are not optimum. Since operating temperature was not adjustable, experimentation with gap size was performed with each probe. The best results of these experiments resulted in the axial probe functioning successfully for nearly all tests, and the radial probes functioning only intermittently throughout the test program.

The main area of work during the "checkout" phase was the control of the two facility flow control valves. One of these valves was located upstream of the turbine, and served to control the flow and inlet pressure to the turbine. The other was located downstream of the turbine and served to control the turbine back-pressure. Working together, these valves controlled the turbine pressure ratio, turbine power and to some extent the axial thrust balance of the TPA. The valves were critical to performing a successful TPA test. The main challenge in controlling these valves was sequencing the valves to maintain the desired pressure and pressure ratio rise rate. A start that was too fast resulted in automatic test kills due to low pump suction pressure, high shaft speed or high pump discharge pressure. Conversely, a start that was too slow resulted in an array of automatic test kills associated with low shaft speed. A slow rate would also cause excessive depletion of turbine supply gas sufficient to limit maximum operating speed.

Chill-in and facility checkout efforts culminated in a successful low speed test, test number 124, on 20 February in which there were no automatic kills. All work after the helium leak-check in this phase was performed with LN_2 as the pumped fluid and ambient temperature GN_2 as the drive gas.

2.2.2 Series C

Test Series C was the first attempt at obtaining performance data from the OTV oxygen turbopump. Series C was further divided into Series C1 and C2. Series C1 consisted of operating the turbopump at five operating points using a GN_2 turbine drive, pumping LN_2. The successful completion of Series C1 qualified the turbopump for operation at high speed and off-design flow without mechanical difficulty. The total run time accumulated on the turbopump through Series C1 was 646 seconds.

With the success of Series C1, it was time to introduce liquid oxygen to the pump and bearings, and perform Series C2. Series C2 consisted of operating the turbopump at seven different operating points (Q/N) using a GN_2 turbine drive, pumping LOX. During the successful completion of Series C2, 748 seconds of run time were accumulated on the turbopump.

The change in pumped fluid from Series C1 to C2 led to a different mode of operation for the bearings in each Series. In Series C1 the hydrostatic bearings were pressurized from the bearing assist supply tank from 1200 psia to 3500 psia prior to shaft rotation. Since pump discharge pressure did not exceed this supply pressure, the bearings were fed from the external pressure source throughout the series. The change to LOX as the pumped fluid in Series C2 resulted in pump discharge pressures high enough to properly supply the bearings. Because of this, the external pressure source was decreased to 500 psia at the start of each Series C2 run. During each run the pump discharge pressure exceeded 500 psia and the pump discharge flow supplied the bearings with propellant. This self pressurization continued throughout the run.

Among the accomplishments of the successful Series C2 were verification of bearing system function, collection of LOX turbopump performance data, and accumulation of run time exceeding that required. Series C2 was completed 4 March, 1989.

2.2.3 Test Series D

Utilizing the same propellants as Test Series C2, Series D consisted of six turbopump starts, accumulating 87 seconds of run time. The reduction of bearing assist pressure to 50-55 psia from 500 psia at the start of each run distinguished Series D from Series C2. This reduction of bearing assist pressure to the range of pump suction pressure resulted in the pump discharge flow feeding the bearings from start to finish of each run.

Six of these "unassisted" starts were performed instead of the single one planned because automatic kills were encountered on the first five runs. These kills were due to low pump suction pressure which was, in turn, caused by the unsupported rotor "sticking" then suddenly rotating as the turbine inlet pressure was increased. The "sticking" could have been due to a number of factors: 1) misalignment of the shaft causing binding that exceeded normal breakaway torque, 2) a particle caught between the bearing and the shaft, or 3) a galled bearing surface contacting the shaft. Its practical effect is to increase the threshold pressure for shaft rotation without bearing assist.

Test Series D demonstrated the turbopump's ability to start without an external bearing supply.

2.2.4 Test Series E

It was in Test Series E testing that an ambient temperature gaseous oxygen turbine drive was first used on the OTV oxygen turbopump. As in Series D, all testing in Series E was performed with the pump operating at its design Q/N value. A total of 787 seconds of turbopump operating time was accumulated during Series E, divided between Series E1 and Series E2.

Test Series E1 consisted of operating the turbopump for the first time with GOX as the drive gas, pumping LOX. While accumulating approximately seven minutes of run time during this series, the turbopump utilized a 500 psia bearing assist pressure for each of the seven "assisted" starts. Series E1 was performed prior to Series D as it was considered to be potentially less risky than Series D.

Test Series E2, GOX/LOX turbopump operation with unassisted bearing starts, was performed last as it was considered to be the highest risk series of the program. Not only was the oxygen in all operating sections of the TPA, but the bearing and shaft surfaces would generate some frictional heating during the rubbing start. The pump operated at design Q/N while accumulating over six minutes of run time and eight more unassisted starts. Test Series E2 ended with the successful completion of Test 190 on 21 March 1989. This brought the test program to a close.

Table 2.2-1 is a listing of sample data at a single time slice for each critical test. The table was originally compiled from quick look data with later corrections from calibrated data where necessary. Total TPA run time as given in the summary included time from the checkout tests not given in this table. Also, the highest TPA speed was recorded on Test 135 where a decay in suction pressure during a kill allowed a brief overspeed to 80,000 rpm. The tests were numbered in the order performed. The "Comments" column denotes the significance of each test, including test series, turbine gas and pump/bearing fluid.

Throughout Test Series C, D and E, the OTV oxygen turbopump was successfully operated for 2268 seconds (counting all rotating time) with a total of fourteen starts without the bearing assist system.

Table 2.2-1. OTV OTPA Testing Summary of Testing Through 3/21/89

TEST NO.	TOTAL RUN TIME (SEC)	TOTAL TIME AT SPEED (SEC)	MAX SHAFT SPEED (RPM)	PUMP DISCH PRESS (PSIA)	BRG INLET PRESS (PSIA)	TURB INLET PRESS (PSIA)	PUMP DISCH FLOW (GPM)	Q/N % OF DESIGN	COMMENTS
1 – 21, 23									CHILL IN AND SEQUENCING TESTS
22, 101 – 123, 126 – 132, 134 – 137, 139 – 141, 143, 145 – 151, 153, 155, 159, 162, 166, 168, 184									SPIN ATTEMPTS: KILLS RELATING TO EITHER (1) FACILITY PROBLEMS OR (2) TURBINE INLET PRESSURE RAMP RATES NOT MATCHING KILL LIMIT TIME SETTINGS
124	68	36	22,000	336	1240	271	11.6	100	FIRST RUN WITHOUT AUTOKILL SHUTDOWN
125	49	35	32,500	688	1217	612	16.6	100	COMPLETES C1.1; GN2/LN2
133	66	45	68,000	2860	3400	2980	32.9	100	COMPLETES C1.2; GN2/LN2
138	26	9	67,000	2700	3000	3000	40.6	120	COMPLETES C1.3; GN2/LN2
142	62	52	53,500	1720	3350	1520	14.4	60	COMPLETES C1.4; GN2/LN2
144	64	55	32,500	640	2300	490	6.1	40	COMPLETES C1.5; GN2/LN2
152	73	63	40,000	1425	1300	1520	27.4	100	COMPLETES C2.1; GN2/LO2
154	82	69	50,000	2330	2200	2300	25.1	60	COMPLETES C2.5; GN2/LO2
156	76	71	31,500	950	875	825	11.9	40	COMPLETES C2.6; GN2/LO2
157	49	33	64,000	3300	3170	4000	44.6	100	RUN #1, C2.2; GN2/LO2
158	39	24	65,800	3480	3340	4250	45.8	100	RUN #2, C2.2; GN2/LO2
160	49	35	67,000	3550	3350	4430	47.5	100	RUN #3, C2.2; GN2/LO2
161	32	21	66,400	3670	3510	4480	47.1	100	RUN #4, C2.2; GN2/LO2
163	47	33	64,000	3830	3660	4680	47.8	100	RUN #5, C2.2; GN2/LO2
164	40	27	68,000	3300	3170	4690	52.9	120	COMPLETES C2.4; GN2/LO2
165	48	34	69,800	4015	3900	4829	46.6	90	COMPLETES C2.7; GN2/LO2
167	81	56	62,200	3340	3240	3630	37.6	80	COMPLETES C2.3; GN2/LO2

Table 2.2-1. OTV OTPA Testing Summary of Testing Through 3/21/89 cont.

TEST NO.	TOTAL RUN TIME (SEC)	TOTAL TIME AT SPEED (SEC)	MAX SHAFT SPEED (RPM)	PUMP DISCH PRESS (PSIA)	BRG INLET PRESS (PSIA)	TURB INLET PRESS (PSIA)	PUMP DISCH FLOW (GPM)	Q/N % OF DESIGN	COMMENTS
169	81	78	40,600	1365	1300	1570	27.3	100	COMPLETES E1.1; GO2/LO2
170	77	69	61,800	3170	3020	3915	41.6	100	RUN #1, E1.2; GO2/LO2
171	48	41	61,980	3185	3036	3925	41.6	100	RUN #2, E1.2; GO2/LO2
172	23	16	62,150	3171	2997	3930	42.0	100	RUN #3, E1.2; GO2/LO2
173	24	17	61,880	3166	2983	3932	41.8	100	RUN #4, E1.2; GO2/LO2
174	81	74	61,520	3164	3024	3933	41.7	100	RUN #5, E1.2; GO2/LO2
175	82	74	61,790	3165	3010	3923	41.5	100	RUN #6, E1.2; GO2/LO2
176	2	2	31,510	855	804	926	21.4	100	START #1, D; GN2/LO2
177	2	2	26,850	919	872	1006	22.2	100	START #2, D; GN2/LO2
178	1	1	17,010	264	176	255	16.3	100	START #3, D; GN2/LO2
179	1	1	15,640	177	122	284	14.4	100	START #4, D; GN2/LO2
180	1	1	19,450	435	402	275	14.6	100	START #5, D; GN2/LO2
181	80	72	41,460	1434	1352	1573	28.0	100	START #6, D; GN2/LO2
182	2	2	26,650	600	565	622	18.4	100	START #1, E2; GO2/LO2
183	82	72	61,920	3128	3068	3937	42.6	100	START #2, E2; GO2/LO2
185	82	75	61,992	3139	2957	3951	42.4	100	START #3, E2; GO2/LO2
186	23	16	61,228	3049	2883	3827	41.6	100	START #4, E2; GO2/LO2
187	81	75	62,017	3168	2987	3949	42.2	100	START #5, E2; GO2/LO2
188	1	1	20,950	419	406	336	15.3	100	START #6, E2; GO2/LO2
189	1	1	21,030	480	454	283	13.1	100	START #7, E2; GO2/LO2
190	99	93	61,880	3168	2988	3958	42.3	100	START #8, E2; GO2/LO2

3.0 DISCUSSION OF RESULTS

3.1 OVERALL TURBOPUMP PERFORMANCE

The completion of Test Series "C", "D", and "E" has succeeded in demonstrating the OTV Oxygen Turbopump to be mechanically sound while being operated to the maximum limits of the testing facility. Testing ranged over a pump Q/N range of 40 to 120% of design. A maximum steady state speed of 69,800 rpm was reached when pumping liquid oxygen, which is 93% of the nominal design speed of 75,000 rpm. A maximum discharge pressure of 4015 psia resulted at that same time, which is 88% of the nominal design pressure of 4575 psia. A maximum turbine inlet pressure 4829 psia was required to achieve this highest demonstrated power point, which is 16% greater than design pressure. At the conclusion of 38 successful data productive tests, the turbopump was found to be in operational condition with minor evidence of wear to the bearing surface plating.

During these test series the turbopump operated with an apparent cyclic axial shaft motion. This anomaly was detected by the axial distance probe and was basically undetected in the radial "Y" distance detector with only a small response in the axial "Z" direction. This axial motion was characterized by a constant frequency of approximately 10,000 cpm. The amplitude was also constant at approximately ± .0005 in. "Waterfall" plots of the axial distance detector for two typical tests are given in Figure 3.1-1 and Figure 3.1-2. The liquid nitrogen pumping test, Figure 3.1-1, used a separate pressurized tank to feed the bearings. The second plot documents the same phenomenon extending right up to the last revolution (see the time line marked F.S.2, fireswitch two) at the termination of the run period (the top time vs frequency plot, Figure 3.1-2).

The predominant displacement peak starting at zero progressing upwards to the right is the shaft speed signal with the amplitude derived from the .002 inch step at the end of the shaft. The vertical predominant peak is the 10,000 cpm frequency (~170 Hz)axial displacement and anomaly. Figure 3.1-1 shows the tank fed bearing system operating with liquid nitrogen. Figure 3.1-2 illustrates the pump fed bearing system operating with LOX showing the same phenomena.

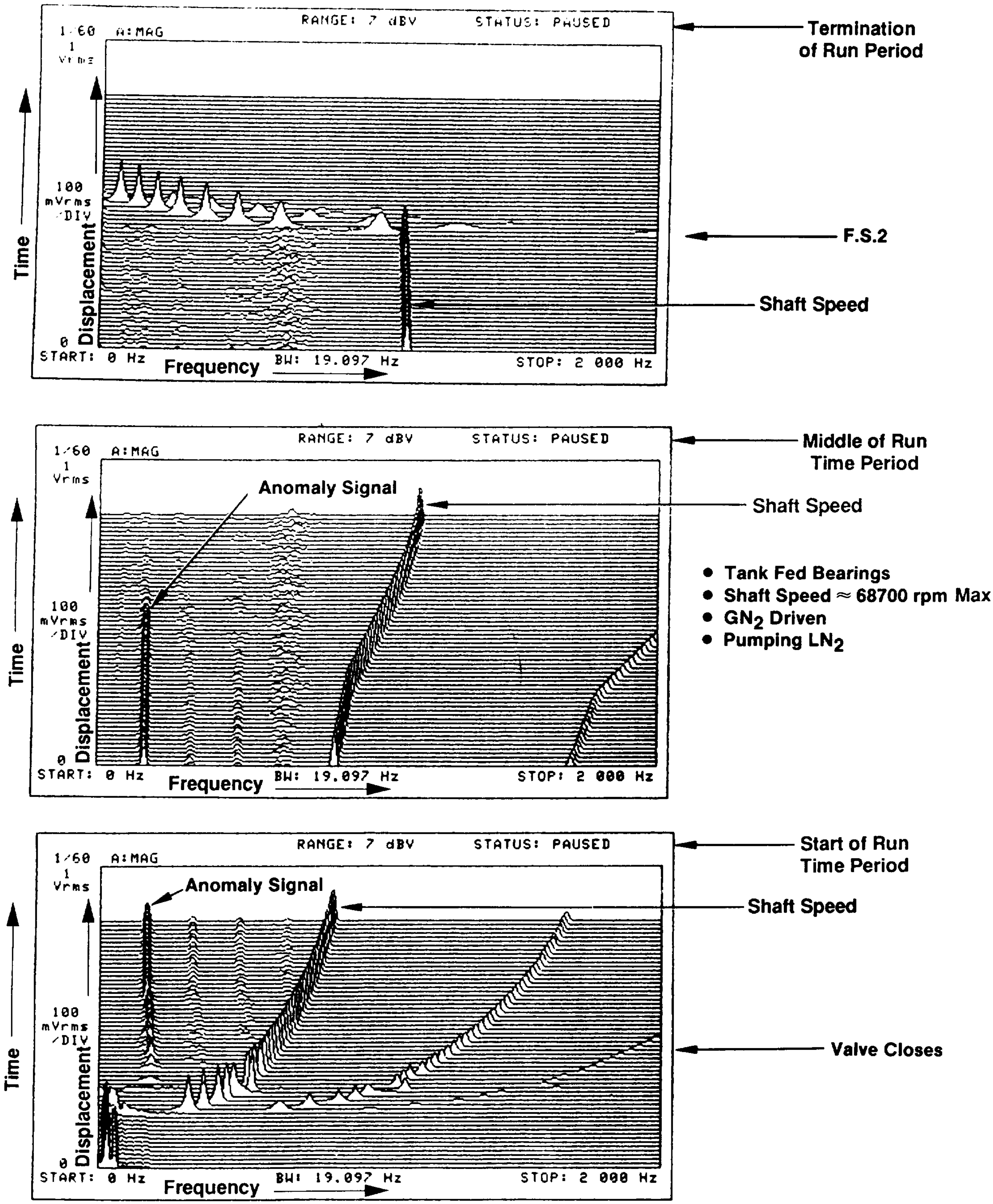

Figure 3.1-1. "Waterfall" Plot for Test 133 Probe Signal NT-Z

3.1 cont

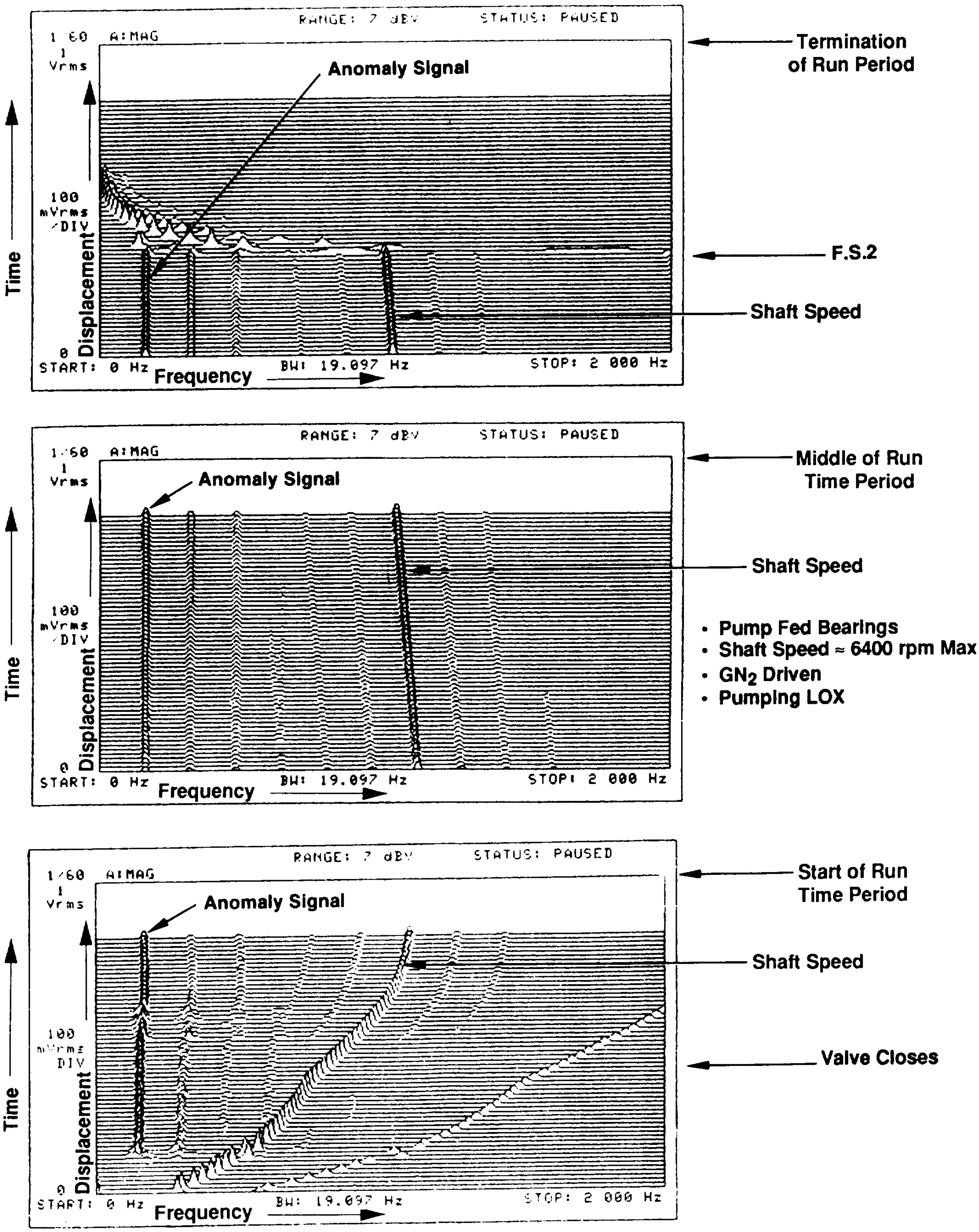

Figure 3.1-2. "Waterfall" Plot for Test 163 Probe Signal NT-Z

The first diagnosis related the closing of the pump discharge flow meter bypass valve with the initiation of the axial displacement signal. Closing of this valve prior to the start of the unassisted bearing transient test, corresponded to the appearance of the displacement signals at about the same shaft speed. Further analysis showed the inducer discharge pressure and the pump inlet pressure to a lesser degree have the same cyclic frequency as the shaft axial motion. Since this is the pressure going into the first impeller it is assumed the pressure in this impeller also experiences the cyclic frequency which is the driving force for the rotating assembly. Other pressure locations did not show this frequency possibly because of lower response rate passages. Additional analysis is recommended prior to testing in the same facility to identify the initial source of the pressure oscillation that causes the rotating assembly axial motion. At this writing it is considered a facility related phenomenon.

The overall TPA efficiency can be determined directly with currently available measurements. The design TPA efficiency is the product of the design values for turbine efficiency (0.67), the pump efficiency (0.59) and the tare efficiency (0.97) for a value of 0.38. For the five 100% Q/N design point tests the average measured value (determined as described below) is 0.31. This lower than design value indicates that either the turbine performance or pump performance or both are below design but does not provide any information for determining which of these possibilities is correct. It should be noted that the pump performance (efficiency) is charged with the bearing and other recirculating flow losses. The recirculating flow losses are much greater than expected.

Measurements are available to allow direct calculation of only the overall TPA efficiency. This quantity is determined by dividing the delivered fluid power at the pump discharge by the turbine isentropic available power. This overall quantity can also be expressed as the product of the turbine efficiency, the pump efficiency and the mechanical efficiency (which accounts for tare losses). In the absence of individual pump and/or turbine test data, the estimation of how this overall value is split up between these different components involves a large amount of subjectivity guided by past experience and knowledge of general pump and turbine characteristics. If separate turbine and/or pump tests had been conducted, characterization of individual component performance would be much more direct and accurate. This is the justification for the data reduction and analysis procedure described in Sections 3.2 and 3.3. It represents a best estimate of individual pump and turbine performance given the current test data constraints.

3.2 PUMP PERFORMANCE

This section summarizes the OTV LOX pump non-cavitating performance test results. Five test series whose test objectives were outlined in Reference 7, were successfully completed. Raw test data, such as pump volumetric flow rates, static pressures and temperatures measured at strategic locations on the test apparatus were recorded many times per second during the test. These raw data were later reduced to engineering units and combined to calculate TPA performance parameters using a data reduction computer program.

Data reduction results of ten tests were reviewed to verify the TPA performance. Test No. 183 of series E2 which has LOX pump flow at 99.8% of the design Q/N and GOX turbine fluid was selected to demonstrate the pump design point operating condition. Q/N is defined as the overall pump delivered volumetric flow rate in gal/min divided by the TPA rotating speed in rpm. Five tests in test series C2 (test No. 154, 156, 165, 167, 164) with GN_2 turbine fluid were selected to represent the off design conditions from 47% to 128% of the design Q/N. Four tests in test series D (test No. 171, 172, 173, 174) at about 100% Q/N and GN_2 turbine fluid without bearing assist systems were also included in this section to verify the repeatability of the test results. Boost pump flow is charged to pump recirculating flows and is, therefore, not considered as part of the overall pump delivered flow.

The data reduction equations which calculated pump flow rate, head rise, overall efficiency and pump horsepower were entered into the computer program to facilitate the data reduction process. Fluid properties, such as density and vapor pressure of the liquid oxygen, were taken from the fluid properties tables (Ref. 8) as a function of local temperature and pressure at the measuring station. Pump overall head rise (H in feet of fluid) was calculated from the total pressure difference between pump inlet and outlet. The total pressure is the sum of the measured static pressure plus the dynamic pressure calculated from the flow rate and pipe area at the measuring station. A method to calculate overall TPA efficiency from available test data is given in Table 3.2-1. This method was used in the data reduction program.

Each test case was run at near constant speed and pump flow rate. Data points were selected at a selected time instant after the shaft speed reached steady state. A portion of Test No. 183 data reduction computer print out is shown in Table 3.2-2 for example. It lists several time points around the selected design point, i.e. 183.023, where the shaft speed, NT-Z, was almost constant at 60626 rpm. Pump performance parameters, i.e., normalized head (H/N**2) and overall pump efficiency vs. normalized flow (Q/N), are better summarized in Figure 3.2-1. It compares the test results from test series E2, D and C2 against the original predicted curves. The slightly higher data points compared with the design curve is due to the increased impeller tip diameter for additional head margin (see Ref. 9). The OTV TPA using propellant fluid bearings has a complicated internal recirculation flow network. At off design Q/N conditions, the slope of the head curve can be offset from the predication due to different internal seal flow. The small variation might be a factor at the 128% Q/N point noted on Figure 3.2-1.

A corrected pump overall efficiency is established by correcting the pump flow rate for the excessive bearing flow rates. At the design operating point, the measured bearing cooling flow rates are about double the design value. These higher measured bearing coolant flow rates are believed to be caused by the internal leakages across the pump housing piston ring seals between the 2nd stage inlet, pump bearing supply inlet, turbine bearing supply and bearing discharge. The pump volumetric efficiency, which is a part of the overall pump efficiency ($Eff_{pump} = Eff_{hyd} * Eff_{vol} * Eff_{dsk\ windage}$), needed to be adjusted from the original design value. This adjustment will decrease pump overall efficiency from 59% to 48% at the design point. The pump off-design efficiencies were back calculated from the

TABLE 3.2-1. Pumping System Calculated Efficiency (Ref. 13)

$$EFF_p = \frac{\text{delivered fluid horsepower}}{\text{shaft input horsepower}} = \text{Total TPA Efficiency}$$

delivered fluid horsepower = (Ç*Q*H)/550/448.8

Ç = average fluid density through pump (lbm/ft**3)

Q = pump discharge volumetric flow rate (gpm)

H = pump total head rise (ft)

shaft input horsepower (not including tare torque) =
delivered pump fluid power + boost pump turbine fluid power +
bearing supply fluid power + friction power sensed as heat

boost pump turbine + bearing fluid power =

$$(\text{Ç}_{bp} * Q_{bpt} * H_{ind} + \text{Ç}_{out} * (Q_{pbi} + Q_{tbi}) * H)/550/448.8$$

friction power sensed as heat = delivered flow fluid losses +
pump bearing fluid losses +turbine bearing fluid losses =

$$(\text{Ç}_{out} * Q * C_p * (T_{p\,out} - T_{ind\,out}) + \text{Ç}_{pb} * Q_{pbi} * C_p * (T_{p\,out} - T_{pi}) + \text{Ç}_{ind} * Q_i * C_p * (T_{ind\,out} - T_{ind\,i}) + \text{Ç}_{tb} * Q_{tbi} * C_p * (T_{p\,out} - T_{p\,i})) * (3600/2545/448.8)$$

<u>Symbols:</u>

- bp = boost pump
- t = turbine
- p = pump
- ind = pump inducer
- i = inlet
- o = outlet
- pb = pump bearing supply
- tb = turbine bearing supply
- T = fluid temperature (°F)
- C_p = fluid specific heat (btu/lbm/F)

TABLE 3.2-2. Data Reduction – Test 183, Sheet 1 of 3

FILE HOTV1

OTV OXYGEN TPA PROGRAM RECORDED DATA TEST NO. 2459-D02-OP-183
TEST DATE 03-20-89 TIME 1913 HOURS DURATION 82.161 SECONDS
PERFORMANCE JOB 692 02/89 NEG. FLOWS QUESTIONABLE; OUTSIDE CJ LIMITS

J0014
04-19-89
10:51:42

RUN,DATA-PT		183.014	183.015	183.016	183.017	183.018	183.019	183.020
0 START TIME		15.0000	16.0000	18.0000	20.0000	22.0000	24.0000	26.0000
1 STOP TIME		16.0000	18.0000	20.0000	22.0000	24.0000	26.0000	28.0000
2 TIME HH,MM		19.1400	19.1400	19.1400	19.1400	19.1400	19.1400	19.1404
3 FMPD-E	GPM	21.7209	21.8249	21.8203	21.8352	21.8154	21.8064	21.7994
4 FMPD-W	GPM	19.9066	20.0004	20.0204	19.9935	20.0107	20.0007	19.9938
5 FMTHI	GPM	3.05198	3.06970	3.07528	3.08240	3.08510	3.08936	3.09170
6 FMPHI	GPM	11.0340	11.0877	11.0769	11.0557	11.0453	11.0365	11.0322
7 FMPHE	GPM	11.9016	12.0093	12.0200	12.0172	12.0327	12.0436	12.0604
8 FMSI	GPM	43.3866	43.5165	43.5576	43.5181	43.4760	43.3921	43.3262
9 FMHPD	GPM	2.93618	2.88438	2.84812	2.80315	2.72493	2.66472	2.61853
10 UAPUT	CTS ADJ	-1657.5	-1657.4	-1657.5	-1657.7	-1657.4	-1657.5	-1657.5
11 PPHI	PSIA	2836.33	2857.06	2854.79	2848.01	2843.71	2837.77	2832.41
12 PTHI	PSIA	2954.54	2976.20	2973.26	2965.63	2960.80	2954.52	2948.97
13 PTD-W	PSIA	1717.41	1734.59	1736.74	1737.25	1737.26	1735.43	1734.26
14 PTD-E	PSIA	1713.28	1730.61	1735.54	1734.47	1734.78	1733.24	1732.23
15 PTDH	PSIA	1752.67	1770.11	1775.05	1773.94	1774.26	1772.06	1771.67
16 PIPI	PSIA	580.341	584.770	584.442	583.546	582.716	581.904	581.093
17 PHF	PSIA	252.938	254.314	253.919	253.023	252.558	251.802	251.437
18 PIT2	PSIA	1094.65	1103.00	1101.62	1097.39	1095.40	1093.29	1091.41
19 PTHC	PSIA	1754.78	1772.09	1776.92	1775.73	1776.10	1774.42	1773.38
20 PS	PSIA	60.5147	60.7732	60.8334	60.9195	60.6226	60.5754	60.6559
21 PD2-W	PSIA	3011.63	3034.59	3031.82	3023.92	3018.85	3012.01	3006.31
22 PD2-E	PSIA	3020.38	3043.11	3039.87	3031.60	3026.72	3019.85	3014.17
23 PPP1	PSIA	1159.19	1167.67	1166.17	1163.48	1161.47	1158.97	1157.12
24 PPP2	PSIA	1211.21	1219.98	1217.60	1213.63	1211.30	1208.48	1206.36
25 PPP3	PSIA	1139.11	1147.78	1146.80	1143.49	1141.97	1138.93	1137.28
26 PPP4	PSIA	1161.99	1170.66	1168.51	1164.65	1162.56	1159.51	1157.71
27 PHPD	PSIA	243.582	244.922	244.675	244.445	243.948	243.456	243.271
28 PTI	PSIA	3783.95	3819.01	3821.53	3814.78	3812.67	3807.49	3804.14
29 PHPH	PSIA	252.883	254.206	253.557	253.067	252.773	252.265	251.818
30 PUTG	PSIA	5326.48	5249.21	5148.02	5049.38	4952.47	4857.31	4763.52
31 PUTR	PSIA	581.739	582.789	584.376	585.439	586.614	587.901	589.333
32 PTIU	PSIA	5304.68	5228.13	5127.00	5028.42	4931.78	4836.37	4742.17
33 DPTIU	PSI	34.9063	34.6769	34.3855	34.1258	33.8818	33.6526	33.4300
34 PUTS	PSIA	67.9782	67.9341	67.8356	67.7609	67.6748	67.5820	67.5487
35 PPOT	PSIA	83.8950	83.8993	83.6749	83.7780	83.9810	83.7447	83.8772
36 TTH7	DEG F	-76.913	-67.576	-58.499	-52.401	-48.396	-45.815	-44.205
37 TBI	DEG F	-285.26	-284.27	-283.03	-281.69	-280.43	-279.58	-279.05
38 TTBH8	DEG F	-256.83	-254.15	-251.01	-248.00	-245.29	-242.60	-240.29
39 TTIOU	DEG F	64.1611	62.7819	61.0174	59.2035	57.3565	55.3982	53.4139
40 TPBE	DEG F	-272.53	-271.49	-270.21	-268.95	-267.81	-266.96	-266.48
41 THX9	DEG F	-285.66	-285.02	-283.98	-282.88	-281.80	-280.62	-279.60
42 TTI	DEG F	51.4957	51.5262	50.7452	49.7694	48.7072	47.5878	46.3803
43 TTCH	DEG F	-35.859	-35.124	-34.968	-35.255	-35.659	-36.337	-37.136
44 TTEUD	DEG F	-42.646	-41.970	-41.874	-42.225	-42.764	-43.417	-44.211
45 TPBI	DEG F	-284.43	-283.41	-282.10	-280.77	-279.63	-278.88	-278.51
46 TTIPH10	DEG F	-269.45	-269.72	-270.12	-270.47	-270.82	-271.07	-271.27
47 TUVS	DEG F	-247.87	-247.35	-246.05	-245.64	-244.58	-243.54	-241.42
48 NT-Z	RPM	60787.4	61099.2	61146.3	61147.4	61153.2	61131.0	61099.2
49 NT-X	RPM	7573.34	39456.0	61118.1	72130.4	82255.8	83754.9	85323.3
50 TPD1	DEG F	-243.90	-243.49	-242.86	-242.18	-241.56	-240.98	-240.64

RUN,DATA-PT		183.021	183.022	183.023	183.024	183.025	183.026
0 START TIME		28.0000	30.0000	35.0000	40.0000	42.0000	44.0000
1 STOP TIME		30.0000	35.0000	40.0000	42.0000	44.0000	46.0000
2 TIME HH,MM		19.1500	19.1500	19.1500	19.1500	19.1500	19.1500
3 FMPD-E	GPM	21.7827	21.7340	21.6638	21.6022	21.5593	21.5000
4 FMPD-W	GPM	19.9766	19.9386	19.8797	19.8163	19.7974	19.7380
5 FMTHI	GPM	3.08938	3.08464	3.07456	3.06089	3.05338	3.04731
6 FMPHI	GPM	11.0279	11.0038	10.9485	10.8666	10.8209	10.7849
7 FMPHE	GPM	12.0701	12.0569	11.9967	11.8991	11.8427	11.7945
8 FMSI	GPM	43.2524	43.1314	43.0059	42.9076	42.8638	42.7800
9 FMHPD	GPM	2.57140	2.54355	2.54497	2.57227	2.59366	2.61115
10 UAPUT	CTS ADJ	-1657.5	-1657.8	-1657.4	-1657.3	-1656.8	-1657.0
11 PPHI	PSIA	2825.51	2811.18	2787.15	2760.85	2747.38	2734.66
12 PTHI	PSIA	2941.80	2927.21	2902.02	2874.17	2859.63	2846.05
13 PTD-W	PSIA	1732.36	1726.11	1713.80	1700.05	1692.38	1684.58
14 PTD-E	PSIA	1730.20	1724.12	1711.79	1698.00	1690.41	1682.57
15 PTDH	PSIA	1769.68	1763.42	1751.20	1737.14	1729.01	1721.03
16 PIPI	PSIA	579.984	576.832	571.946	567.197	564.297	562.328
17 PHF	PSIA	250.838	249.906	248.128	245.795	244.860	243.695
18 PIT2	PSIA	1089.97	1084.88	1075.97	1067.30	1061.06	1056.27
19 PTHC	PSIA	1771.49	1765.28	1753.16	1739.32	1731.52	1723.64
20 PS	PSIA	60.2437	60.4222	60.3000	60.1534	60.3444	59.8897
21 PD2-W	PSIA	2999.45	2984.36	2956.47	2930.24	2915.39	2901.69
22 PD2-E	PSIA	3007.51	2992.53	2966.79	2936.23	2923.82	2909.81
23 PPP1	PSIA	1154.57	1148.59	1139.01	1128.22	1122.76	1117.50
24 PPP2	PSIA	1203.68	1197.90	1188.28	1177.34	1171.90	1166.51
25 PPP3	PSIA	1134.81	1129.27	1119.70	1109.42	1103.84	1098.82
26 PPP4	PSIA	1155.17	1149.46	1140.39	1129.94	1124.41	1119.33
27 PHPD	PSIA	242.558	242.009	240.463	238.225	237.571	236.193
28 PTI	PSIA	3798.53	3784.29	3757.55	3726.42	3710.11	3692.24
29 PHPH	PSIA	251.352	250.371	248.670	246.685	245.742	244.720
30 PUTG	PSIA	4671.58	4515.77	4303.46	4161.67	4083.68	4007.62
31 PUTR	PSIA	590.551	592.755	595.999	598.114	599.089	600.276
32 PTIU	PSIA	4650.22	4494.55	4281.95	4140.41	4062.26	3986.05
33 DPTIU	PSI	33.2148	32.8579	32.3969	32.1155	31.9729	31.8666
34 PUTS	PSIA	67.4823	67.3177	67.1526	66.9966	66.9004	66.8698
35 PPOT	PSIA	83.7941	83.8170	83.8237	83.7909	83.5997	83.7919
36 TTH7	DEG F	-43.388	-43.137	-44.185	-45.361	-46.014	-46.841
37 TBI	DEG F	-278.86	-278.72	-278.76	-278.85	-278.93	-279.07
38 TTBH8	DEG F	-238.31	-235.69	-233.31	-232.27	-231.80	-231.48
39 TTIOU	DEG F	51.4452	47.9830	42.8606	39.2651	37.1883	35.1195
40 TPBE	DEG F	-266.24	-266.21	-266.33	-266.50	-266.64	-266.75
41 THX9	DEG F	-278.72	-277.65	-276.80	-276.57	-276.44	-276.48
42 TTI	DEG F	45.1312	42.8893	39.5676	37.0979	35.7131	34.3158
43 TTCH	DEG F	-37.994	-39.690	-42.361	-44.364	-45.566	-46.680
44 TTEUD	DEG F	-45.104	-46.764	-49.333	-51.326	-52.455	-53.655
45 TPBI	DEG F	-278.37	-278.39	-278.55	-278.70	-278.77	-278.90
46 TTIPH10	DEG F	-271.41	-271.57	-271.59	-271.54	-271.51	-271.45
47 TUVS	DEG F	-239.92	-239.29	-238.16	-236.63	-236.05	-235.36
48 NT-Z	RPM	61034.7	60879.1	60626.1	60363.0	60206.7	60048.2
49 NT-X	RPM	86677.6	86279.9	85436.5	83355.5	81925.8	82222.9
50 TPD1	DEG F	-240.38	-240.12	-239.93	-239.82	-239.79	-239.77

TABLE 3.2-2. Data Reduction – Test 183, Sheet 2of 3

FILE MOTV1

OTV OXYGEN TPA PROGRAM RECORDED DATA TEST NO. 2459-D02-OP-183
TEST DATE 03-20-89 TIME 1913 HOURS DURATION 82.161 SECONDS
PERFORMANCE JOB 892 02/89 NEG. FLOWS QUESTIONABLE; OUTSIDE CJ LIMITS

J0014
04-19-89
10:51:42

	RUN.DATA-PT		183.014	183.015	183.016	183.017	183.018	183.019	183.020	183.021	183.022	183.023	183.024	183.025	183.026
51	TPD2	DEG F	-270.07	-270.07	-270.00	-270.03	-270.06	-270.03	-270.05	-270.03	-270.06	-270.06	-270.04	-270.05	-270.05
52	TBPD	DEG F	-253.44	-252.38	-251.63	-251.54	-251.27	-250.91	-250.62	-250.43	-250.15	-249.57	-249.34	-249.33	-249.35
53	TS	DEG F	-298.02	-297.08	-295.79	-294.45	-293.36	-292.62	-292.25	-292.12	-292.13	-292.18	-292.21	-292.21	-292.27
54	TPD2-E	DEG F	-255.57	-254.74	-253.60	-252.42	-251.33	-250.51	-249.93	-249.59	-249.28	-249.09	-249.08	-249.00	-249.08
55	TPD2-W	DEG F	-251.26	-250.61	-249.69	-248.67	-247.73	-247.04	-246.57	-246.27	-245.97	-245.67	-245.66	-245.65	-245.62
98	MIDPT	SECONDS	15.5000	17.0000	19.0000	21.0000	23.0000	25.0000	27.0000	29.0000	32.5000	37.5000	41.0000	43.0000	45.0000
102	RHOIN	LB/CUFT	71.3946	71.2334	71.0099	70.7759	70.5863	70.4561	70.3906	70.3674	70.3690	70.3786	70.3836	70.3833	70.3944
103	DIN	IN	1.76000	1.76000	1.76000	1.76000	1.76000	1.76000	1.76000	1.76000	1.76000	1.76000	1.76000	1.76000	1.76000
104	RHOOUT	LB/CUFT	67.1674	67.0782	66.9145	66.7326	66.5670	66.4395	66.3508	66.2911	66.2249	66.1548	66.1173	66.0928	66.0799
105	PIN	PSIA	60.7672	61.0266	61.0865	61.1714	60.8733	60.8247	60.9041	60.4910	60.6682	60.5445	60.3968	60.5874	60.1317
106	DOUT	IN	.620000	.620000	.620000	.620000	.620000	.620000	.620000	.620000	.620000	.620000	.620000	.620000	.620000
107	DELTAPO	PSI	2969.44	2992.14	2989.05	2980.83	2976.12	2969.27	2963.47	2957.09	2941.81	2916.01	2887.68	2872.81	2859.33
109	DELTAHI	FT	413.250	416.739	416.739	417.008	418.399	418.416	417.892	418.070	415.581	412.002	407.787	405.153	403.786
110	POUT	PSIA	3030.21	3053.17	3050.13	3042.01	3036.99	3030.10	3024.38	3017.58	3002.48	2976.56	2948.07	2933.40	2919.46
111	NSI		4368.49	4369.83	4375.26	4371.24	4358.63	4352.72	4351.24	4341.56	4343.84	4347.59	4357.25	4364.92	4360.21
112	PVI	PSIA	14.1140	14.9052	16.0523	17.3194	18.3941	19.1595	19.5533	19.6916	19.6828	19.6239	19.5925	19.5957	19.5258
114	NPSPI		46.6531	46.1214	45.0342	43.8520	42.4792	41.6652	41.3508	40.7994	40.9854	40.9206	40.8043	40.9916	40.6059
115	NPSPT(D)		563.245	563.466	563.257	563.073	562.685	562.531	562.494	562.326	562.293	562.605	563.332	563.554	563.241
116	NPSHI		94.0975	93.2355	91.3242	89.2209	86.6599	85.1564	84.5924	83.4921	83.8706	83.7267	83.4828	83.8665	83.0642
117	NPSHPT		434.817	433.991	427.793	421.742	416.353	411.636	408.397	406.306	404.025	400.836	397.324	395.888	394.175
118	SI		13252.8	13433.1	13660.4	13895.1	14196.5	14364.9	14418.2	14532.8	14426.4	14364.0	14316.6	14223.3	14274.5
119	SPT		4060.18	4096.00	4147.56	4192.47	4235.38	4268.93	4291.04	4301.63	4303.89	4304.79	4307.79	4304.84	4302.07
120	RHOPMI	LB/CUFT	71.7149	71.5806	71.3816	71.1766	71.0017	70.8850	70.8240	70.7971	70.7870	70.7890	70.7871	70.7857	70.7942
121	RHOMP	LB/CUFT	67.0322	66.8388	66.5937	66.3518	66.1321	65.9709	65.8720	65.8254	65.8179	65.8376	65.8692	65.8943	65.9149
123	PVBP	PSIA	50.7280	53.0190	55.9747	58.9900	61.8131	63.9305	65.2478	65.8687	65.9503	65.6497	65.1830	64.8270	64.5309
124	RHOPME	LB/CUFT	67.0322	66.8389	66.5942	66.3517	66.1318	65.9702	65.8714	65.8246	65.8172	65.8368	65.8679	65.8930	65.9134
125	HPLOSS		198.788	199.009	197.834	196.045	195.273	194.937	195.239	195.688	196.101	196.114	195.159	194.655	194.114
127	EPAP		.260193	.262447	.263732	.264708	.265236	.265027	.264240	.263161	.261248	.258824	.257250	.256436	.255489
128	PMPD		6.23028	6.25126	6.23830	6.21456	6.20374	6.19904	6.17872	6.16816	6.14921	6.12367	6.10179	6.09041	6.07176
129	QI/N * 1.E4	GPM/RPM	7.13743	7.12227	7.12350	7.11691	7.10936	7.09821	7.09113	7.08653	7.08477	7.09364	7.10826	7.11944	7.12428
130	QP/N * 1.E4	GPM/RPM	4.53114	4.52836	4.52824	4.52850	4.52891	4.52818	4.52858	4.52891	4.53097	4.53937	4.55428	4.56466	4.56397
131	PHO/NTSQ*1E6	FT/RPMSQ	1.67031	1.66896	1.66933	1.66972	1.67109	1.67159	1.67195	1.67289	1.67355	1.67349	1.67211	1.67245	1.67342
132	U	FT/SEC	353.558	355.372	355.646	355.652	355.686	355.557	355.372	354.997	354.092	352.620	351.090	350.181	349.259
133	DBAR	IN	1.33300	1.33300	1.33300	1.33300	1.33300	1.33300	1.33300	1.33300	1.33300	1.33300	1.33300	1.33300	1.33300
134	PHS		2.15896	2.15749	2.15292	2.15045	2.14887	2.14790	2.14720	2.14645	2.14599	2.14570	2.14515	2.14580	2.14537
135	CP PUMP		.405000	.405000	.405000	.405000	.405000	.405000	.405000	.405000	.405000	.405000	.405000	.405000	.405000
137	GAM TURBINE		1.37000	1.37000	1.37000	1.37000	1.37000	1.37000	1.37000	1.37000	1.37000	1.37000	1.37000	1.37000	1.37000
138	DHT	BTU/LB	19.0908	19.0767	19.0002	18.9364	18.8826	18.8310	18.7790	18.7249	18.6370	18.5109	18.4137	18.3689	18.3128
139	CPHI		977.617	977.257	975.296	973.708	972.272	970.943	969.601	968.204	965.928	962.655	960.125	958.957	957.490
142	W TURBINE		1.29608	1.29608	1.29608	1.29608	1.29608	1.29608	1.29608	1.29608	1.29608	1.29608	1.29608	1.29608	1.29608
143	WDOT	LB/SEC	4.61770	4.58628	4.54470	4.50571	4.46800	4.43174	4.39589	4.36061	4.30097	4.21998	4.16689	4.13818	4.11200
144	HPOIS	HP	46.2580	46.8445	46.8477	46.7364	46.6759	46.5424	46.4217	46.2627	45.9030	45.3675	44.8638	44.6102	44.2693
145	ETATPA		.370955	.378511	.385538	.387197	.391112	.394262	.397545	.400542	.404840	.410573	.413358	.414882	.415604
146	U/CPHI		.361653	.363642	.364654	.365255	.365829	.366197	.366513	.366655	.366582	.366300	.365671	.365169	.364765
147	WRTP		.027591	.027152	.026868	.026659	.026423	.026215	.025995	.025792	.025479	.025093	.024923	.024825	.024753
148	NPSPI(E)		202.406	201.441	197.835	194.329	191.211	188.563	186.819	185.731	184.667	183.265	181.746	181.158	180.431
149	FMPDT	GPM	41.8295	41.8253	41.8407	41.8287	41.8201	41.8071	41.7932	41.7593	41.6726	41.5435	41.4185	41.3566	41.2380
150	PU2	PSIA	3016.01	3038.85	3035.84	3027.76	3022.78	3015.93	3010.24	3003.48	2988.44	2962.63	2934.23	2919.60	2905.75
151	TPC	DEG R	206.256	206.996	208.022	209.123	210.141	210.899	211.417	211.743	212.046	212.289	212.304	212.344	212.318
153	CP TURBINE		.199000	.199000	.199000	.199000	.199000	.199000	.199000	.199000	.199000	.199000	.199000	.199000	.199000
154	DELTAHO		6171.96	6230.40	6241.43	6243.11	6249.37	6246.73	6241.56	6231.90	6202.62	6150.96	6092.64	6062.37	6034.01

TABLE 3.2-2. Data Reduction – Test 183, Sheet 3 of 3

FILE HOTV1

OTV OXYGEN TPA PROGRAM RECORDED DATA TEST NO. 2459-D02-OP-183
TEST DATE 03-20-89 TIME 1913 HOURS DURATION 82.161 SECONDS
PERFORMANCE JOB 892 02/89 NEG. FLOWS QUESTIONABLE; OUTSIDE CJ LIMITS

J0014
04-19-89
10:51:42

RUN.DATA-PT		183.014	183.015	183.016	183.017	183.018	183.019	183.020	183.021	183.022	183.023	183.024	183.025	183.026
155 RHOTBI	GPM	71.9370	71.8092	71.6232	71.4170	71.2261	71.0935	71.0091	70.9737	70.9399	70.9232	70.9118	70.9120	70.9200
156 HPHEAT		174.802	174.714	173.369	171.869	171.153	170.888	171.251	171.774	172.374	172.717	172.150	171.853	171.489
157 HPBLEED		23.9861	24.2953	24.2651	24.1767	24.1195	24.0488	23.9882	23.9138	23.7266	23.3967	23.0088	22.8018	22.6250
158 HPPT		69.9145	70.8143	70.7926	70.5989	70.4899	70.2932	70.1180	69.8898	69.3477	68.4845	67.5927	67.1315	66.6128
159 HPSF		268.702	269.823	268.426	266.644	265.763	265.250	265.357	265.578	265.448	264.599	262.751	261.787	260.727
160 HPPUMP		93.7452	94.9262	94.9324	94.7076	94.5860	94.3137	94.0701	93.7487	93.0254	91.9624	90.9809	90.4944	89.8010
161 HPTURB		96.6445	97.8621	97.8685	97.6367	97.5113	97.2306	96.9795	96.6482	95.9025	94.8065	93.7947	93.2932	92.5783
162 ETAS		.775018	.790741	.801240	.808890	.817078	.823643	.830510	.836778	.845807	.857994	.864190	.867640	.869132
163 C*		.650000	.650000	.650000	.650000	.650000	.650000	.650000	.650000	.650000	.650000	.650000	.650000	.650000
164 Y		.997957	.997921	.997897	.997872	.997846	.997819	.997790	.997761	.997708	.997628	.997568	.997533	.997494
165 BETA		.485800	.485800	.485800	.485800	.485800	.485800	.485800	.485800	.485800	.485800	.485800	.485800	.485800
166 HPPFL		46.2580	46.8445	46.8477	46.7364	46.6759	46.5424	46.4217	46.2627	45.9030	45.3675	44.8638	44.6102	44.2693
167 NRT		2688.64	2702.35	2706.50	2709.14	2712.23	2714.23	2716.06	2716.54	2715.66	2713.35	2708.28	2705.04	2701.73
168 ETAST		.751767	.767019	.777203	.784623	.792566	.798934	.805595	.811675	.820433	.832254	.838264	.841611	.843059
169 HPSFPD		93.7452	94.9262	94.9324	94.7076	94.5860	94.3137	94.0701	93.7487	93.0254	91.9624	90.9809	90.4944	89.8010
170 DELPB	PSI	2583.40	2602.74	2600.87	2594.99	2591.15	2585.97	2580.98	2574.67	2561.27	2539.02	2515.05	2502.52	2490.97
171 DELTB	PSI	1199.76	1204.11	1196.34	1189.90	1184.70	1180.10	1175.60	1170.31	1161.93	1148.86	1134.85	1128.11	1122.41
172 EFFPD		.493444	.493483	.493485	.493481	.493475	.493486	.493480	.493475	.493446	.493326	.493112	.492961	.492971
173 DURI	IN	.650000	.650000	.650000	.650000	.650000	.650000	.650000	.650000	.650000	.650000	.650000	.650000	.650000
174 RHO-WDOT	LB/CUFT	29.5082	29.3016	29.0178	28.7406	28.4666	28.1987	27.9305	27.6637	27.2074	26.5694	26.1352	25.8931	25.6537

turbine efficiency and the overall TPA efficiency (see turbine performance section for details). As shown in Figure 3.2-1, the adjusted efficiencies fit into a revised predicted efficiency curve. The lower efficiency calculated from last data is credited to the following three sources. First, the pump flow is not a fully adiabatic process. There are heat transfers between the turbine and the pump fluids, and some heat losses to the ambient. These heat exchanges were not considered in the data reduction calculation. Second, the calculation was based on a simplified internal recirculation flow model. The internal flows can not be verified with the external flow measurements available. Therefore significant uncertainty occurred from the leakage power loss calculation. Third, the pump discharge fluid temperatures were measured with the film RTD (Resistance Temperature Detector) attached on the pipe outside surface. Although this type of temperature measurement is very accurate and responsive, it is inappropriate to use the wall temperature as the inside fluid temperature without a correction during transient conditions.. The thermal power loss in the efficiency calculation may therefore have some error. For this TPA as tested, the efficiency corrected for bearing flow losses ("X" in Figure 3.2-1) are considered representative of the final pump efficiency.

In general, this series of tests demonstrated that the TPA can be operated close to the original design requirements. For the later TPA test series, the interstage data, such as pressure and temperature measurements in the external crossover pipes should be obtained to separate the pump stage performance. This can provide more detailed information about the multistage pump performance characteristics with hydrostatic bearings for future design improvements.

3.3 TURBINE PERFORMANCE

Turbine performance estimates were based in part on the pump shaft horsepower estimates presented in Section 3.2 of this report. Initially, the values for the pump shaft horsepower were added to tare horsepower estimates and divided by the ideal isentropic horsepower available to the turbine to define turbine efficiency. However, when compared to the design turbine efficiency vs. U/Co curve, (Reference 10), these data did not show the typical parabolic shape that is to be expected (Ref. 1). Upon examination of the pump data, as described in the Pump

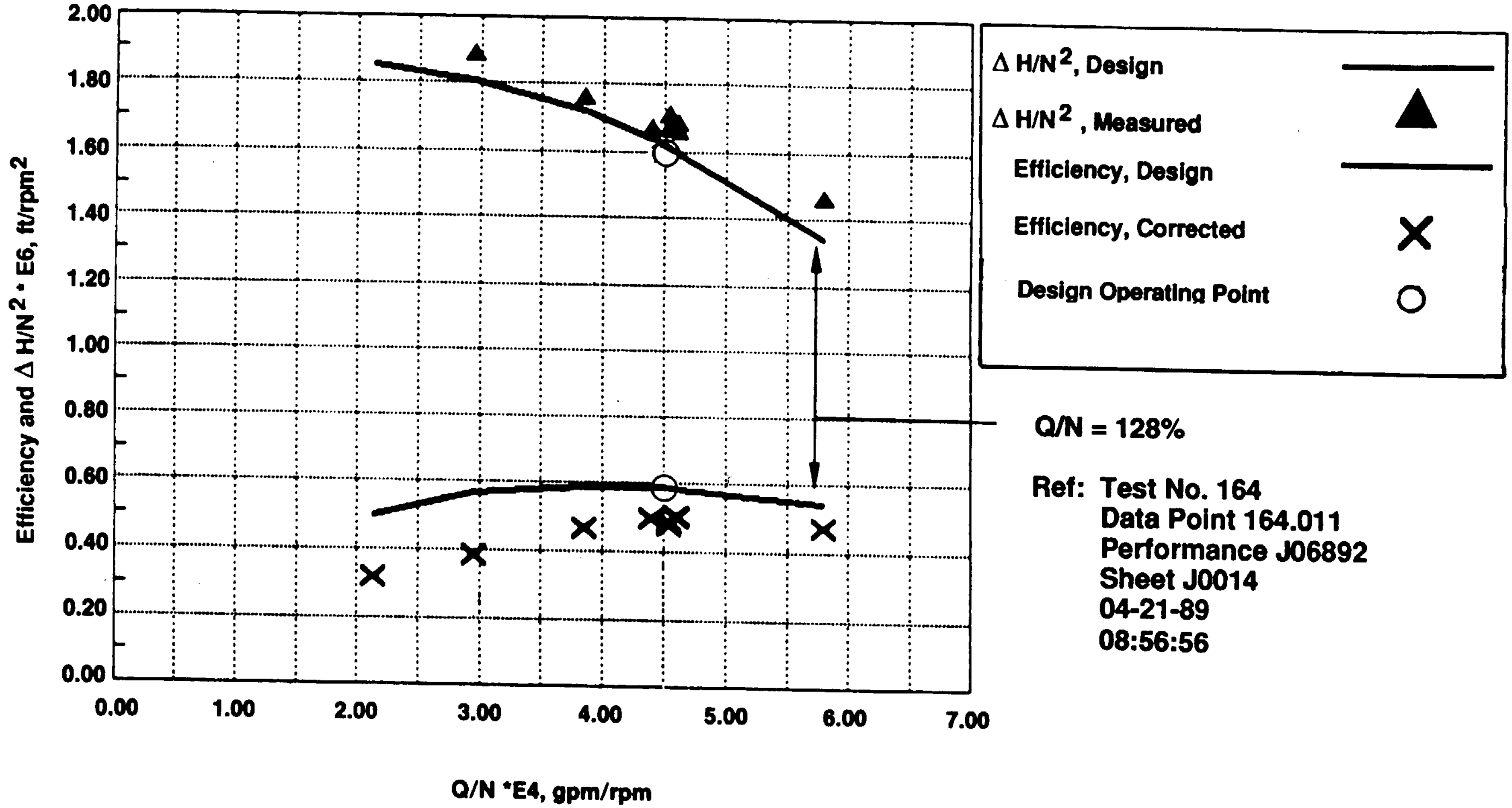

Figure 3.2-1. Pump Performance

Performance, Section 3.2, of this report, it was felt that the pump efficiency curve was too high at Q/N values below design and too low at Q/N values above design. This would account for some of the distortion to the turbine efficiency curve mentioned above.

To adjust these curves to better reflect the real efficiency characteristics, it was decided that a parabola should be fit from the zero efficiency point, through the average of the turbine efficiencies at the design Q/N operating point, peaking at a U/Co of 0.50. (The peak efficiency location was determined from previously run computer simulations of turbine off-design performance). Turbine efficiencies were then determined from the fitted parabolic curve for each test at the test values of U/Co. These values of turbine efficiency, Figure 3.3-1, and the subsequently derived TPA tare efficiencies were then divided into the corresponding values of overall TPA efficiency to give the respective pump efficiencies. These calculated pump efficiencies were then used as described in the pump analysis in Section 3.3.2 of this report and noted as the corrected values.

3.3.1 Analysis Details

The analytical relationships used for turbine data reduction are based on ideal gas properties and characteristics. Unfortunately, at the 2000 to 4000 psia turbine pressures involved, neither the GN_2 nor the GOX working fluids behaved as ideal gases with constant properties over the ranges of interest. It was therefore necessary to derive "pseudo-ideal" gas properties. This was done by picking a characteristic turbine test operating point for each gas, determining the isentropic enthalpy drop across the turbine inlet-to-exit conditions from the gas properties program MIPROPS (Ref. 8) and using the isentropic ideal gas relations to back out the pseudo values for the specific heat at constant pressure (Cp), the gas constant (R) and the ratio of specific heats (Gamma). The results of these calculations are presented in Tables 3.3-1 and 3.3-2. These are the gas properties used in the subsequent analysis for the respective gases. Comparing turbine efficiency calculations using these properties to the efficiency calculated for one GOX and one GN_2 case calculated using enthalpies determined directly from MIPROPS showed an

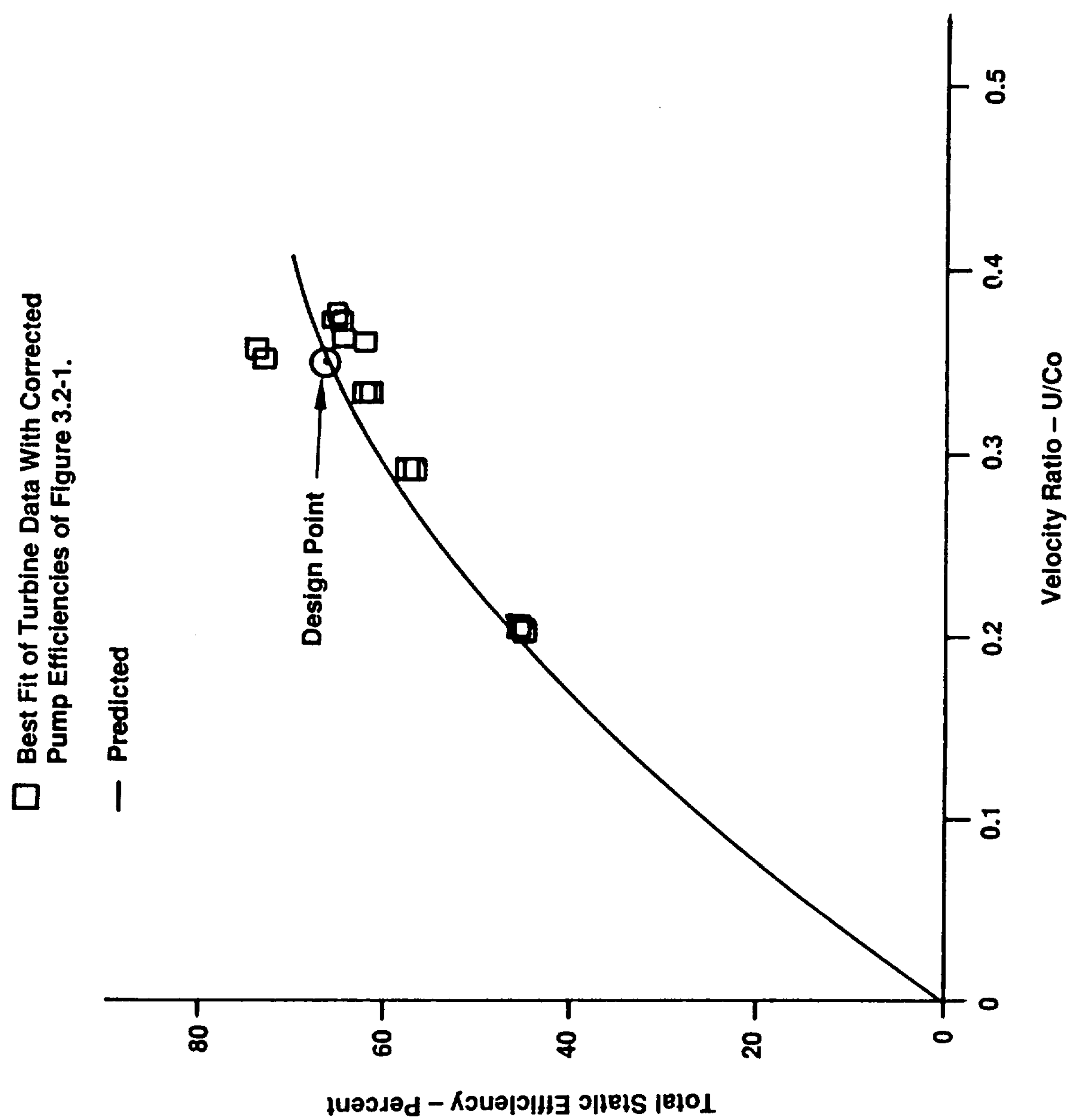

Figure 3.3-1. Turbine Efficiency Ratio

TABLE 3.3-1

GN$_2$ PSEUDO-IDEAL GAS PROPERTIES

h in, enthalpy	101.1	Btu/lbm
h ex	77	Btu/lbm
T in, temperature	491.81	°R
T ex	400	°R
p in, pressure	4422.5	psia
p ex	2083.2	psia
rho in, density	20.73	lbm/ft^3
rho ex	14.909	lbm/ft^3
s, entropy	1.165	Btu/lbm-°R
Cp, specific heat, p = constant	0.262499	Btu/lbm-°R
Gamma ratio of specific heats	1.37832	
R, gas constant	56.38326	ft-lbf/lbm-°R

TABLE 3.3-2

GOX PSEUDO-IDEAL GAS PROPERTIES

h in, enthalpy	82.1	Btu/lbm
h ex	63.8	Btu/lbm
T in, temperature	499.57	°R
T ex	403	°R
p in, pressure	3757.6	psia
p ex	1751.2	psia
rho in, density	24.075	lbm/ft^3
rho ex	16.563	lbm/ft^3
s, entropy	1.128	Btu/lbm-°R
Cp, specific heat	0.1895	Btu/lbm-°R
Gamma ratio of specific heats	1.391514	
R, gas constant	41.38437	ft-lbf/lbm-°R

approximately 1 percentage point difference in overall TPA efficiency. Since this is far less than the discrepancy observed between calculated and predicted in the values discussed below, this "pseudo-ideal" gas property approach was deemed to be reasonable.

An important quantity used in data reduction is the turbine flow rate. Provision was made for measuring this quantity with an orifice flow meter between the turbine and gas source. It was intended to use the standard orifice flow meter relations from Ref. 12 but these yielded erroneous values, possibly due to improper static pressure tap locations. Also, for several tests, valid static pressure measurements were unavailable due to transducer problems. After the completion of the testing and the teardown inspection of the hardware, an actual flow test of the turbine nozzle was made to determine the actual "as-build" flow area. This was considered necessary as all earlier calculations involving turbine flow area or flow coefficient used "as designed" area and flow coefficient (0.945). A minor discrepancy between these values could significantly effect the calculation of overall turbopump efficiency. A test apparatus was setup and the turbine nozzle pressure drop was carefully measured while flowing gaseous nitrogen of known temperature and pressure. The results of this calibration testing are presented in Figure 3.3-2. Based on this flow data a flow area of 0.06237 square inches was calculated. This was less than the design value by five percent, and served to reduce the TPA efficiency. This measured flow area was then used to calculate overall turbopump efficiency.

TPA tare losses were calculated by multiplying the tare horsepower at the design point, (3% of the design turbine shaft horsepower), by the square of the ratio of the test speed to the design speed. Turbine tare efficiency is then simply one minus the ratio of tare horsepower to turbine shaft horsepower.

3.3.2 Discussion of Results

The turbine efficiency vs. velocity ratio (U/Co) data are presented in Figure 3.3-1. The test data values were calculated as described in the previous section. The test data show slightly lower efficiencies than the predicted curve. Insufficient data and analysis time hinder the investigation as to the reasons but several possibilities should be considered:

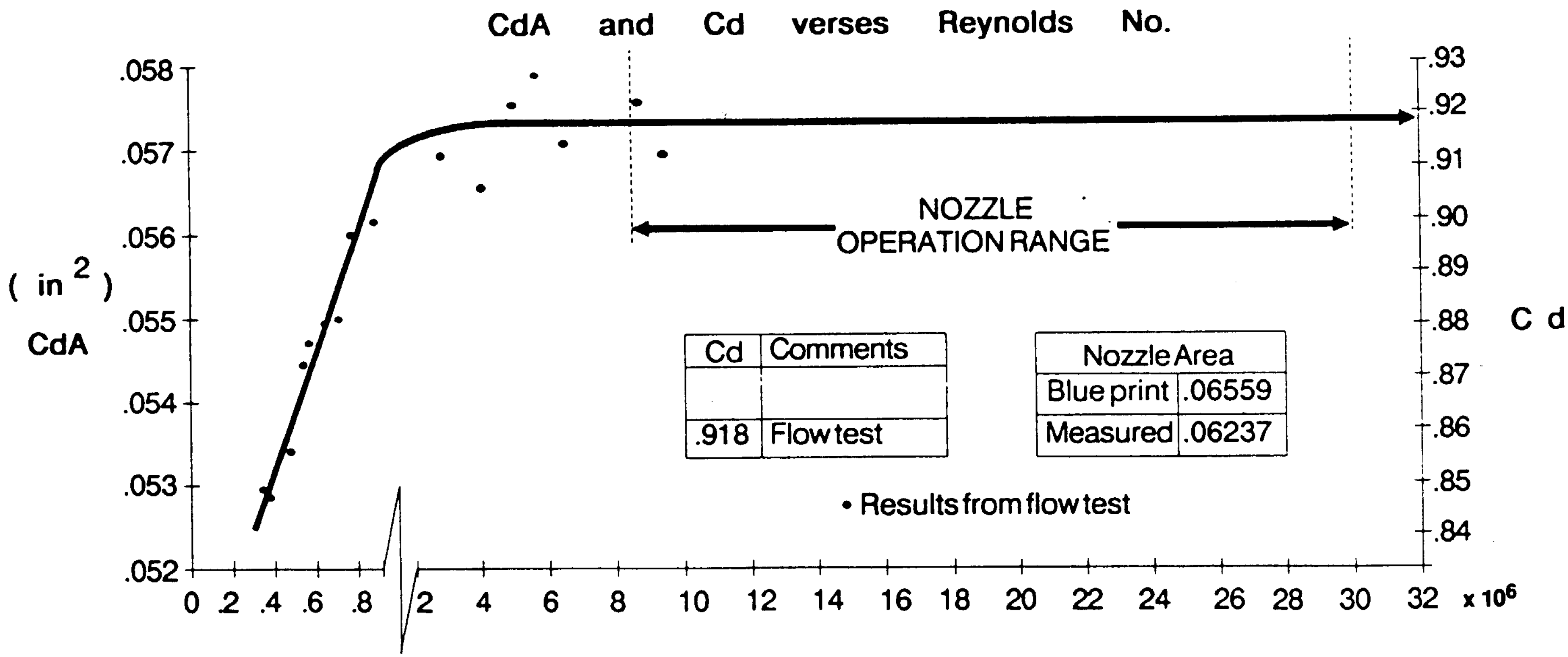

Figure 3.3-2. Turbine Nozzle Flow Test and Measured Value After Disassembly

1) A potential leak was detected upon post-test teardown inspection at the "V" seal of the turbine nozzle to turbine housing interface resulting in possible turbine by-pass flow. This would reduce the working fluid flow through the turbine resulting in reduced power output.

2) Upon post-test teardown inspection, the turbine nozzle vanes were found to have a very rough surface finish compared to the drawing value of 32 micro-inches. Also the rotor blades were found to have parallel surface grooves running from hub-to-tip on the central portion of the blades (the leading and trailing edge regions had been polished smooth as far as possible along the blade chord until interference with the adjacent blade would not allow access to the central portions of the blade surfaces). These large surface roughnesses would increase blade losses but the ultimate effect on turbine performance was not quantified for this report. A more detailed acceptance inspection prior to assembly and testing would possibly have detected these hardware deficiencies.

3) Calculated turbine performance is dependent on the accuracy of the calculated pump performance at the 100% pump design Q/N point. Any inaccuracies in the pump calculations and efficiencies will also be found in the calculated turbine efficiency.

4) Design predictions are based on nozzle inlet and rotor exit conditions whereas the test data reduction is based on turbine inlet and turbine exit conditions. That is, the results presented in this report include inlet and exit manifold losses lumped into turbine performance.

3.4 BEARING SYSTEM PERFORMANCE

When operating the turbopump it is difficult to separate bearing performance characteristics especially in this design where functions of the bearings and seals are combined. Some bearing performance can be inferred by the success of the turbopump. Characteristics to be rated are:

- Clearance Control
- Flow Rate
- Radial Motion of Shaft
- Axial Motion of Shaft
- Load Capacity
- Stiffness
- Rotor Critical Speed
- Oxygen Ignition Resistance
- Wear Resistance
- Start Transient Capability

<u>Clearance Control</u>

The rotating assembly to stationary housing clearances were established during the buildup procedure and are shown in Figure 3.4-1. These are the minimum clearances for potential rub zones in the propellant. The only close clearance in the GOX is the turbine tip seal at .005 in. All other close clearances exist in the liquid oxygen. The bearing radial and axial clearances limit the rotating assembly position. As shown in the figure the radial and axial bearing clearances are very small and prevent other zones from having contact. Thermal deflection and hydraulic loading will contribute to clearance change. This design controls thermal differential by using the same material throughout, by adequate cooling passages

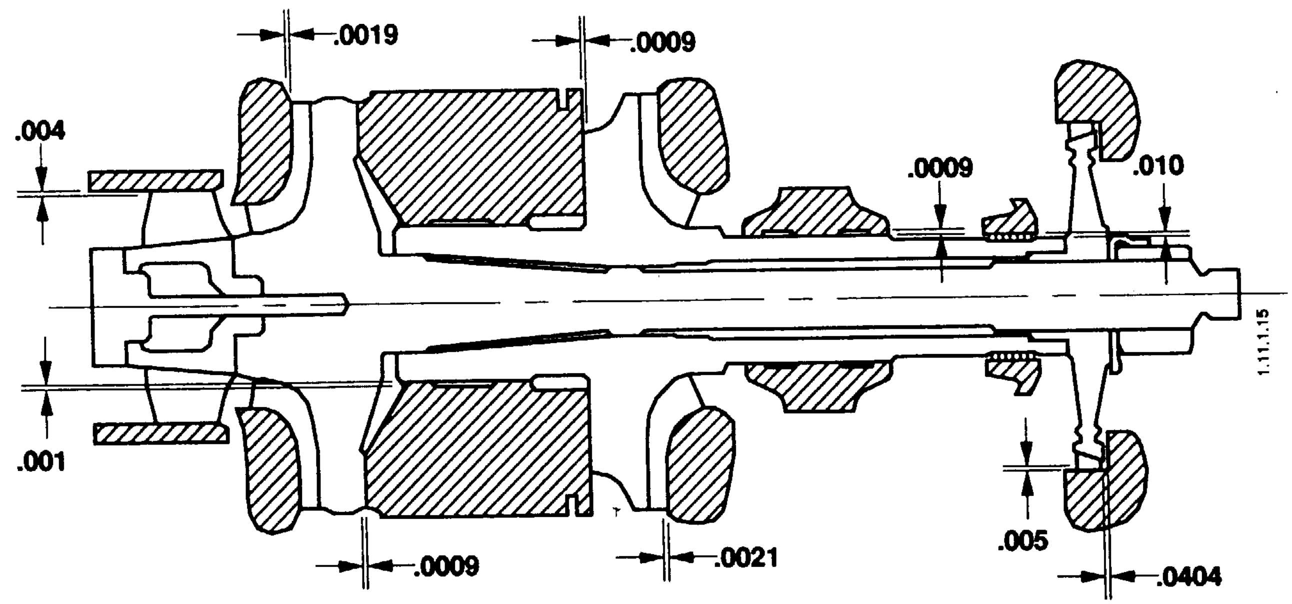

Figure 3.4-1. Nominal Assembly Clearances Between Rotating and Stationary Parts

(including the shaft bore) and by allowing radial temperature growth without mechanical restraint. The housing and rotor are of robust proportions and the bearing load capacities are large resulting in minimum deflections.

Flow Rates

Flow rates to both the turbine end and pump end bearings were supplied from the pump discharge line. Bearing supply flow passed through 2 micron filters, and each flow was measured with a turbine type flowmeter. All flow through the turbine end bearing passes through a flowmeter. The flow rate to the turbine end bearing is shown in Figure 3.4-2. The measured flow and the predicted flow differ considerably. The measured flow is approximately 2.5 times the predicted flow. The flow through the bearing is controlled by the compensating orifices with a pressure ratio of approximately 0.4.

Even with zero back pressure on the pocket the flowrates would be less than what was measured. There are other leakage paths for this bearing supply flow as it crosses housing joints. The bearing supply is fed through the housing across the circumferential joints sealed by piston rings. Assuming the piston ring gap is small, i.e., .0001 inch, the piston ring flow area is equivalent to the bearing flow area. As is true for most ring seals, the effective gap will vary with the installation and the groove dimensions. In the Series A and B tests (Ref. 1) two ring seals were found to be stuck in their grooves allowing a 50 percent increase in flow. Despite reasonable care in the installation for this TPA buildup a recurrence is possible accounting for the higher recirculation flow. The ring grooves were reworked prior to this test series, and the test data indicates the flowrate was reduced, but some leakage around the ring seals is likely.

The pump bearing flowrate is shown in Figure 3.4-3 as a function of pressure difference between orifice supply and the pump bearing exit cavity. This is the flowrate supplied to three bearing faces, the pump journal, the first stage thrust face

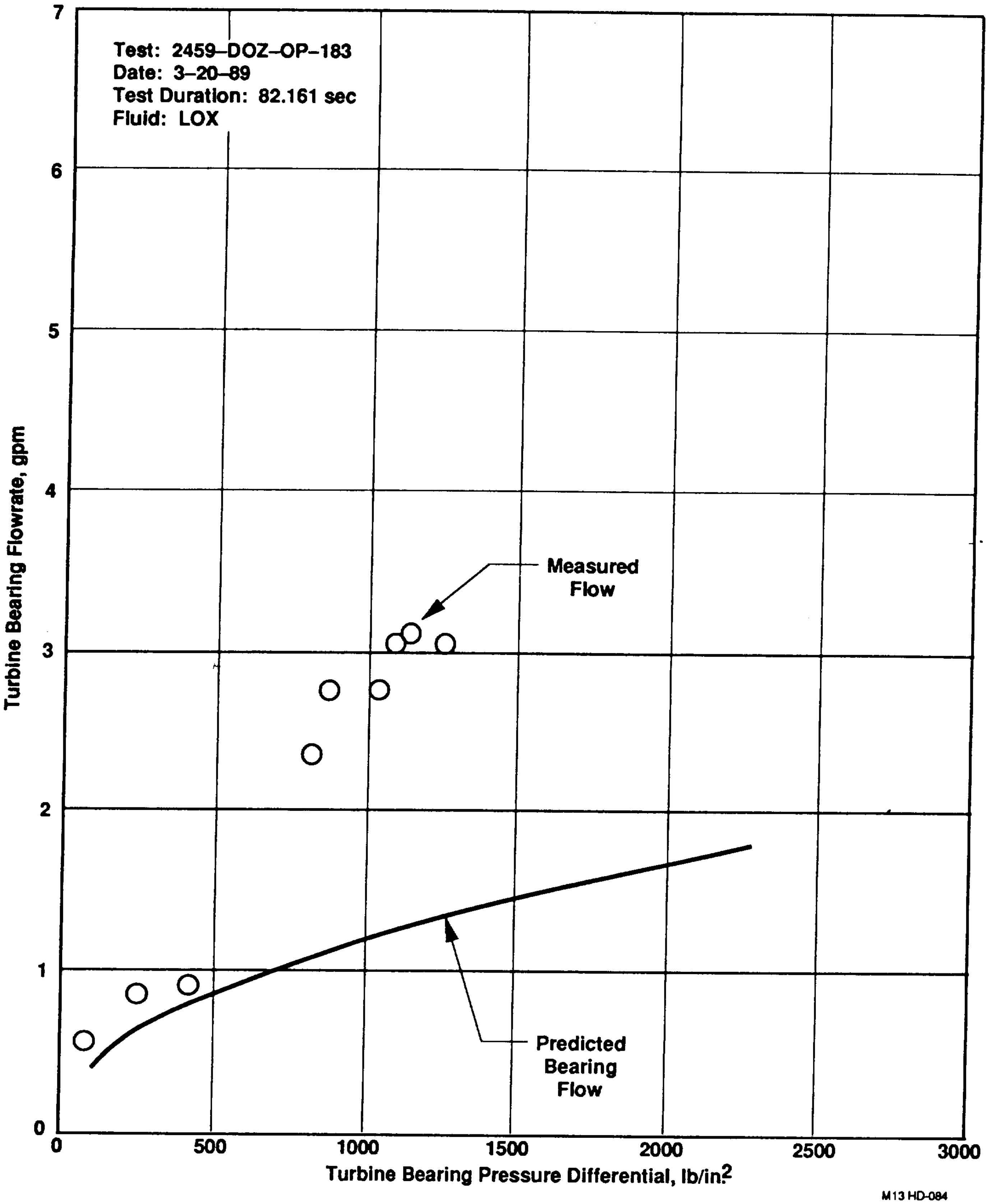

Figure 3.4-2. Turbine Bearing Flowrate vs Pressure Differential

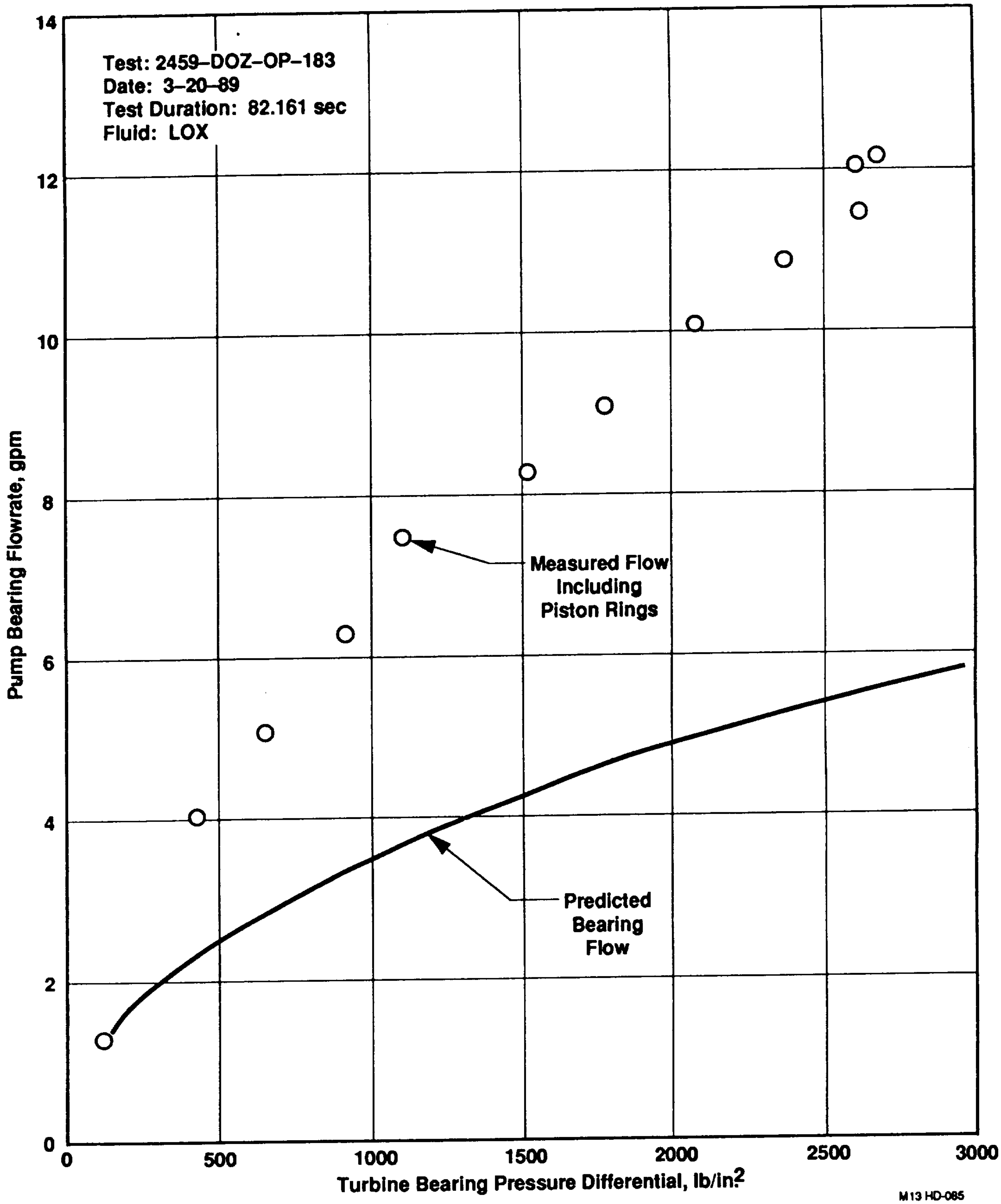

Figure 3.4-3. Pump Bearing Flowrate vs Pressure Differential

and the second stage thrust face. The solid curve is the predicted flowrate for the bearing alone while the data points include any leakage the piston rings may allow. The test flowrate appears to follow a square root of pressure differential curve for a relative to bearing flow area that would account for the additional flow area. It should be noted here that the outer cylinder of piston ring seals will not exist in a flight type turbopump which will eliminate a significant proportion of bearing supply flowrate.

Shaft Radial Motion

The shaft radial motion was monitored by a set of "X" and "Y" distance detectors adjacent to the turbine end journal bearing. This cavity is a high pressure zone exposed to the turbine exhaust pressure. This pressure reaches a design point maximum of about 2300 psi. In order to make an oxygen compatible, low ignition potential distance detector and accommodate the high pressure a distance detector probe tip of alumina ceramic was used. This tip reduces the gap sensing range of the probe and makes it very sensitive to temperature changes. As a result obtaining reliable distance detectors readings is difficult. The probes were calibrated to operate near LOX temperature and the axial probe in the pump inlet performed reasonably well. The radial "X" and "Y" probes were in a zone prone to exceeding their range due to temperature shifts. When the "X" probe was reading during a test the shaft motion was stable with very small deflections approximately the same magnitude as the surface runout. The pump "X" and "Y" distance probe signals combined to display a shaft orbit. Several orbits from the series A and B for the pump end at approximately 70,000 rpm are shown in Figure 3.4-4. A .002 inch step in the shaft was used for speed signal generation and displacement calibration.

Shaft Axial Motion

An anomalous 170 Hz cyclic motion was present during most of the test runs. It is discussed in some detail in Section 3.1, and is considered an installation caused phenomenon. It caused no problems during the TPA operation and is a concern only because the actual shaft displacement during the cycling reduces the clearances between the rotating assembly and stationary surfaces. Minimum clearances of 1 to 2 mil are reduced to 1/2 to 1 mil during the cyclic motion.

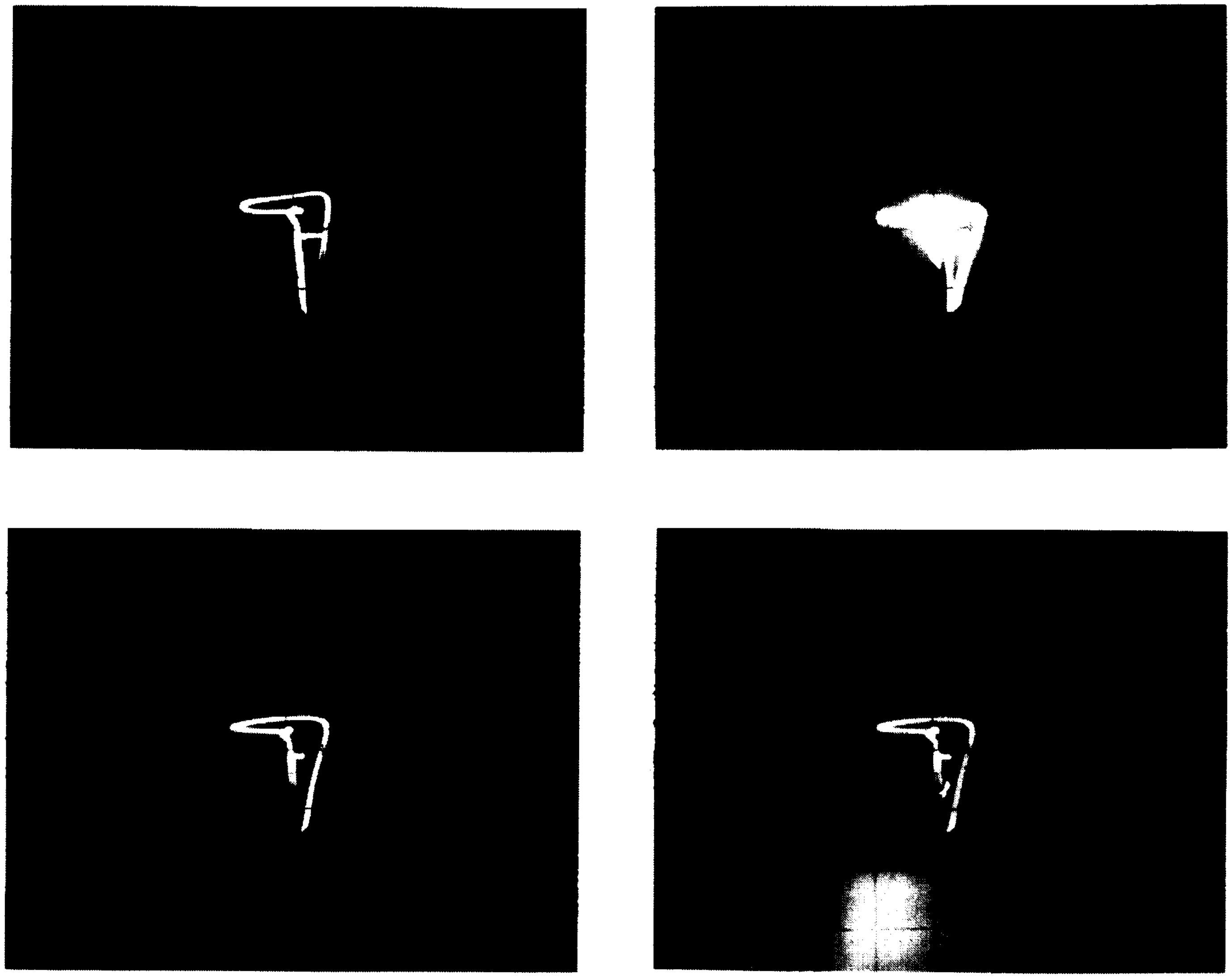

- Test Series A and B
- Inducer End Motion

Figure 3.4-4. "X" Vs. "Y" Orbits at 72,000 rpm

Load Capacity

The thrust bearings provided high axial load support, high pressure impeller sealing, high axial stiffness, and unassisted lift-off during start and stop transients. The bearings were operated to high pressures subjecting the rotating assembly to high axial forces. Typical calculated nominal net axial loads were approximately 150 lb. The absolute loads on each impeller disk are quite high on the order of 5000 lb. The thrust bearing axial capacity is shown in Figure 3.4-5 for the design pressure differential. The bearing capacity is a direct ratio of this pressure differential which is determined by pump speed. The first thrust bearing sealing pressure differential was 962 lb/in.^{2} while the bearing orifice supply pressure differential was 2612 lb/in.^{2} (P_{PBI}-P_{BE}). Axial motion of the shaft at a low constant frequency existed (displacement probe output signal) during this test series. It obviously loaded the thrust bearing. Thrust cyclic excursions were in the range of ±.0005 in. This requires several hundreds of pounds cyclic axial load to produce this motion. Even with this adverse loading situation the thrust bearing maintained adequate impeller vane clearance and thrust bearing clearance. The calculated thrust bearing load during the unassisted "start transient" started at 24 lb on the first stage thrust bearing. This load definitely created metal-to-metal contact initially. Fourteen unassisted starts were performed in LOX. The thrust bearings were found to be in excellent condition posttest.

Radial loads on the journal bearings were determined by the impeller peripheral pressure distribution. Loads cannot be measured directly but can be calculated from the pressure distribution and the projected area. A summation of radial load over the first stage impeller port width as a function of Q/N is shown in Figure 3.4-6. The off-design Q/N tests were not all at the same speed. The speed and Q/N followed a throttled engine operating requirement for flow and pressure. The lower Q/N values were run at lower speed and pressure. In order to determine the bearing radial loads the full impeller load must be calculated. Therefore, assuming the pressure distribution is constant over the axial width of the impeller disk and that the second stage impeller has the same peripheral pressure distribution, the two impeller radial loads were calculated. These radial loads as a function of Q/N are shown in Figure 3.4-7. The resulting radial bearing loads are shown in Figure 3.4-8

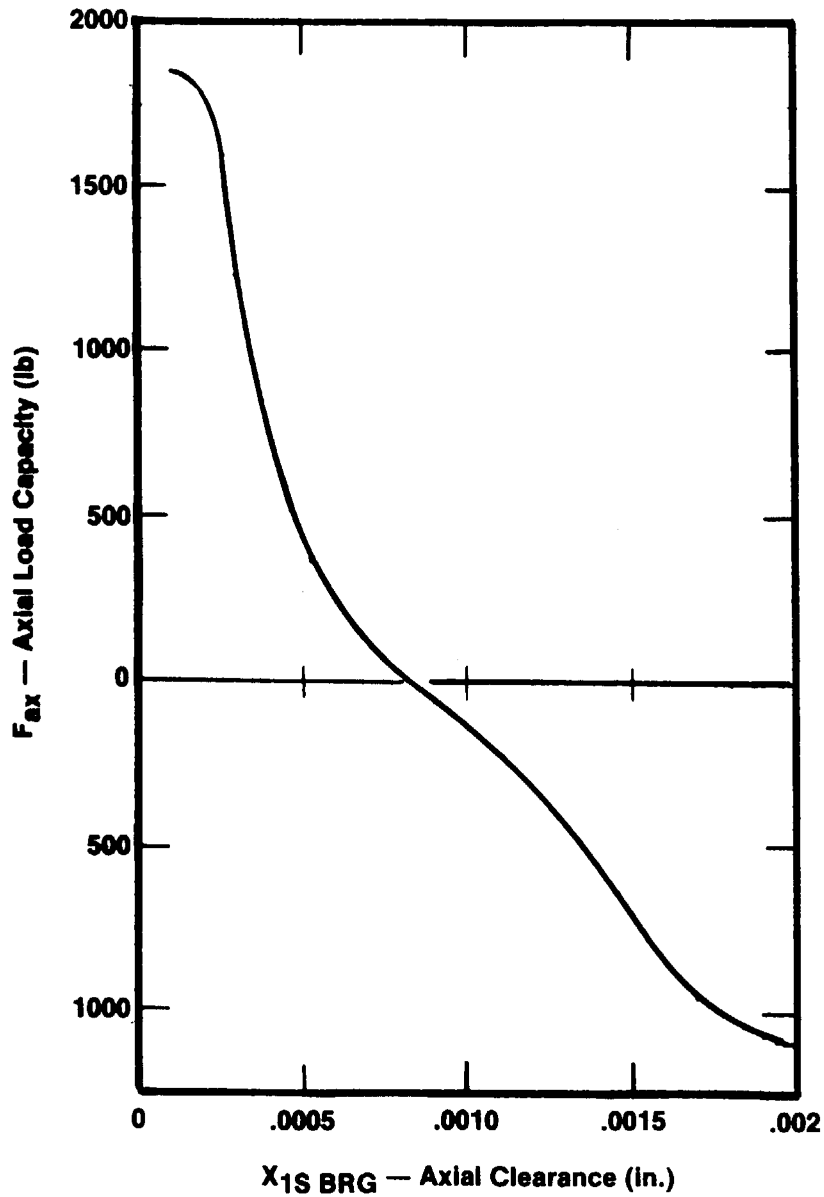

- Shaft Speed N = 75000 rpm
- Fluid LO_2
- First Stage Thrust Bearing
- Supply Pressure, P_s = 4600 lb/in.^{2}
- Exit Pressure, P_e = 500 lb/in.^{2}
- Number of Recesses, N_R = 4
- Diameter of Orifice, D_o = .020 in.
- Land Radius, R_1 = .60 in.
  R_2 = .64 in.
  R_3 = .69 in.
  R_4 = .81 in.
- Second Stage Thrust Bearing
- Supply Pressure, P_s = 4600 lb/in.^{2}
- Exit Pressure, P_b = 2100 lb/in.^{2}
- Number of Recesses, N_R = 4
- Diameter of Orifice, D_o = .020 in.
- Land Radius, R_1 = .35 in.
  R_2 = .39 in.
  R_3 = .45 in.
  R_4 = .65 in.

Figure 3.4-5. Thrust Bearing Axial Load Capacity vs Axial Clearance, First Stage

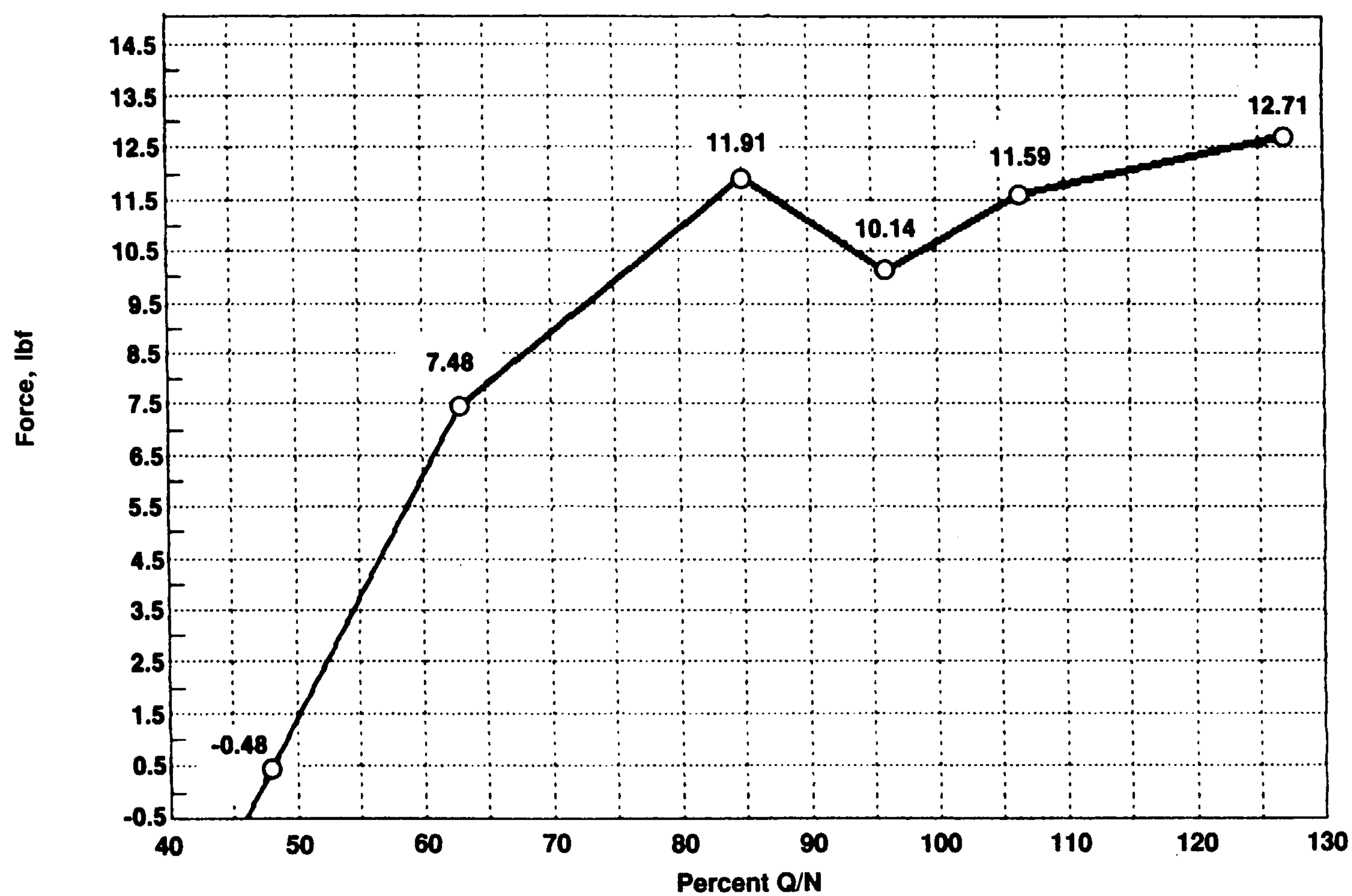

Figure 3.4-6. Radial Load Across Impeller Port Width vs Percent Design Q/N

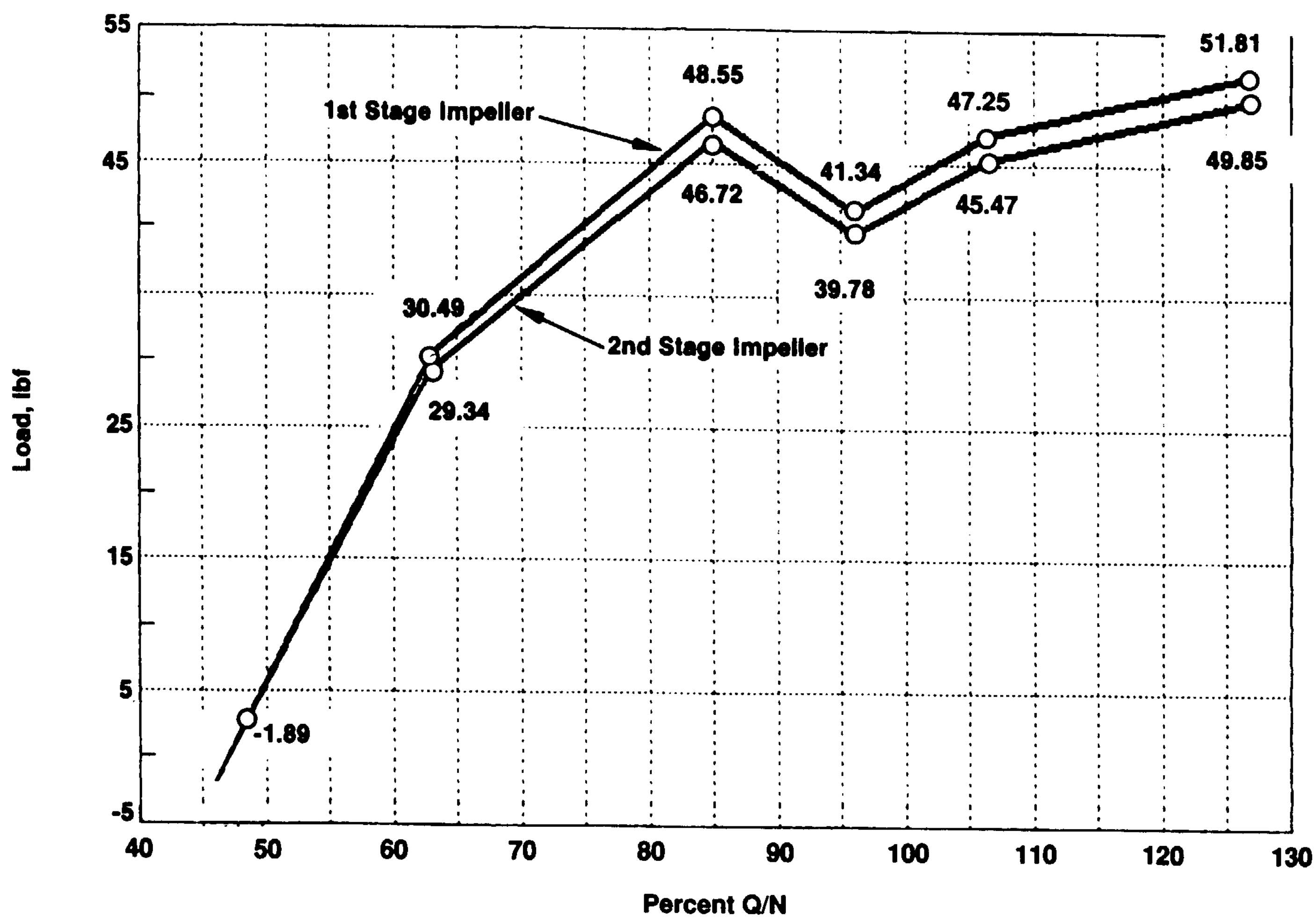

Figure 3.4-7. Radial Load on Impeller vs Percent Design Q/N

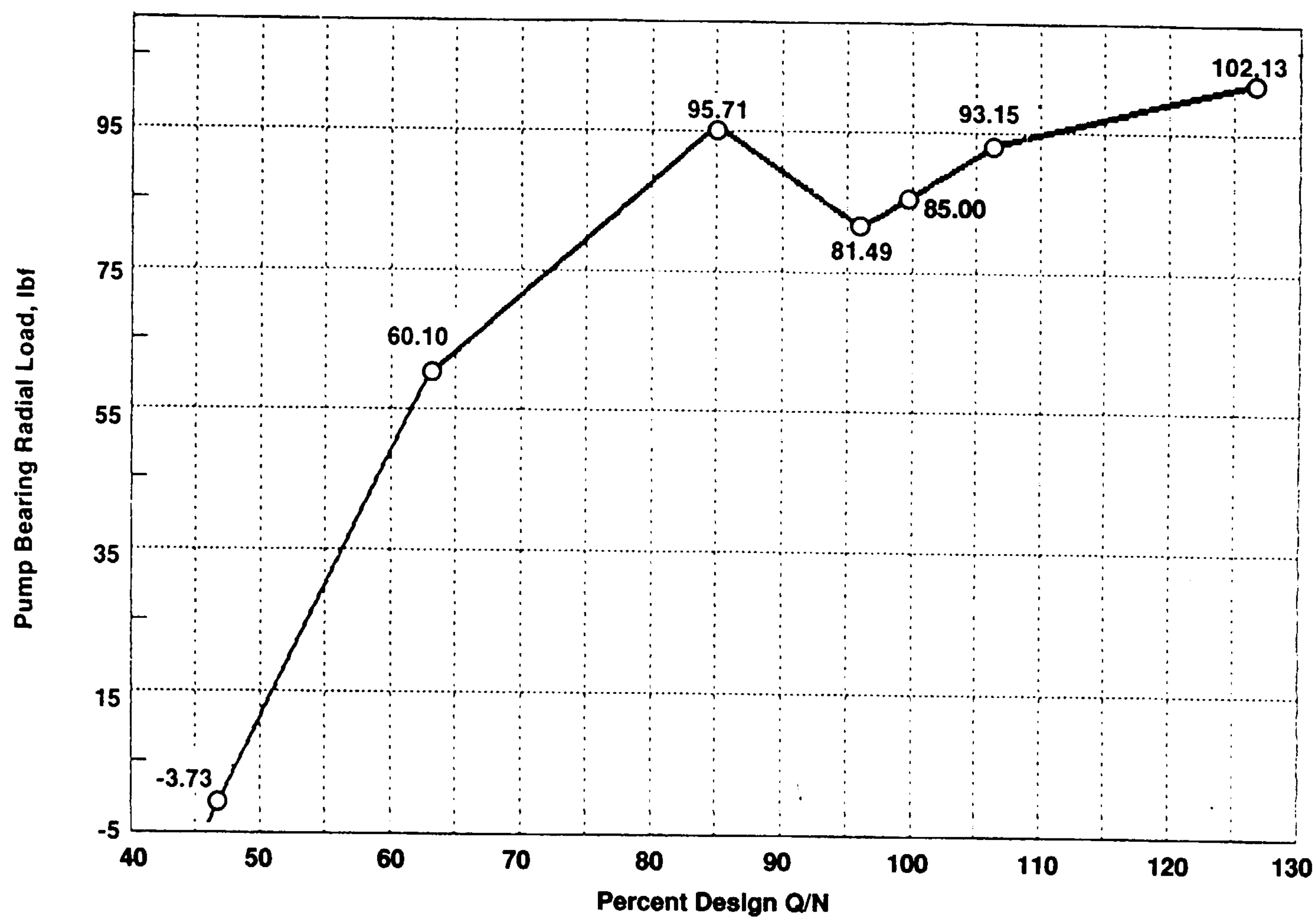

Figure 3.4-8. Radial Load on Pump Bearing vs Percent Design Q/N

for the pump end journal bearing. The turbine journal bearing loads are less than 1 pound. At the 100% Q/N design point and maximum speed of 67000 rpm and pump discharge pressure of 3350 lb/in.^{2} the calculated pump journal bearing load is 85 lb. This radial load is equivalent to a bearing unit load of 295 lb/in.^{2}, which is significant, but well within the capability of the bearing (approximately 1440 psi at 67,000 rpm).. Some excursions were experienced during start transients that resulted in much higher radial loads. On one LN_2 test the peripheral pressure distribution resulted in a pump bearing radial load of 230 lb which is equivalent to 800 psi unit loading.

Stiffness

The bearing stiffness of this turbopump was designed to control the rotor radial and axial motion and prevent contact with the stationary components, especially in the turbine tip seal area. This means the bearings must be of adequate stiffness to react to both static and dynamic loads. No direct measurement of stiffness was made for two reasons: 1) special loading devices were not incorporated and, 2) the distance detectors were very sensitive to temperature and accurate load deflection characteristics were difficult to measure. The fact that only incidental minor contact was made between the rotating assembly and the housing during the extensive testing would indicate that the stiffness was adequate over the operating range experienced.

Rotor Critical Speed

The rotor critical speed also a function of the bearing stiffness, was designed to be above the operating speed by a wide margin at all times. Even though distance detector operation was erratic, no indication of any resonance or amplified whirl orbit or any indication of excess vibration on the accelerometers was recorded. This includes all speeds up to a maximum speed of 80,394 rpm logged in Test 135.

Oxygen Ignition Resistance

The turbopump oxygen ignition resistance feature is achieved through two methods. First, the turbopump was designed to prevent contact between the stationary and rotating components.

Secondly, materials were selected that have minimum burn factors and sufficient strength while sustaining rubs and particle impact in oxygen. There were a few minor rubs in the impeller vane area and a significant rub in the exit land at the pump end journal bearing. There is no way of knowing the pressure velocity of this rub. It appears to involve a third party wear particle. The results to date confirm the adequacy of the design as there is no evidence of any melting or localized ignition.

Wear Resistance

Wear of this turbopump would likely occur only in the loss of close operating clearances between the rotating assembly and the stationary mating housings. The close clearance locations are identified in Figure 3.4-1. Section 3.5, Teardown and Inspection, defines the type of wear experienced at each location. Photographs show the mating surfaces. Profile traces are provided for each bearing surface. The inspection results showed the pump end journal bearing exit land experienced the most wear. The turbine journal bearing also experienced a small amount of wear in one land but the remainder of the surface experienced very minor wear. There was no significant symptom during the test program that would indicate wear was occurring.

Some wear was anticipated during unassisted bearing starts. Since the highest start load was in the axial direction it was expected that the thrust bearings would experience the most wear. Several operational and mechanical anomalies that could have precipitated the bearing wear are listed below.

1. The overspeed excursion during turbine valve malfunction
2. Unsymmetrical impeller pressure distribution during start transient
3. Excessive radial load during operation

4. Misaligned bearing (would cause contact at the outer corners of the thrust bearing)

5. Disbond of silver plating

6. Debris particle(s) in the system (from a ruptured filter)

These are potential causes that could have happened during the test program.

Wear of the bearing exit land will increase the bearing flowrate. Fortunately the pump journal bearing combined with the first stage thrust bearing exit flowrate, Q_{PBE}, was measured. Also the flow supplied to the compensating orifices, Q_{PBI}, was measured. Not all the flow through the bearing was measured by Q_{PBI} but a relative comparison may be made at different pressures. Comparing Q_{PBE}/Q_{PBI} vs. test sequence in Figure 3.4-9 shows a significant change between tests 125 and 131 indicating wear occurred early in the test series. These are the first rotating tests in LN_2 with high pressure assist to the bearings before shaft rotation.

The material loss in the bearings, which occurred on the downstream exit land of the pump journal bearing, appears to have been mechanically removed. Debris from the fluid system or silver debris from a rub could have caused this wear. An overload during the start transient may have created silver debris, but journal overloads usually have unidirectional wear patterns. The observed wear was not unidirectional. In addition, a small groove was worn on the shaft surface as discussed in Section 3.5. Since the shaft is relatively hard, this groove could not have been caused by soft silver. It is more likely that a hard particle from the fluid system caused the wear on both the shaft and pump journal bearing surface. If particles came from the supply system flow, the fluid velocity would direct them towards the journal bearing and not to either of the two thrust bearings.

Since upon disassembly the upstream pump bearing filter was found to be ruptured and since the pressure drop across this filter was higher than the turbine filter and varied with time, it is concluded that hard debris passed through the pump journal bearing and caused the exit land wear.

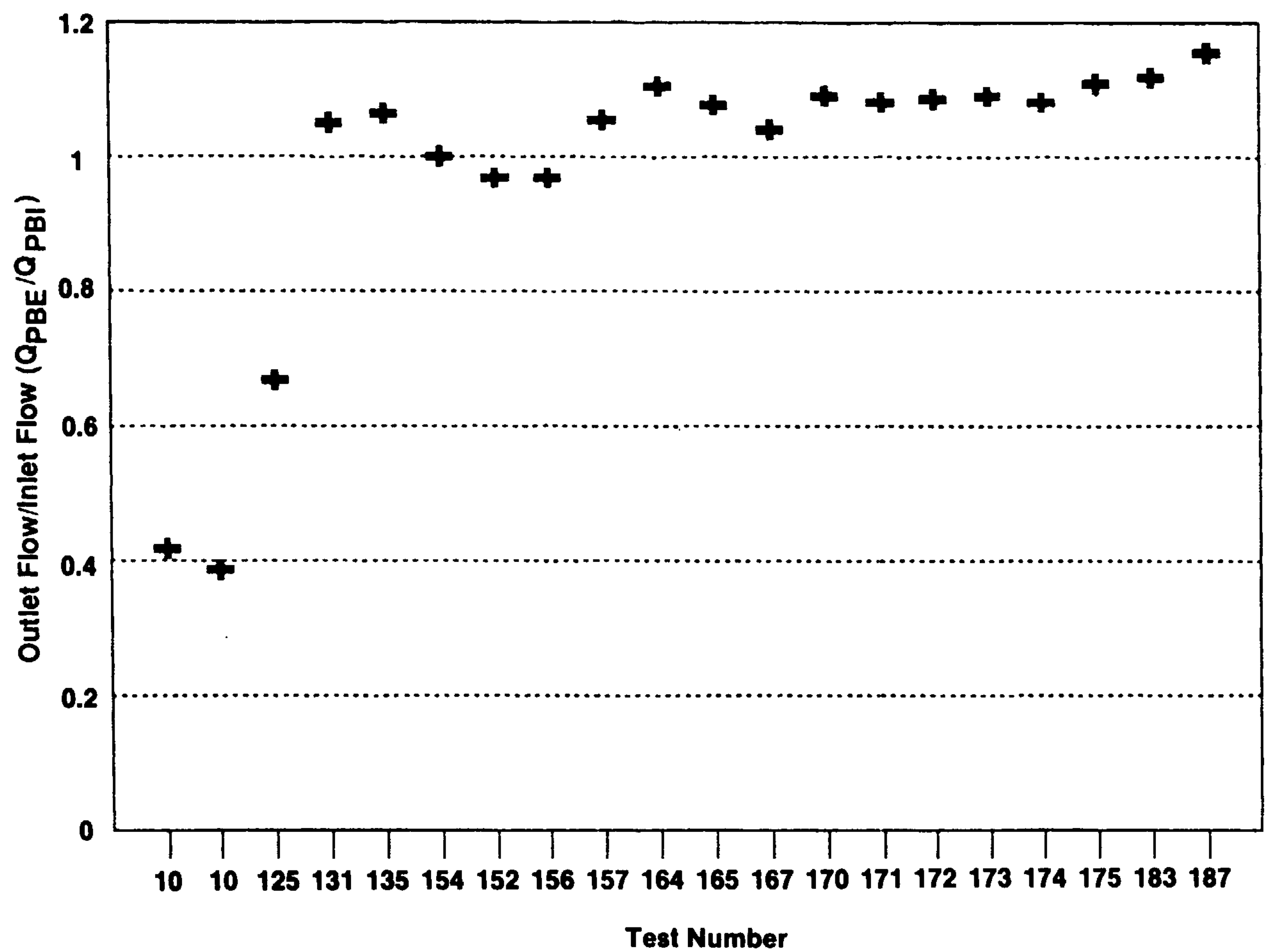

Figure 3.4-9. Pump Bearing Flow Ratio vs Test Number

Start Transient

Several options for dealing with bearing start stop transients when using hydrostatic bearings are:

1. Unassisted start (rubbing-hydrodynamic-hydrostatic)

2. Series hybrid ball bearing/hydrostatic.

3. Parallel hybrid ball bearing/hydrostatic

4. Accumulator

5. Magnetic lift-off.

Two of these options considered for the OTV turbopump are the accumulator and the unassisted start. Factors to consider when selecting the start technique are the applied radial and axial loads, material wear resistance, number of revolutions until pump pressure rises, turbine torque available, and the condition of the propellant in turbopump (phase, temperature, and pressure).

In this test series the bearing assist start (accumulator) was used for most of the tests. The unassisted starts with transition to pump discharge fed bearings were done only in the final LOX tests. All of the LN_2 tests were tank fed at higher pressure than the pump discharge pressure. This was done to maintain high bearing stiffness. The rotor speed was designed for oxygen, but the fluid density of LN_2 is lower than LOX and, therefore, the pump discharge pressure was lower. Also on all LN_2 tests the bearings were lifted prior to rotation with external tank pressure. The relative pressures vs. speed for LN_2 are shown in Figure 3.4-10. In the turbopump performance test series with LOX, (C2 and E1), the bearing assist was set to 200 to 500 lb/in.^{2}. When the pump discharge pressure surpassed the bearing assist pressure, the bearing feed line check valve opened and the bearings were pump fed. The pressure vs. speed data for this type of transient is shown in Figure 3.4-11. This bearing assisted start maximizes the life of hydrostatic bearings during transients.

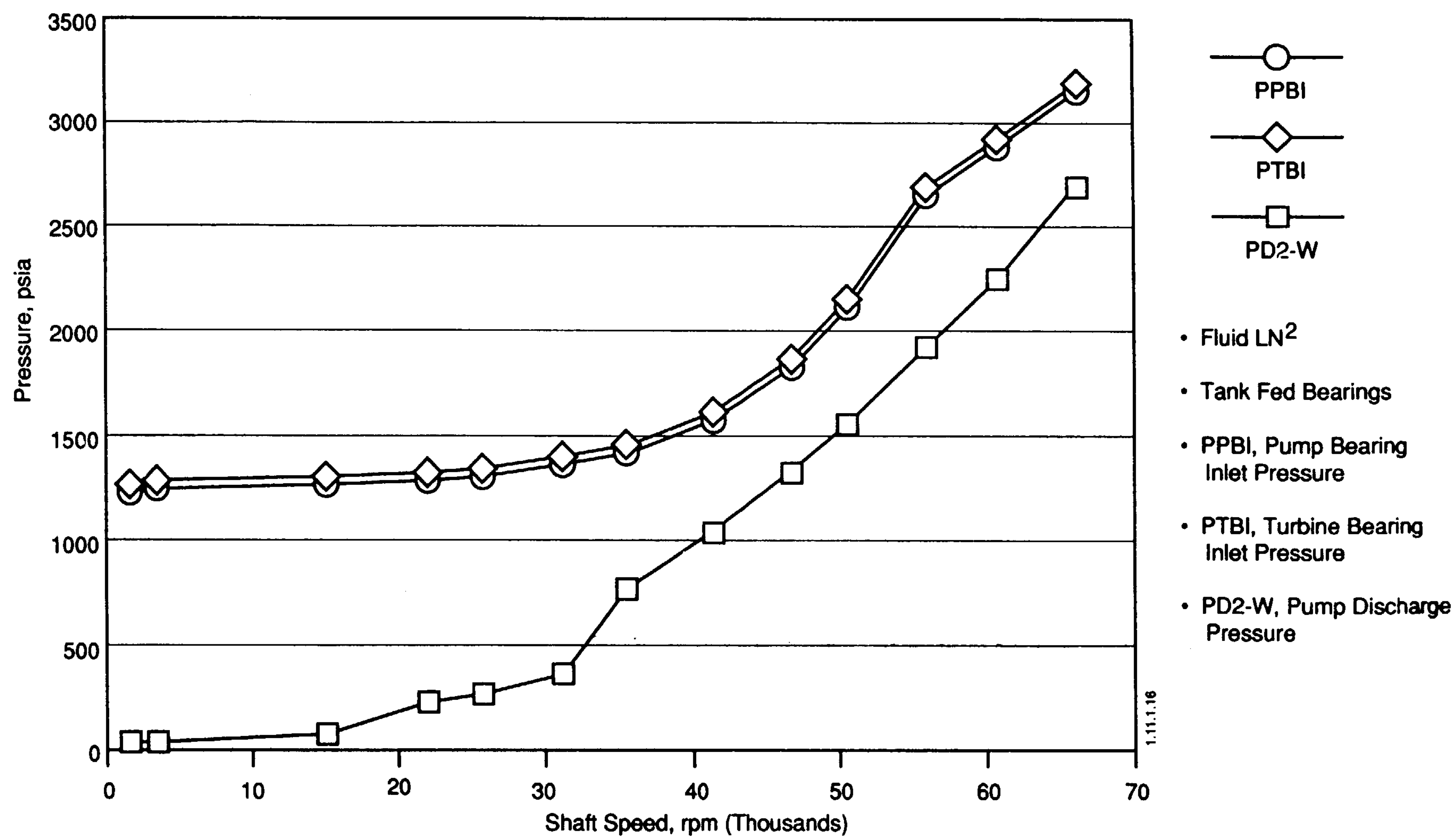

Figure 3.4-10. Bearing Inlet and Pump Discharge Pressures vs Shaft Speed — Test 131

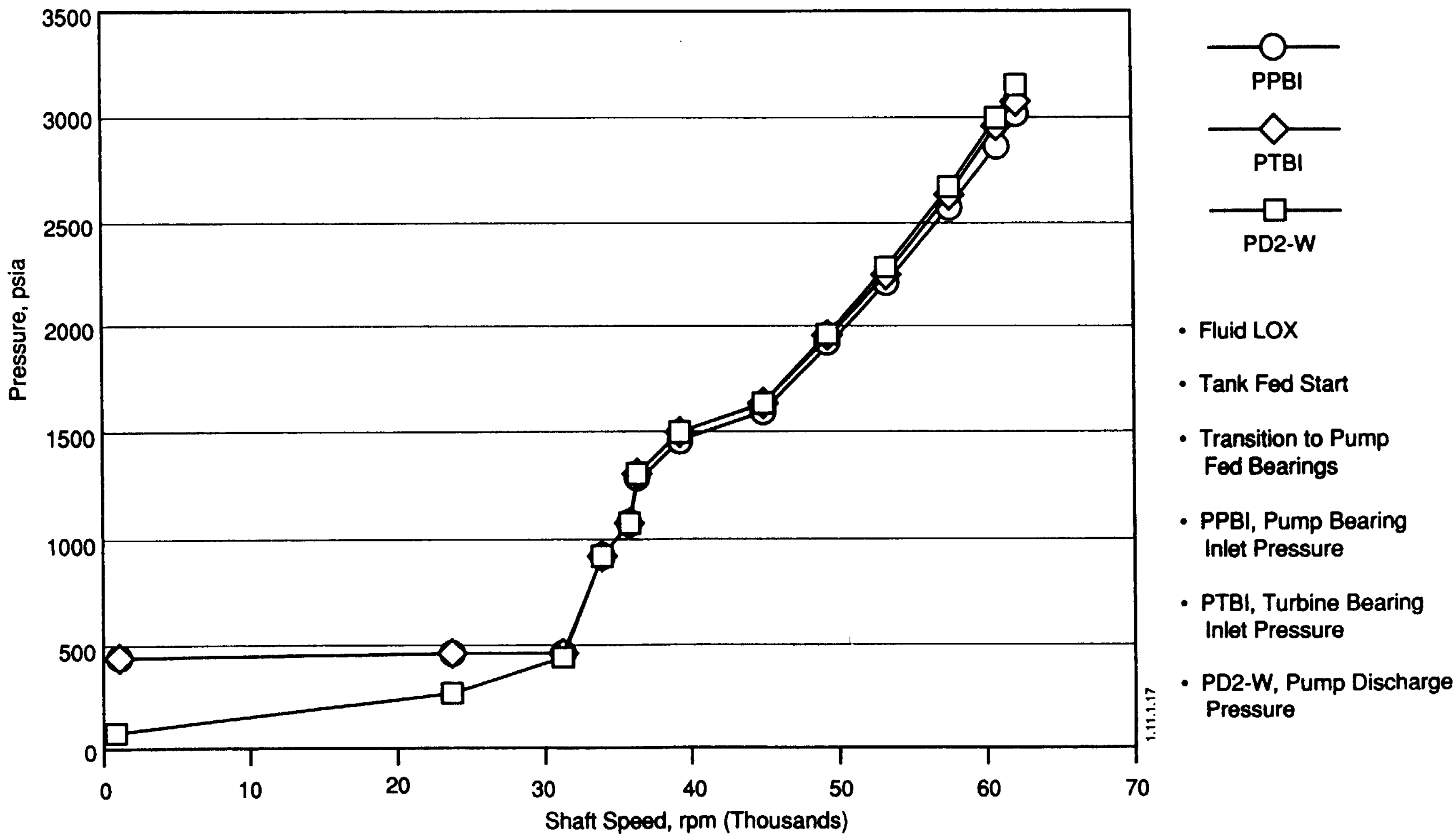

Figure 3.4-11. Bearing Inlet and Pump Discharge Pressures vs Shaft Speed — Test 174

During its operational life the turbopump will have hundreds of starts that begin with a low speed shaft rotation at low oxygen pressure. The LOX has very low viscosity which reduces its lubrication effectiveness. The contacting surface must provide their own capability to rub without significant wearing. It must be a low friction rub otherwise the energy generation becomes a hazard with LOX at all rub points. A well-proven design for such a situation is to have a hard, slick rotating material contacting a softer, yielding stationary material. If there is any wear it should be to the stationary surface which will have sufficient sacrificial thickness to last through the life of the component. A design corollary is that material removed by rubbing must be of a size and composition that will not harm the components downstream. The materials selected were silver bearing plating operating against a hard chrome shaft surface. Silver is a low burn factor material which has high resistance to ignition in oxygen. Energy generated during the transient is dependent on the applied load, the rubbing distance and speed just before lift-off. The pump discharge and bearing pressure as a function of speed is shown in Figure 3.4-12 and Figure 3.4-13 for an unassisted bearing start transient with GN_2 in the turbine (Figure 3.4-12) and with GOX in the turbine (Figure 3.4-13). The load on the rotating system during the start transient is the rotor weight, .6 lb, on the journal bearings and approximately 24 lb axial load on the first stage thrust bearing. This load comes from the pressure-area force differential between the pump inlet (50-70 psi) and the turbine exhaust (ambient). This causes an axial load that would not be there in a flight type turbopump system. The real system is an arrangement where the boost pump, main pump, heat exchanger, and turbine are in series. In that situation only a small pressure drop exists on the rotor, which is a small axial load, during the start transient. In our test setup the inlet pressure was fixed and the turbine back pressure was a function of turbine supply pressure. The pump inlet pressure and the turbine inlet pressure were two separate sources. The start transient was controlled by the turbine inlet supply pressure. As the turbine pressure increased the turbine torque increased and turbine back pressure increased, decreasing the rotor axial load. Turbine pressure ramp rates were keyed to acceleration rates slow enough that they did not decrease pump inlet pressure to less than 40 psia yet

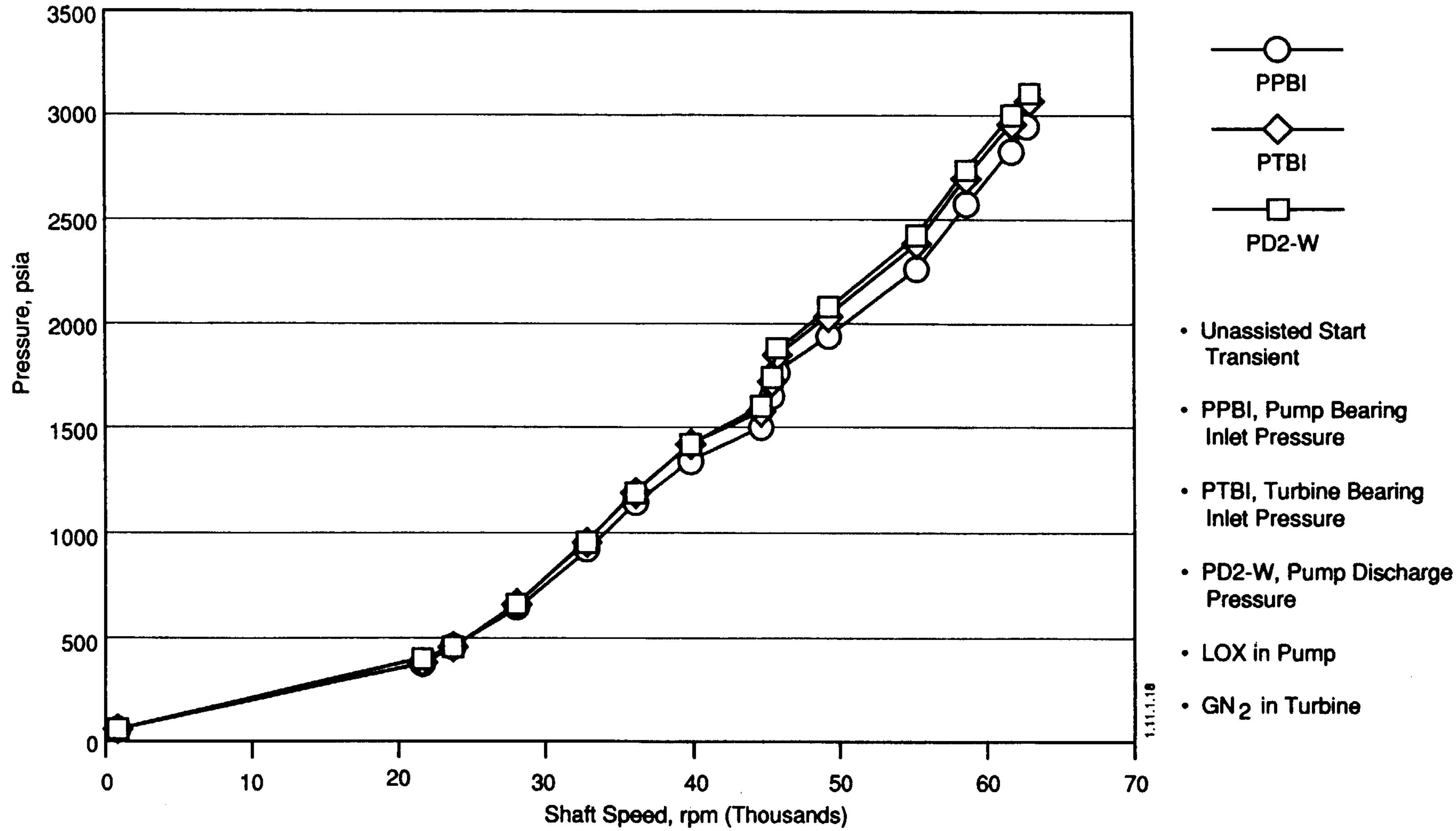

Figure 3.4-12. Bearing Inlet and Pump Discharge Pressures vs Shaft Speed --- Test 183

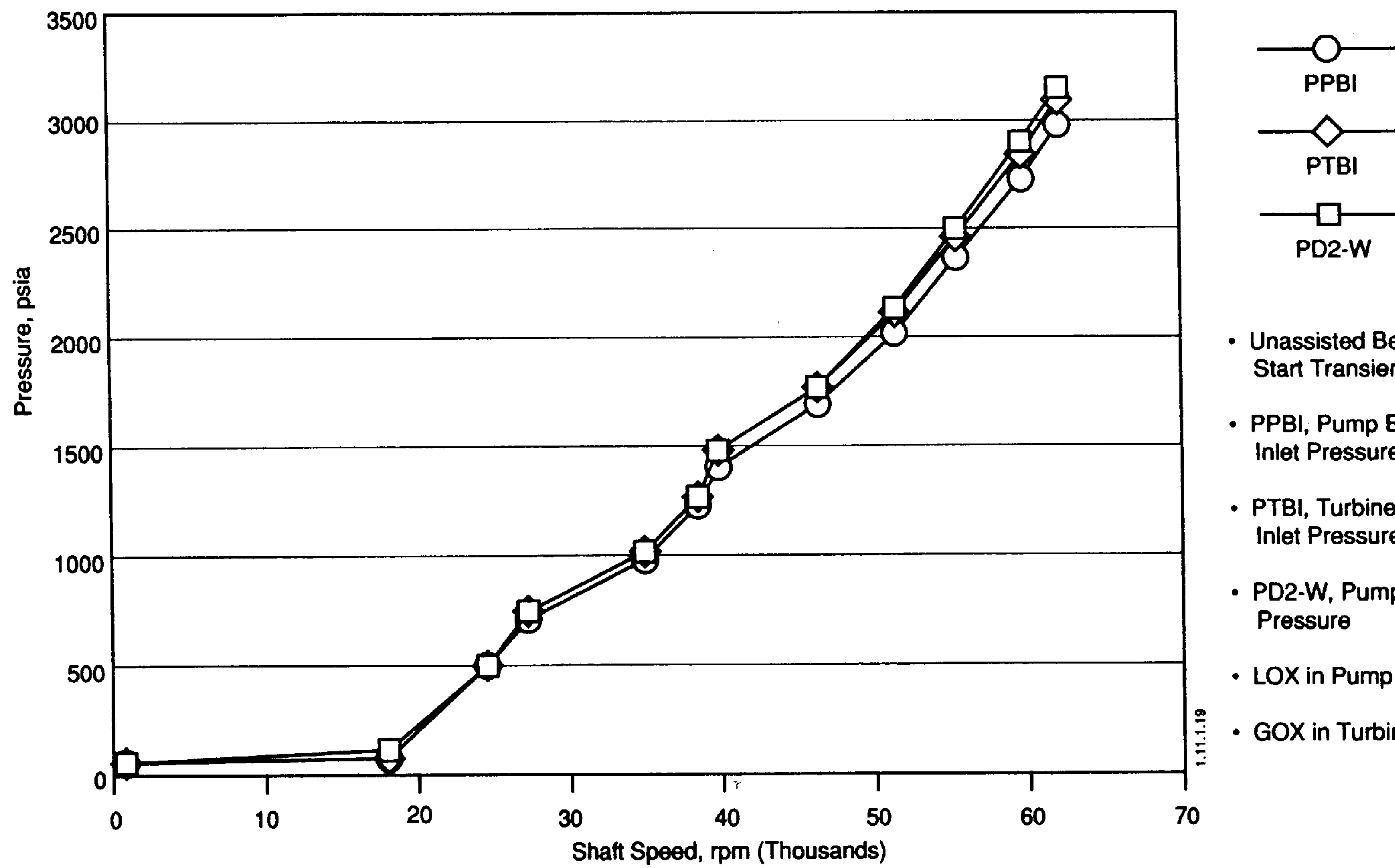

- Unassisted Bearing Start Transient
- PPBI, Pump Bearing Inlet Pressure
- PTBI, Turbine Bearing Inlet Pressure
- PD2-W, Pump Discharge Pressure
- LOX in Pump
- GOX in Turbine

Figure 3.4-13. Bearing Inlet and Pump Discharge Pressures vs Shaft Speed — Test 190

fast enough to achieve the highest shaft speed and pump discharge pressure before supply tank pressure decayed. Typical test pressure vs. time characteristics are shown in Figure 3.4-14.

During these start transients the axial distance detector indicated non-contact rotation after approximately 10 revolutions. The speed at this time was in the range of 15,000 rpm. During the test series D and E1 which were LOX/GN_2 and LOX/GOX tests, respectively, 14 unassisted start/stop transients were performed. The axial thrust bearing condition on teardown after the entire test series was excellent. The journal bearings had some wear which was diagnosed as occurring during the initial rotation tests in LN_2.

Both tank fed and unassisted bearing start transients were demonstrated for this turbopump and both techniques were successful. The bearings did contact with the shaft during unassisted start transients. These tests demonstrated the material wear resistance and oxygen ignition resistance of the design, and the bearing ability to maintain impeller and turbine clearances over the full range of operating conditions.

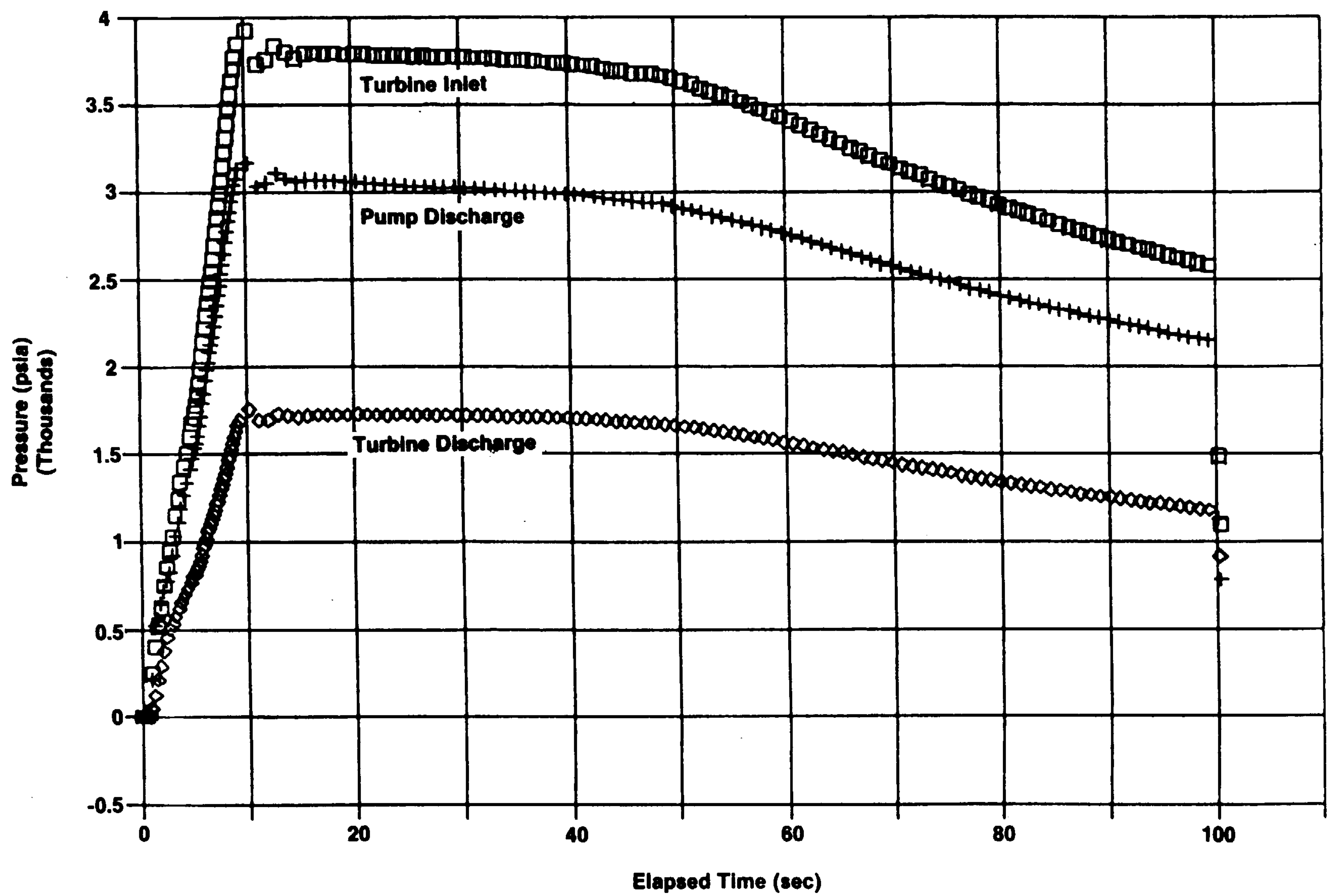

Figure 3.4-14. Typical Pressure vs Time Plot for GOX Driven, Unassisted LOX Bearing Run

3.5 TEARDOWN AND INSPECTION

After completion of test series C, D, and E, the turbopump was taken to Development Operations Assembly clean room for post test inspection. The turbopump was basically in very clean condition. The bolt removal was very positive without any suggestion of galling. Two fittings on the turbine end of the outside housing were starting to gall and therefore were not removed. The outer housing inlet elbow and the the turbine nozzle were removed. At this point, shaft rotation and turbine tip clearance at the tip seal was checked. The shaft rotated freely and the radial clearance between the turbine rotor and the turbine tip seal was consistent with the pre test dimensions. A slight post test eccentricity was observed which is due to the minor rubbing/wear experienced by the bearing components. The measured tip seal clearance is shown in Figure 3.5-1 for concentric and eccentric positions.

The turbopump disassembly was completed and the condition of the major parts are shown in Figure 3.5.2. The general condition was excellent with some local rubs on the journal bearings, shaft journals and impeller vane mating contours. The rotating assembly cross section is shown in Figure 3.5.3 and the rotating assembly after testing in Figure 3.5.4. The turbine end journal surface shows minor scratches and the pump end journal surface shows the burnish work from the balancing procedure and a small groove towards the pump end of the journal. A close up of these two journal surfaces are shown in Figures 3.5-5 and 3.5-6. A profile of the turbine end surface is shown in Figure 3.5-7 indicating minor scratches. An axial profile trace at the pump end journal surface is shown in Figure 3.5-8. This shows a sharp groove approximately .0013 in. deep at the approximate axial location of the pocket to exit land entrance. This groove would suggest a particle possibly trapped in the pocket wearing on the chrome coated shaft surface.

The first stage impeller thrust surface, Figure 3.5-9, shows some minor circumferential scratches in the area of the mating hydrostatic bearing pocket. This was the highest loaded bearing of the system during the unassisted start transients.

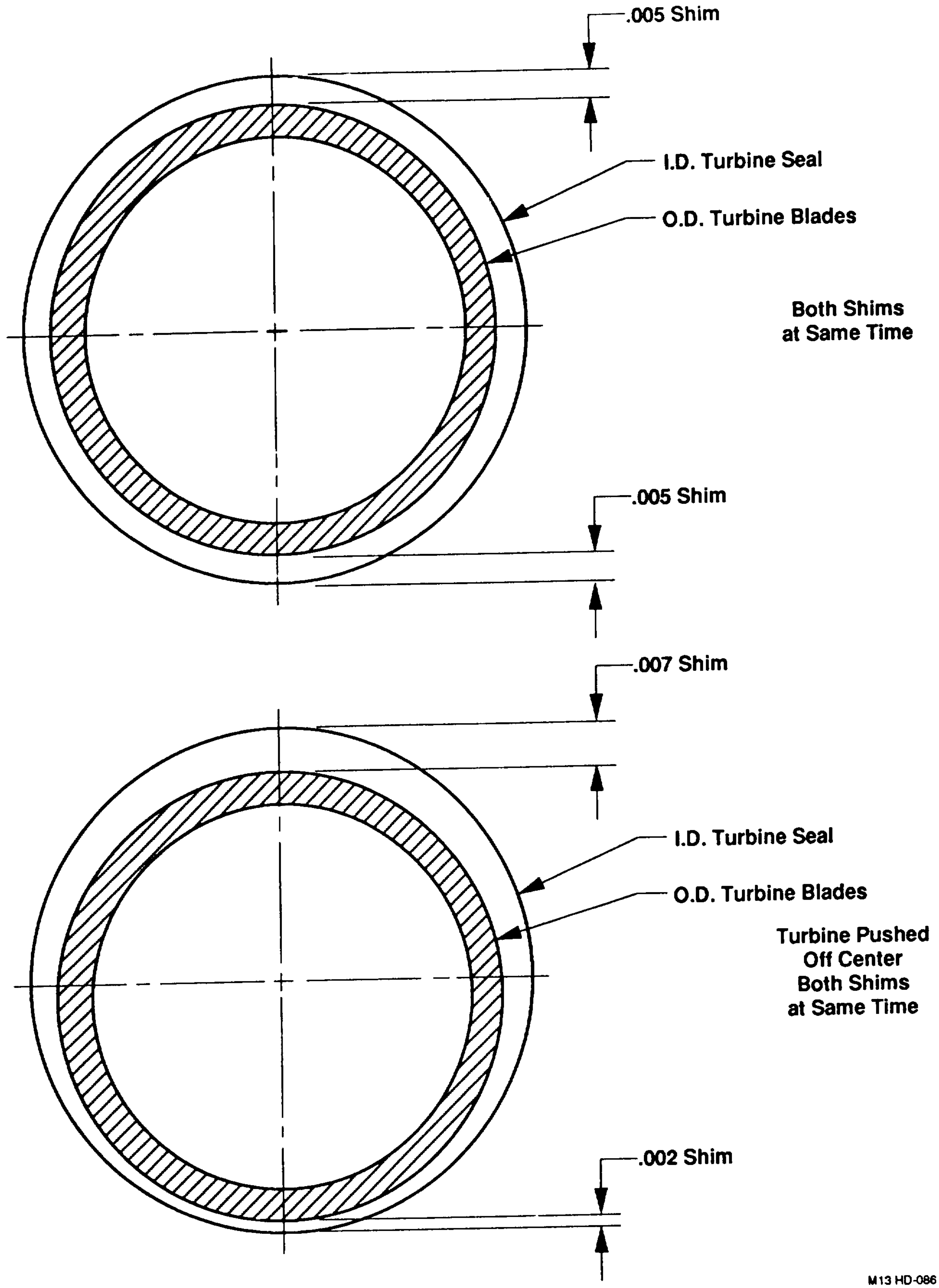

Figure 3.5-1. Turbine Tip Clearance Check

ATC Photo #C0489 1875

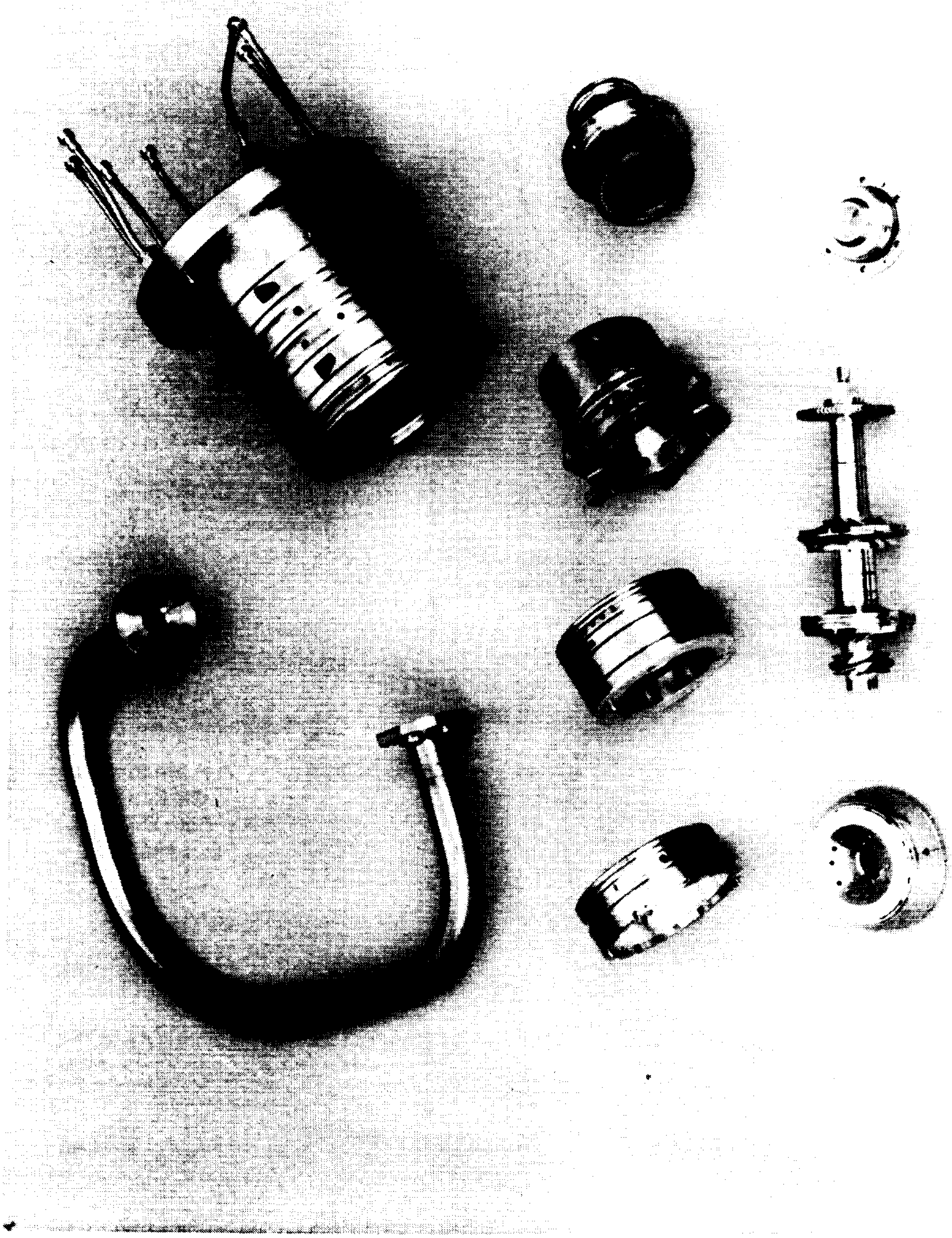

Figure 3.5-2. OTV TPA Components

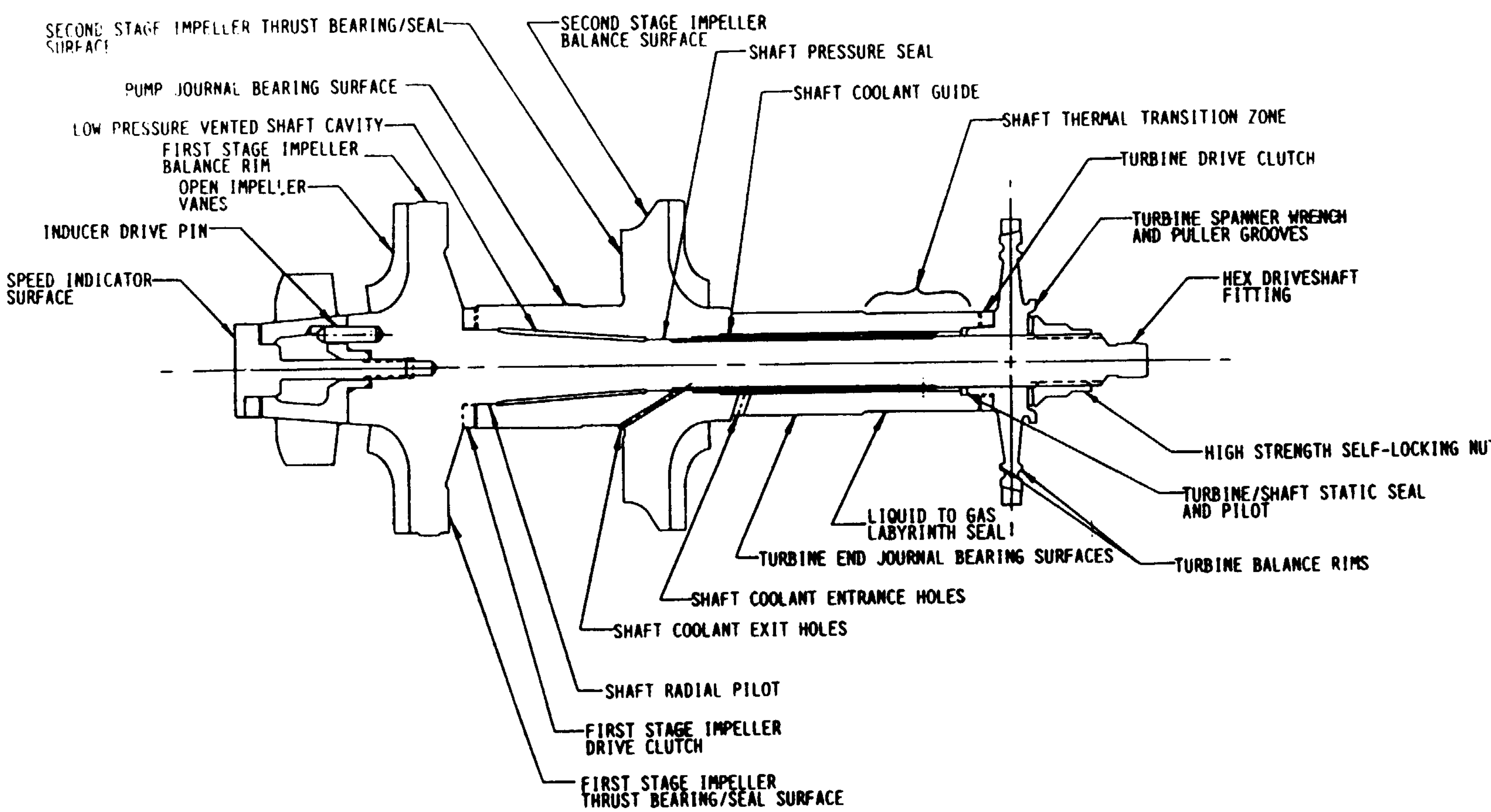

Figure 3.5-3. OTV OTPA Rotating Assembly

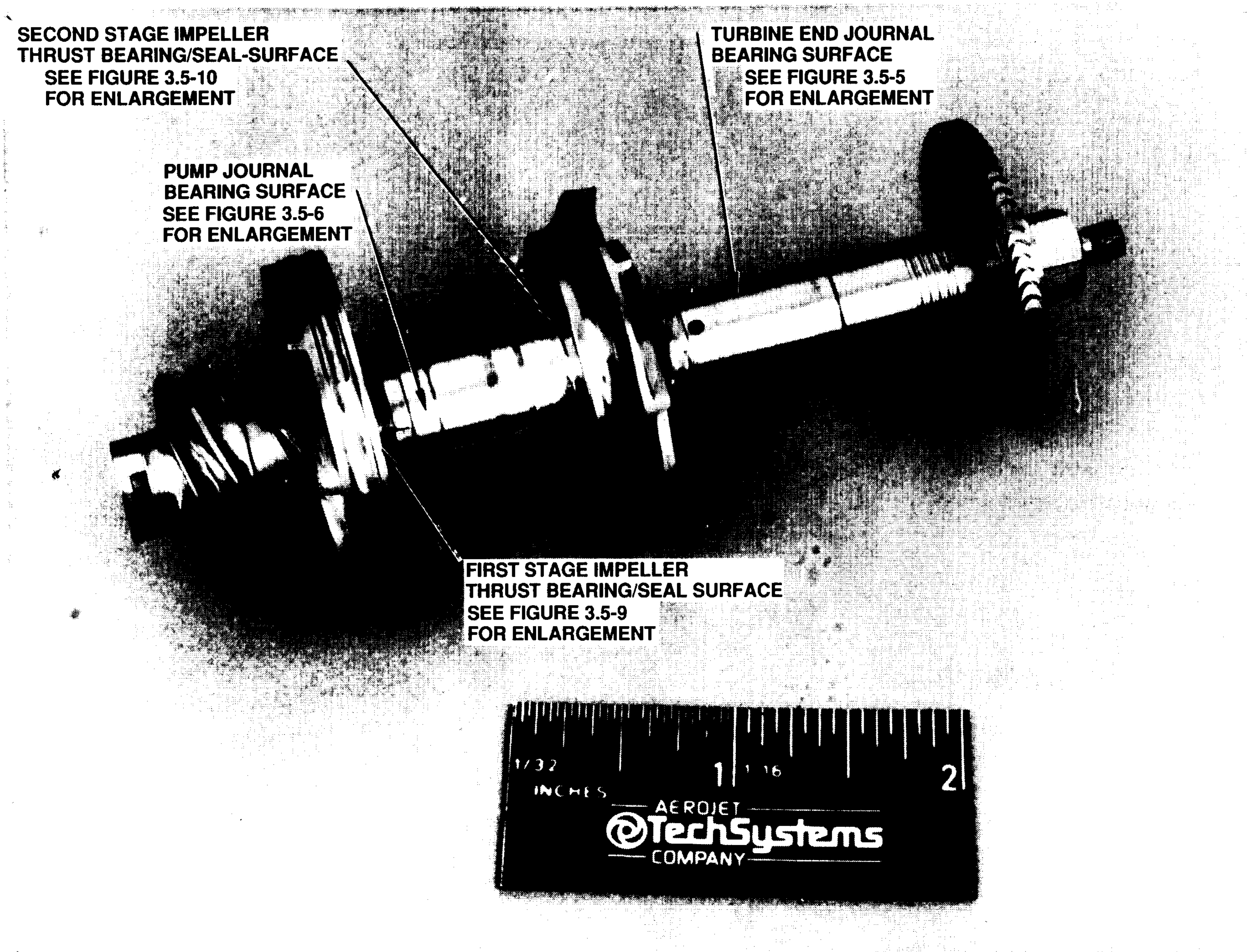

Figure 3.5-4. OTV Oxygen Turbopump Rotating Assembly – Post Test

ATC Photo #C0489 1874

Figure 3.5-5. Turbine End Journal Bearing Shaft Surface – Post Test

ATC Photo #C0489 1861

ORIGINAL PAGE
BLACK AND WHITE PHOTOGRAPH

Figure 3.5-6. Pump Journal Bearing Shaft Surface – Post Test

ATC Photo #C0489 1860

C-2

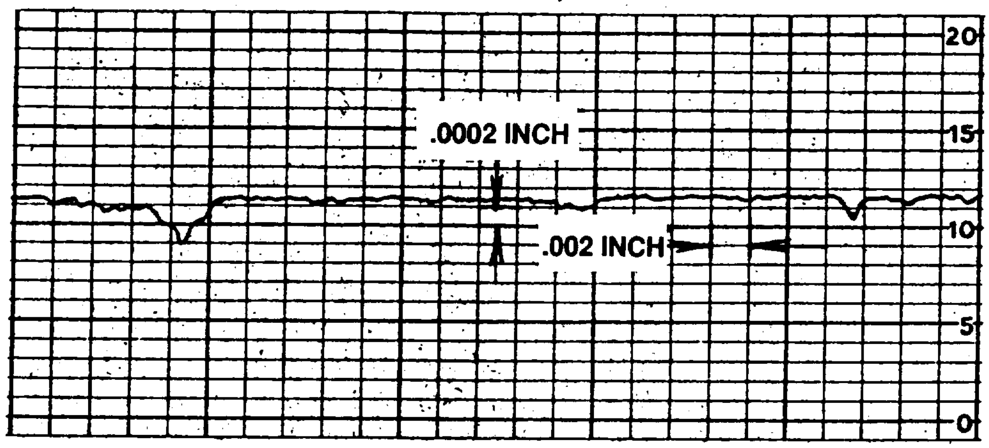

Figure 3.5-7. Profile of Turbine Bearing Journal Surface Along Shaft Axis

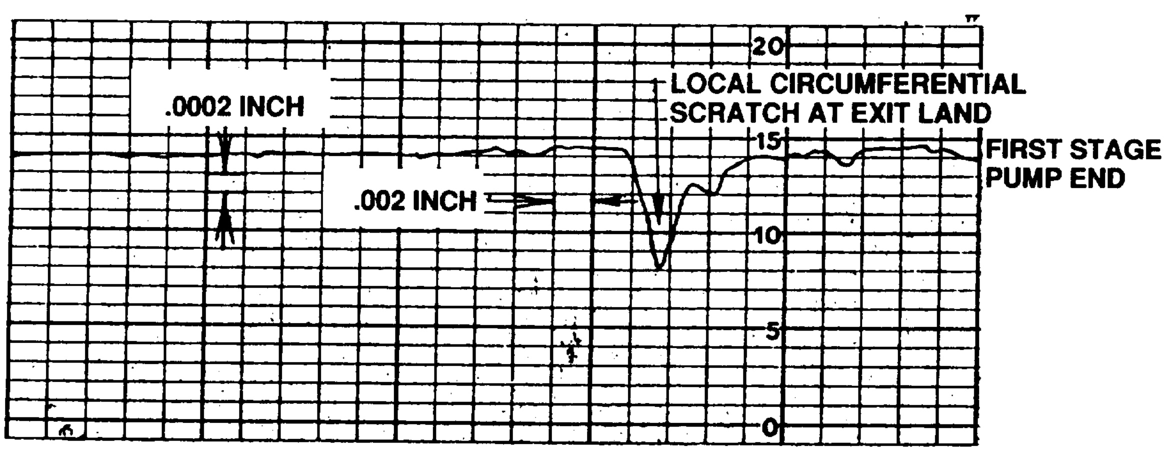

Figure 3.5-8. Profile of Pump Bearing Journal Surface Along Shaft Axis

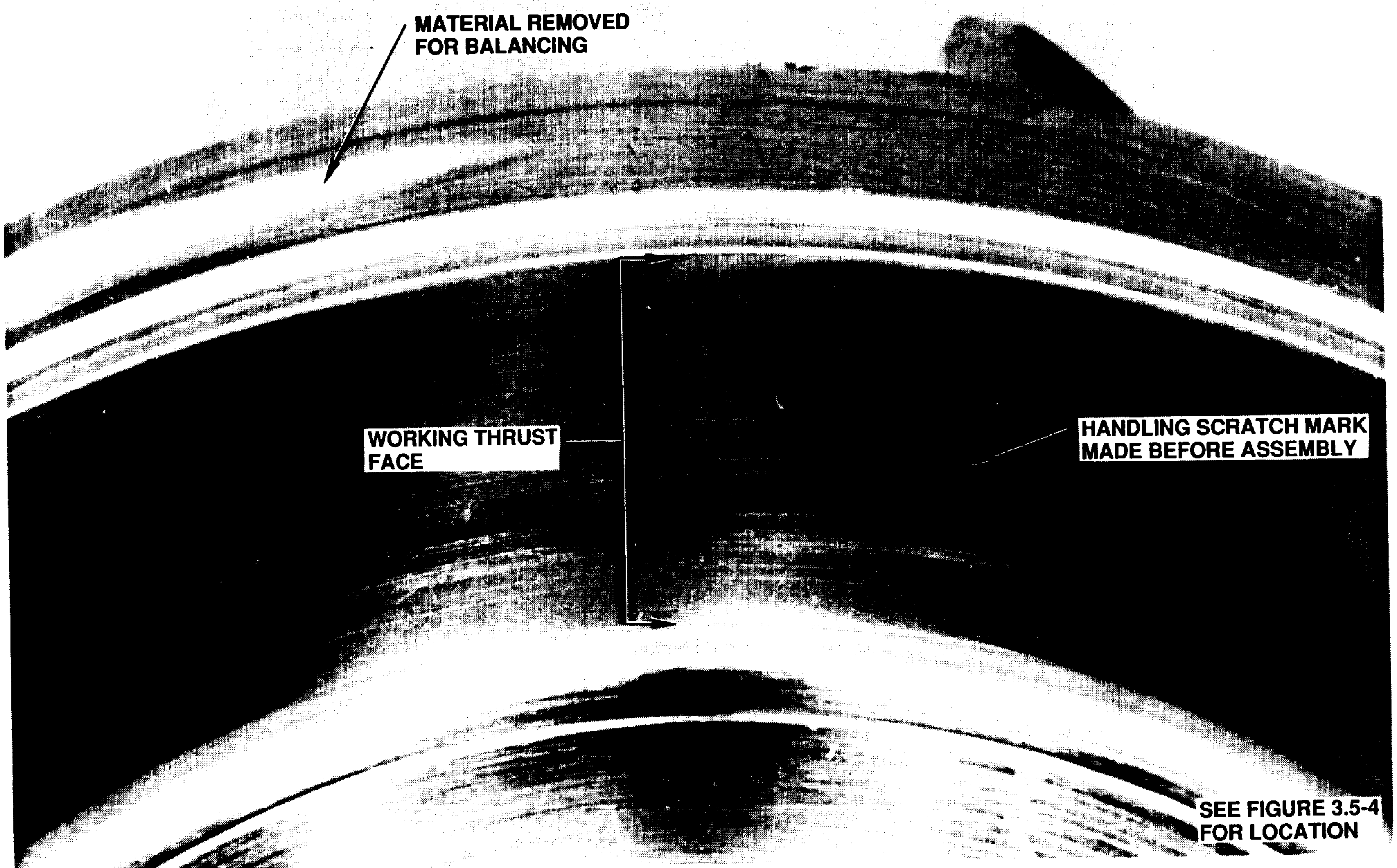

ATC Photo #C0489 1859

Figure 3.5-9. First Stage Impeller Thrust Surface – Post Test

ORIGINAL PAGE
BLACK AND WHITE PHOTOGRAPH

The second stage impeller thrust surface, Figure 3.5-10, indicates essentially no contact. The radial marks over the surface are grinding marks under the thin dense chrome coating on this surface.

The condition of both the pump end bearing and the turbine end bearing are shown in Figure 3.5-11. Generally the condition of both bearings is very good. The pump and thrust bearing face shows some material collection at the end of the pockets and material removed from the journal bearing bore at the exit land adjacent to the first impeller. The spherical surface was in excellent condition and all passages within the bearing were clean and free of any obstructions. The turbine end bearing had some material removed from the exit land at the turbine side. Disassembly of this part showed the spherical surface to be in excellent condition again with all passages clean and free of any obstructions. A close up view of this bearing surface is shown in Figure 3.5-12. From the close up photo it appears that some of the silver plate may have been mechanically dislodged or smeared and became a third member wear particle. The profile of this surface is shown in Figure 3.5-13.

Close up photos of the pump bearing from the first stage side, Figure 3.5-14, and from the second stage side Figure 3.5-15 show that the wear occurs at the first stage exit land. A significant portion of the silver plating on the exit land has been removed or smeared in the circumferential direction. An axial surface profile across the bearing bore between the four pockets is shown in Figure 3.5-16. From these profiles and the photos it is obvious that the predominant wear occurred on the exit land. The rest of the bore is close to original condition. It appears that once wear started on the exit land the debris moved circumferentially removing the silver plating. Mentioned earlier was the fact that a groove was carved in the chrome coating on the shaft. This would indicate a hard particle to wear a groove in the hard chrome surface. With this exit land worn the journal bearing flowrate will increase. Subsequent disassembly of the pump end bearing supply filter showed a ruptured filter element. In addition, the pressure drop on this filter was higher than the turbine end filter and also varied with time. The conclusion is that debris passed through the pump journal bearing.

ATC Photo #C0489 1858

Figure 3.5-10. Second Stage Impeller Thrust Surface – Post Test

ORIGINAL PAGE
BLACK AND WHITE PHOTOGRAPH

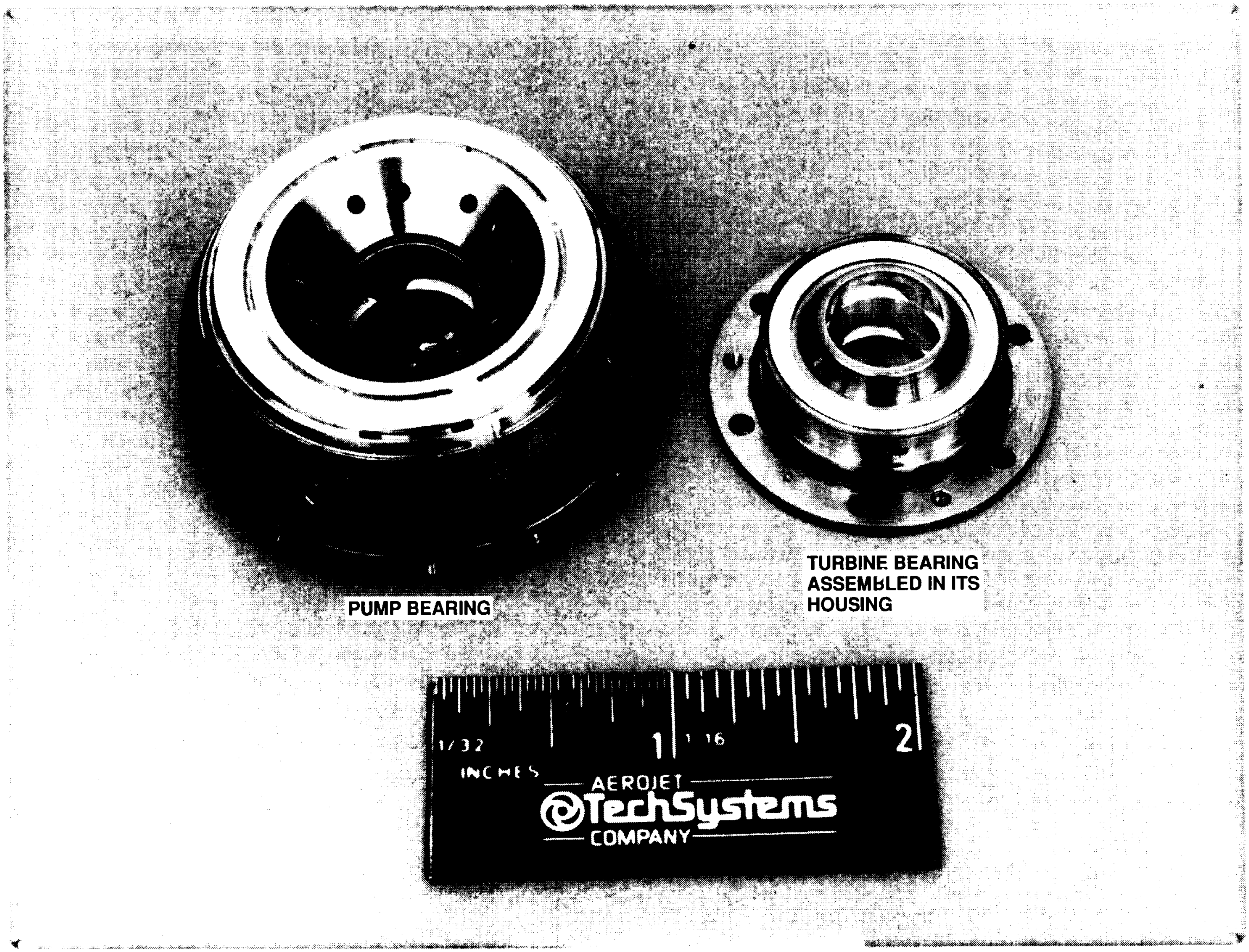

Figure 3.5-11. Pump and Turbine Bearing Post-Test

ATC Photo #C0489 1873

ORIGINAL PAGE
BLACK AND WHITE PHOTOGRAPH

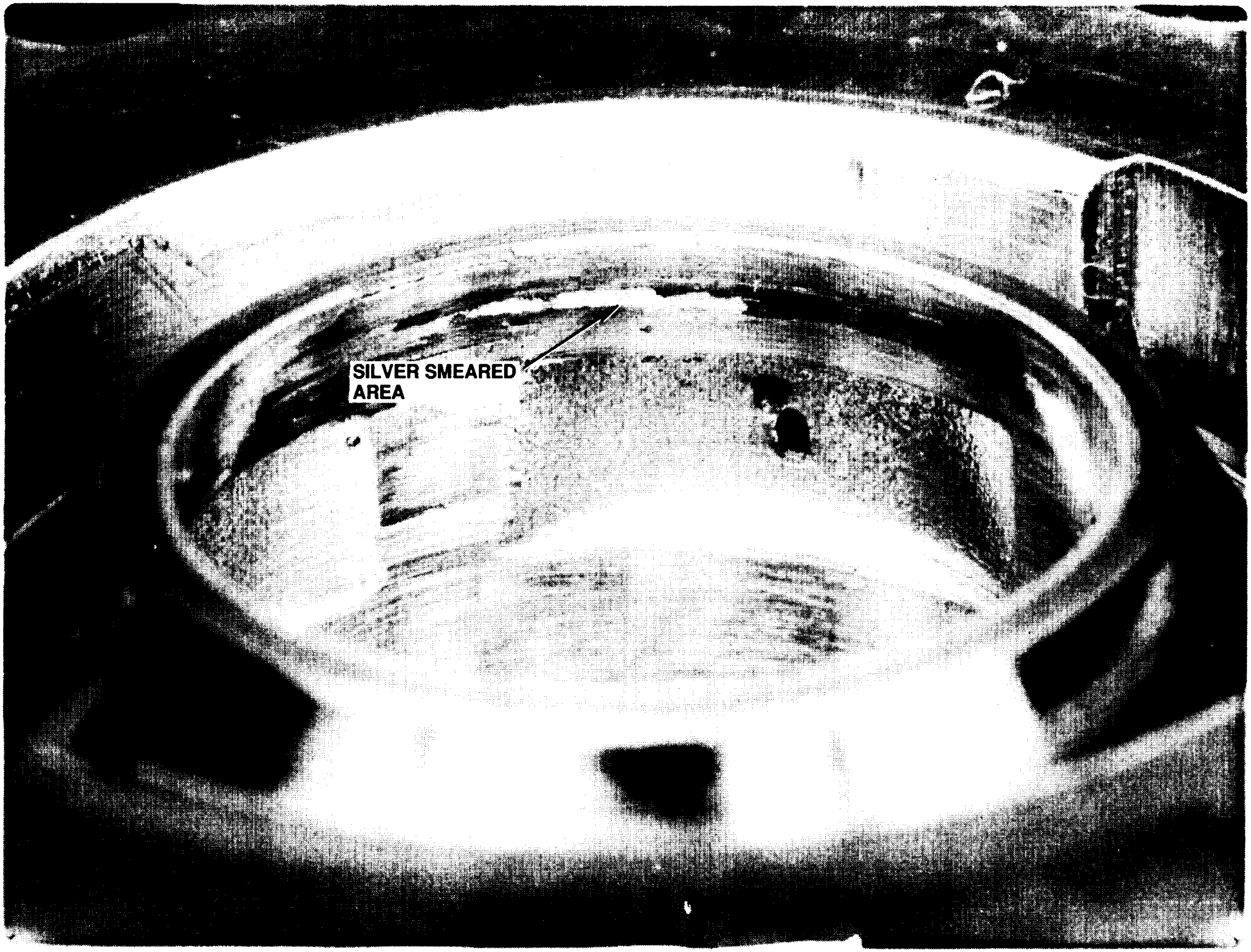

ATC Photo #C0489 1865

Figure 3.5-12. Turbine Bearing Bore

ORIGINAL PAGE
BLACK AND WHITE PHOTOGRAPH

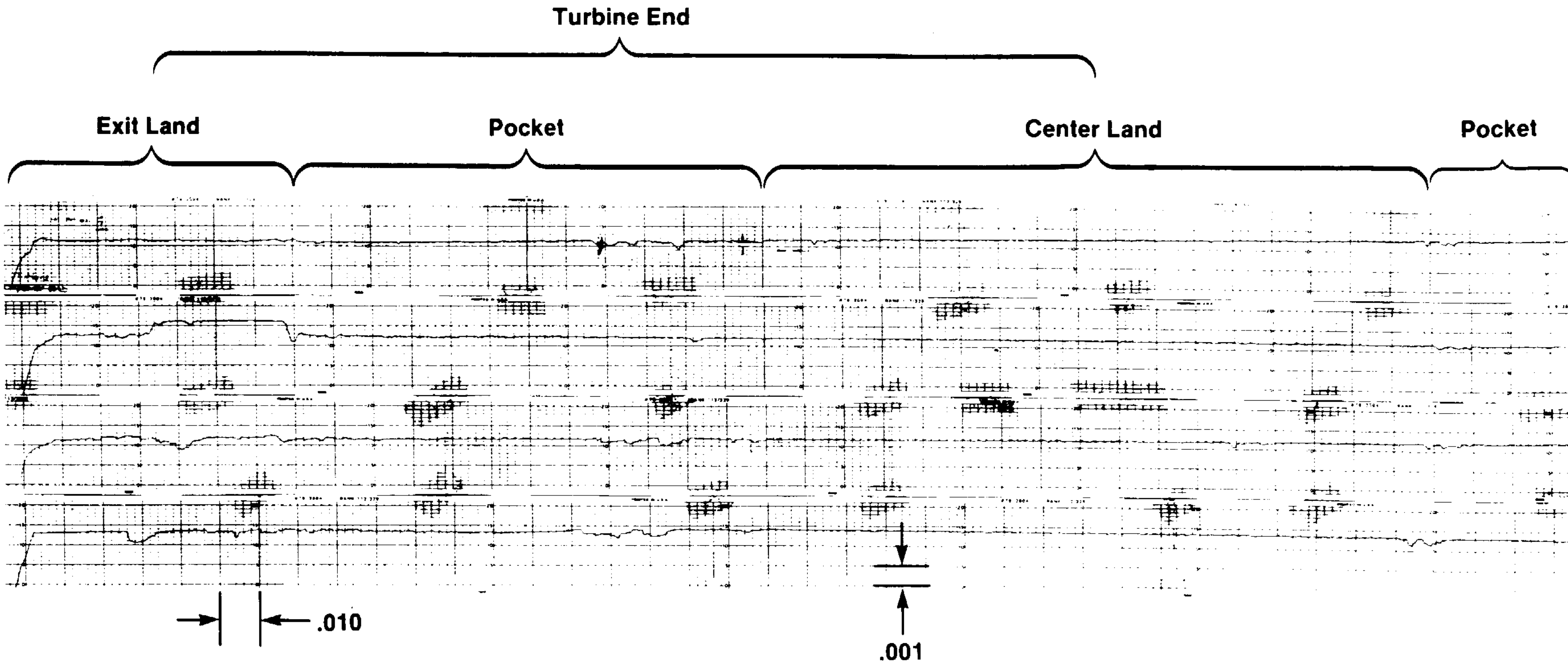

The Four Profiles Represent Surfaces at 90° Circumferential Between Pockets

Figure 3.5-13. Turbine Bearing Journal Profiles

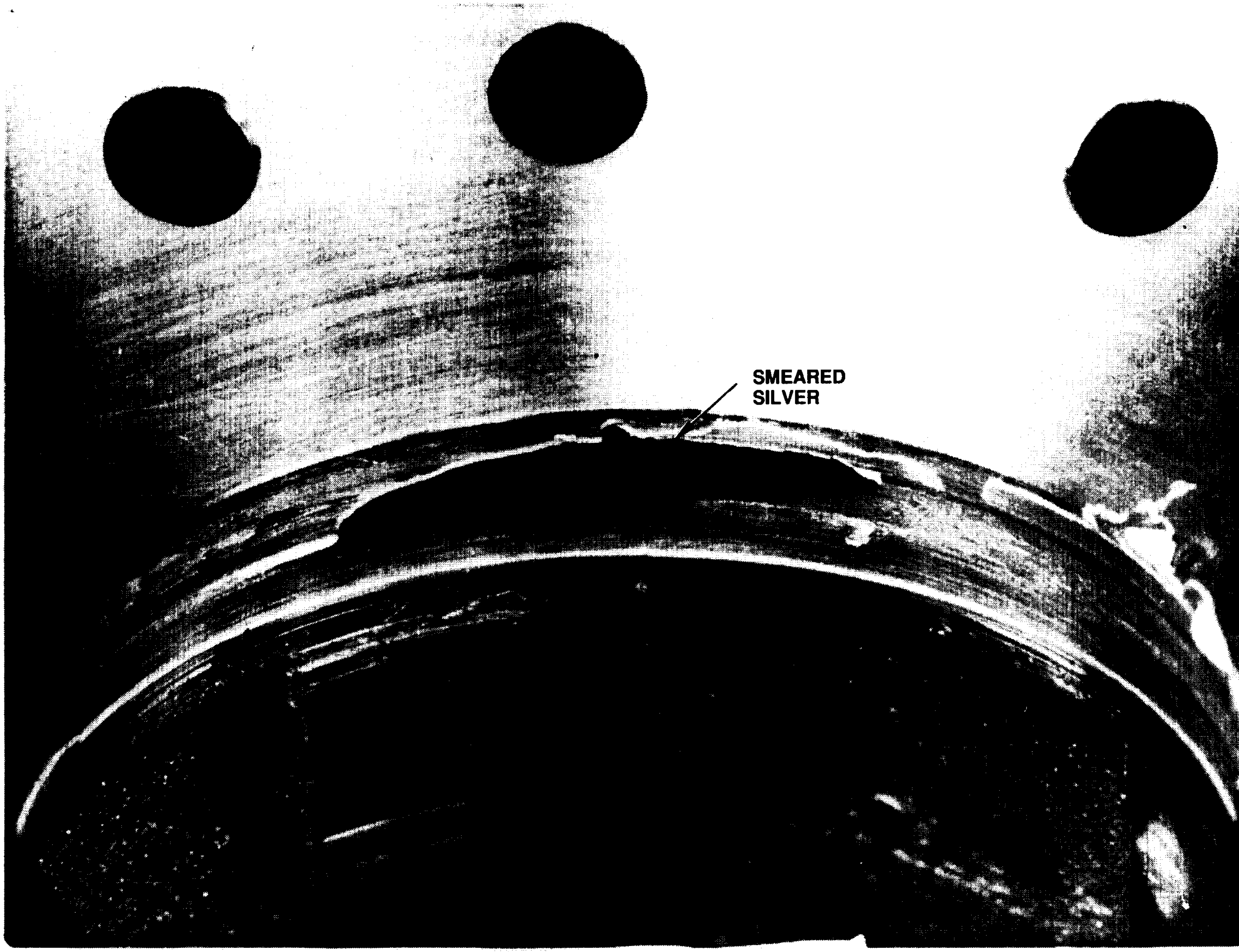

Figure 3.5-14. Pump Bearing Bore View Looking From the First Stage Impeller Side ATC Photo #C0489 1855

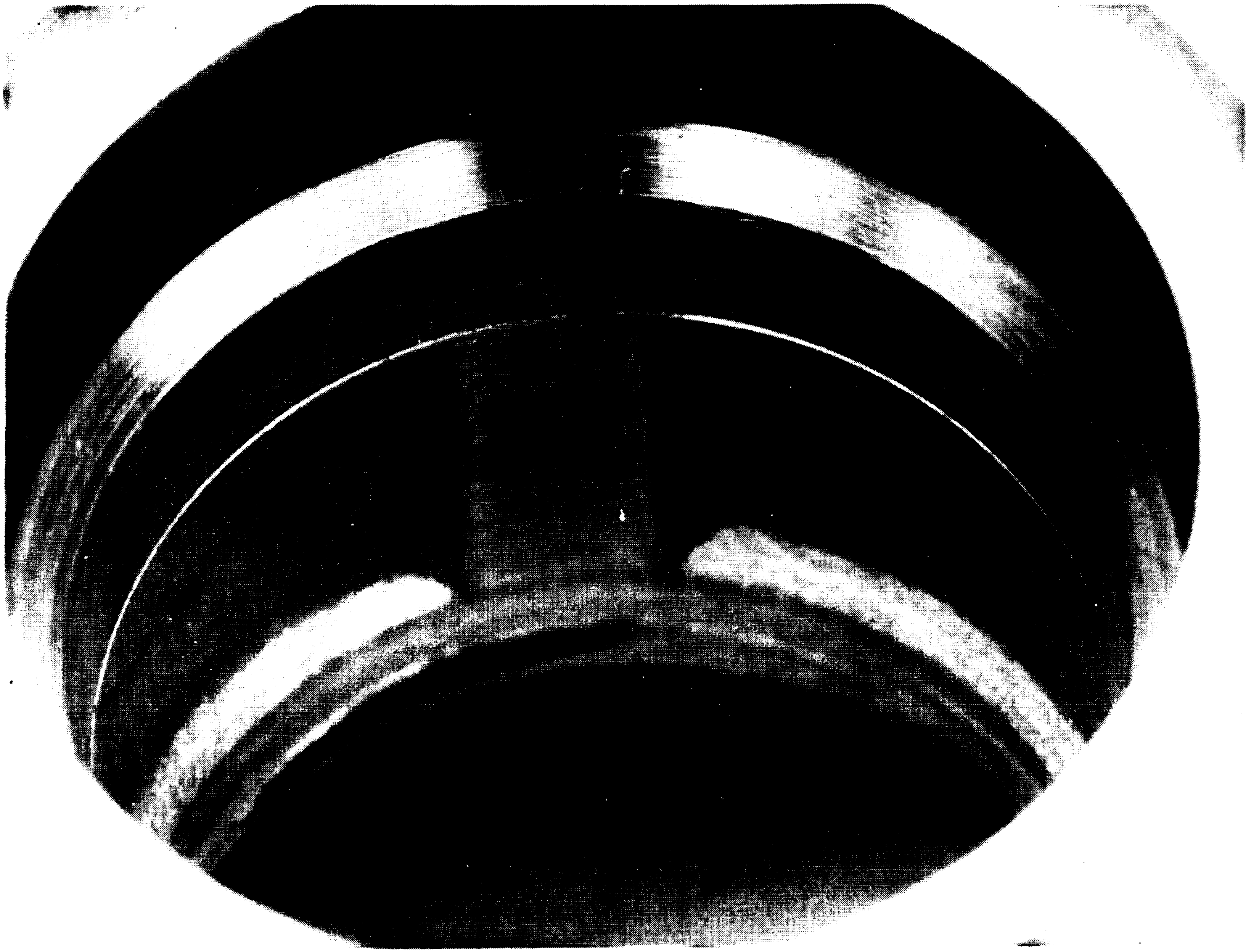

Figure 3.5-15. Pump Bearing Bore View From 2nd Stage Pump Side

ATC Photo #C0489 1854

FOLDOUT FRAME /

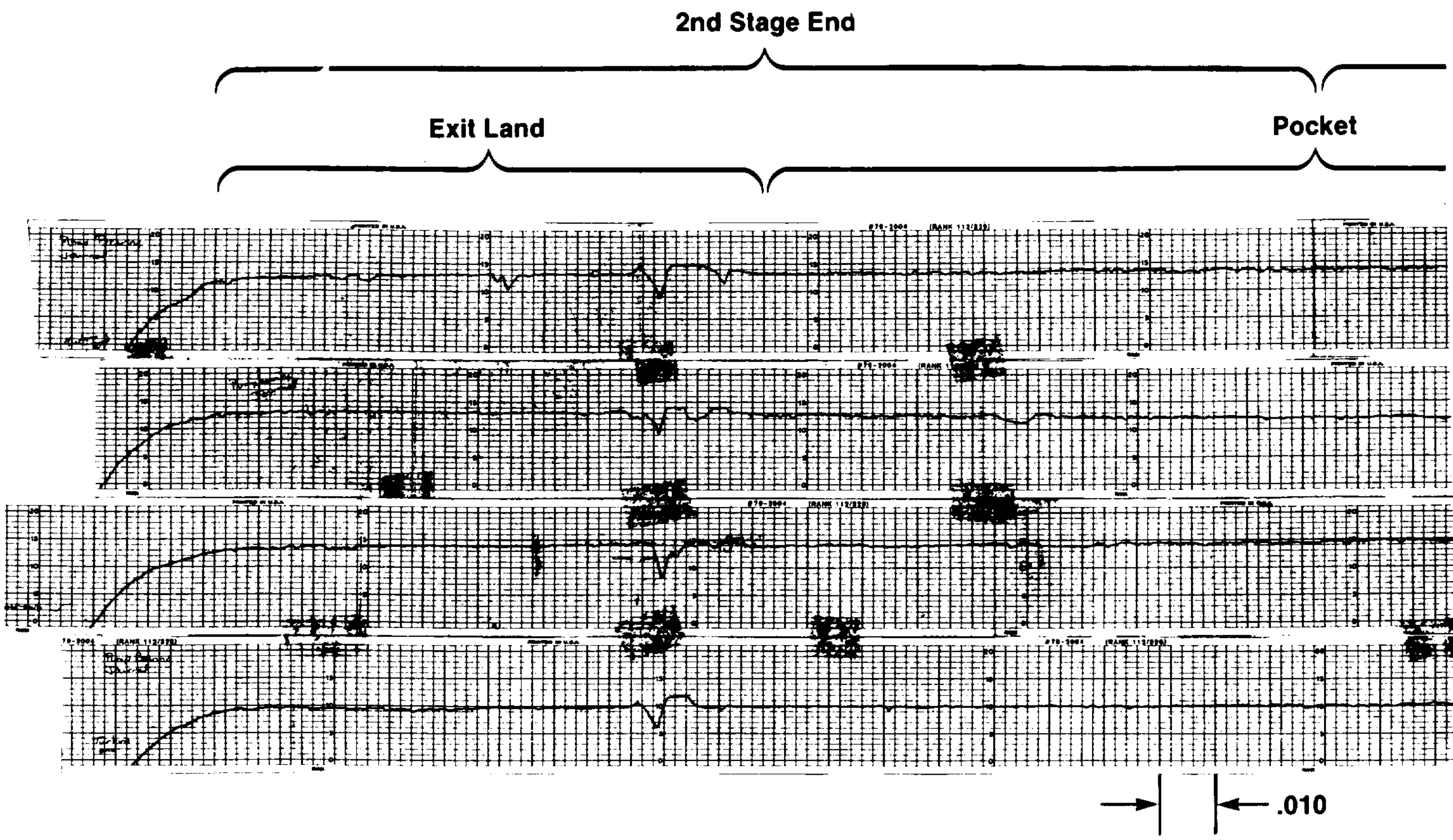

FOLDOUT FRAME 2

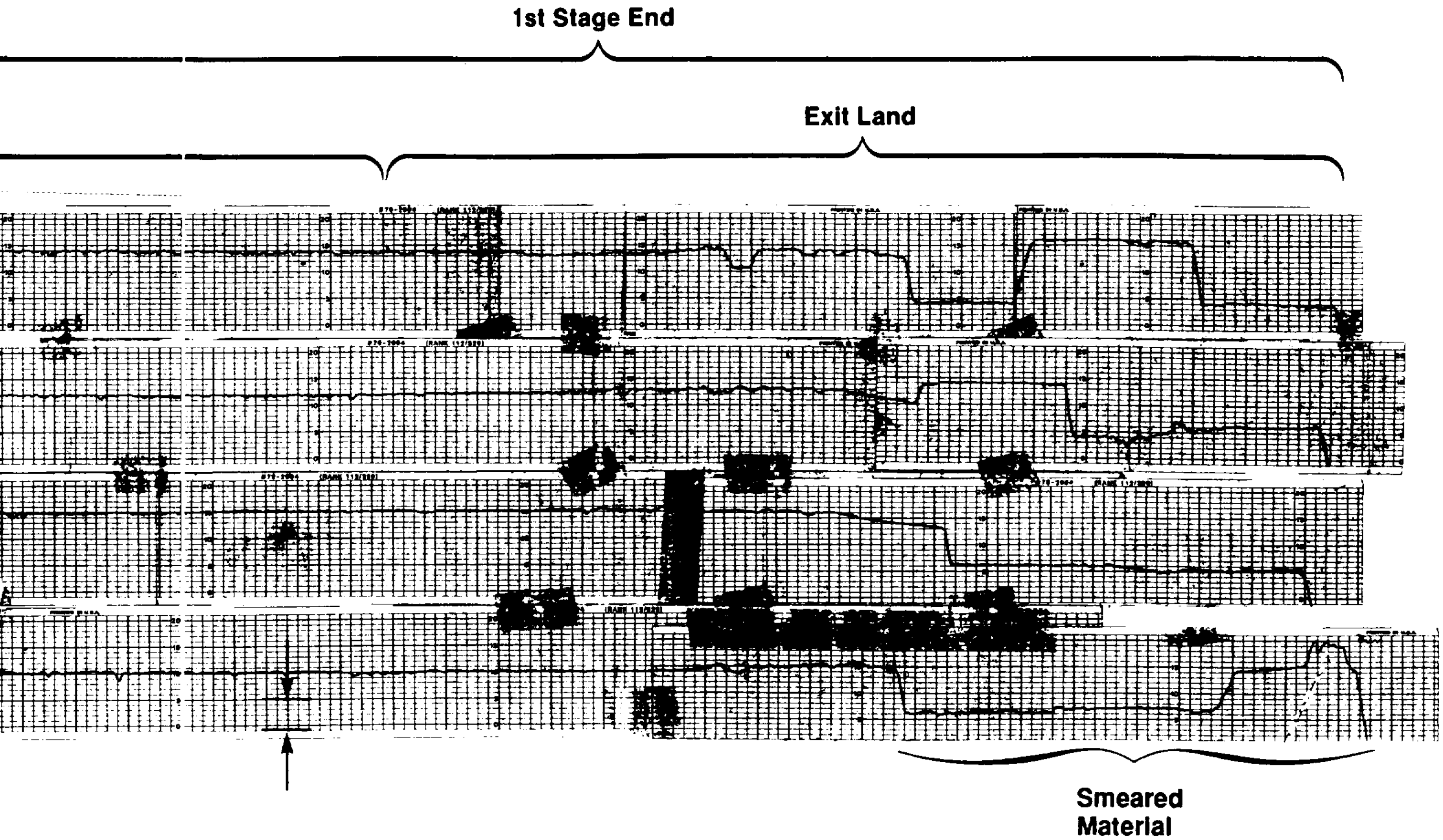

Note: The Four Axial Profiles Represent Surfaces at
90° Circumferential Between Pockets

Figure 3.5-16. Pump Bearing Journal Profile

3.5, Teardown and Inspection (cont.)

The first stage thrust bearing is shown in Figure 3.5-17. There is some scuffing of material between the pockets and the mating rotating surface and this is the highest loaded bearing surface during the start transient. There are slight burnish marks on the inlet and exit lands. The second stage thrust bearing surface is shown in Figure 3.5-18. This surface shows some minor circumferential scratches between pockets and just inside the pockets. In evidence are random surface scratches that have occurred during manufacturing and handling over the past two years.

The pump bearing cup is shown in Figure 3.5-19. The silver sphere is in excellent shape but with several discoloration marks near the sphere outside diameter. These marks are shown close up in Figure 3.5-20. Contact scratches were evident in this zone with corresponding discolored marks on the pump bearing sphere. Contact at this location on the sphere is a logical condition. This location on the sphere is at a maximum diameter and the radial clearance is not adjustable. The axial clearance is adjustable to compensate for increasing load with increasing pump pressure. In addition as axial load is applied to the bearing cup the cup tends to twist about a diametral axis inward at the maximum diameter. Contact locations are diagrammed in Figure 3.5-21 for the sphere and the pump journal bearing. Light contact is not considered detrimental.

The second stage impeller housing shown in Figure 3.5-22, is in excellent condition. Two things were found on this part. First, there was slight trace of discoloration in the pump inlet and a small amount in the bearing area. This substance was a very thin tan powder (oxidation?). There was the same substance in the first stage diffuser passage but not in the crossover passages. Second, a small amount of impeller vane contact on the silver housing contour was experienced. This minute contact is shown close up in Figure 3.5-23. This contact occurred where the radial surface of the impeller housing contour enters the housing inner radius. This was the point of minimum clearance during the turbopump assembly and probably contacted during assembly.

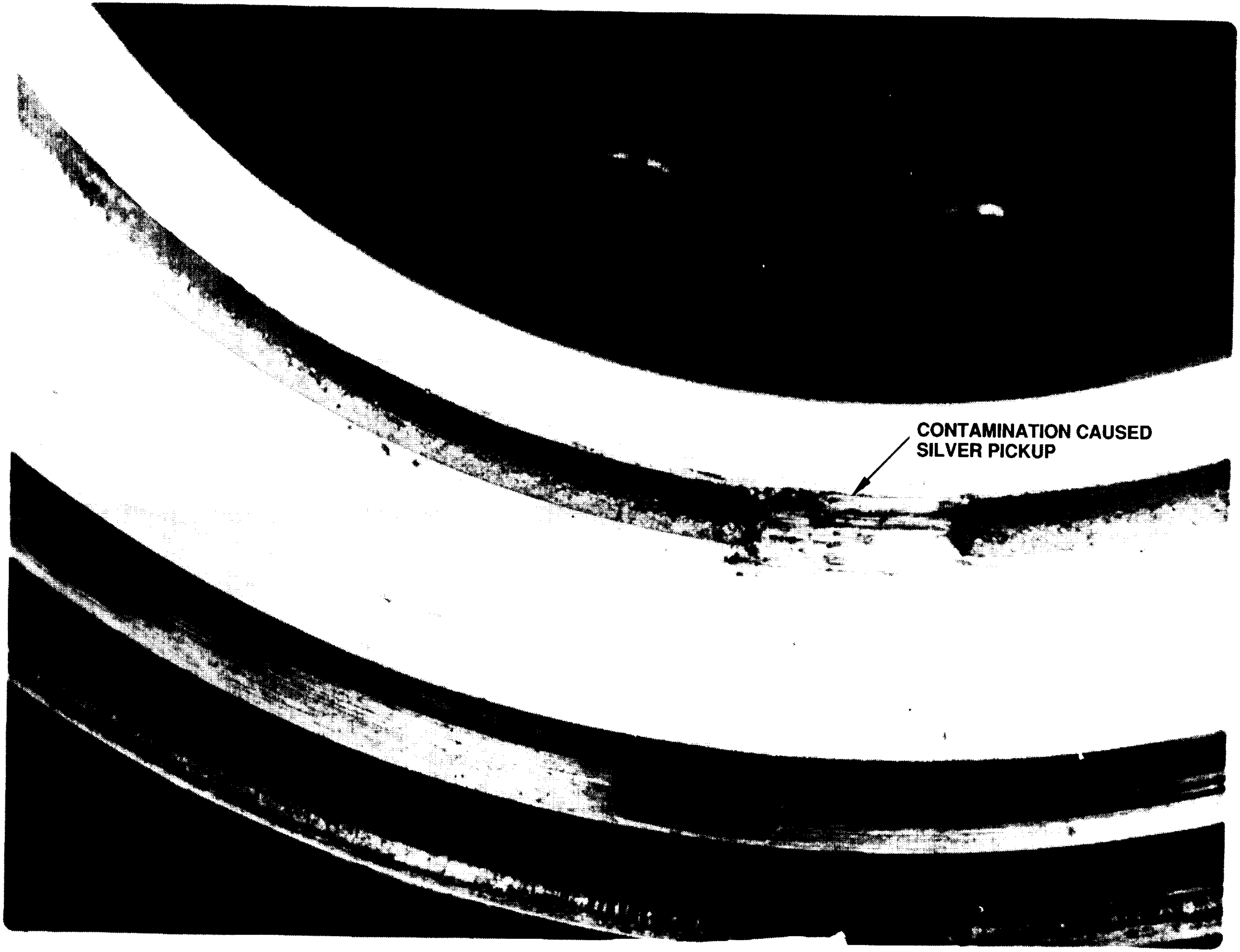

Figure 3.5-17. First Stage Thrust Bearing Surface

ATC Photo #C0489 1864

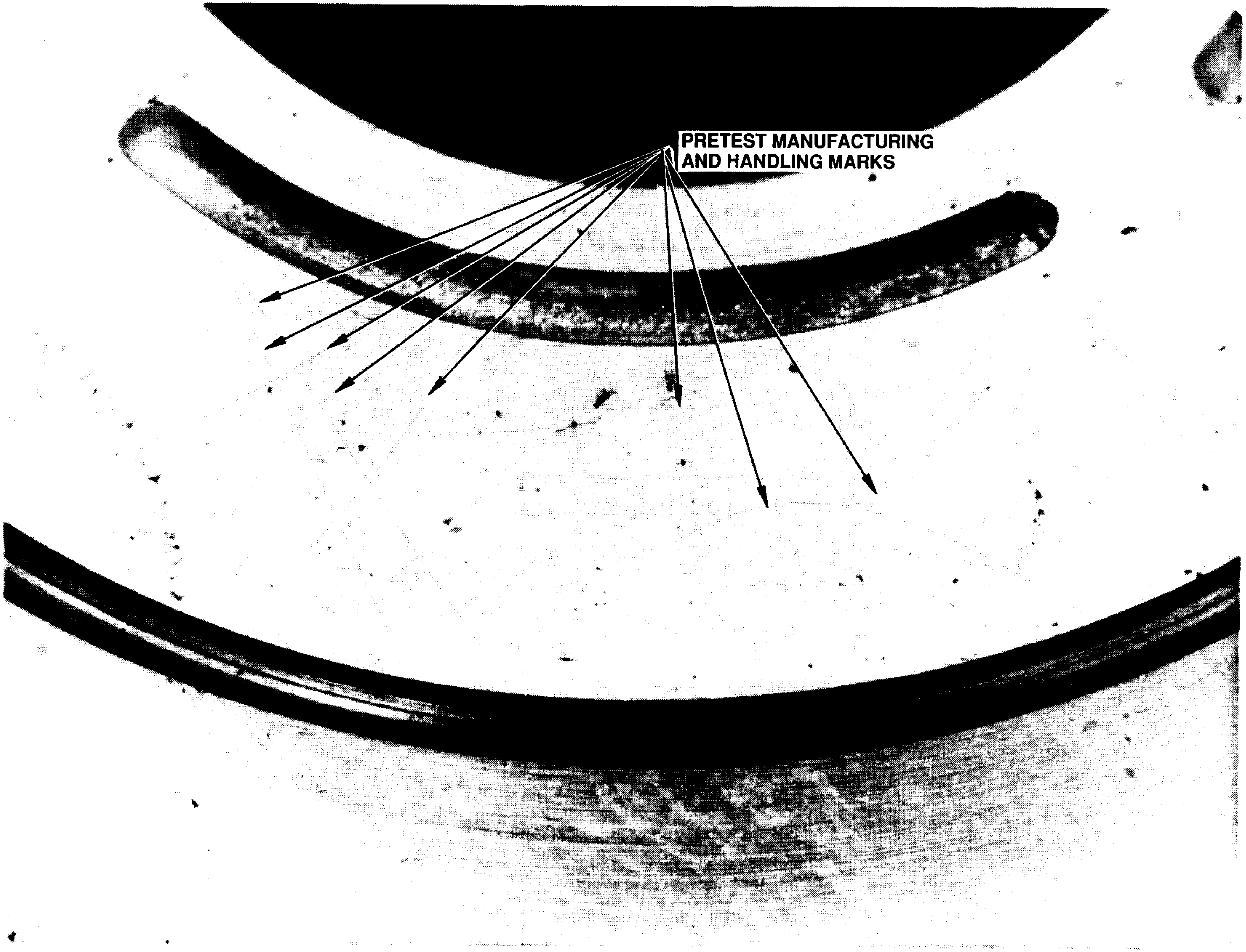

Figure 3.5-18. Second Stage Thrust Bearing Surface Post Test

ATC Photo #C0489 1863

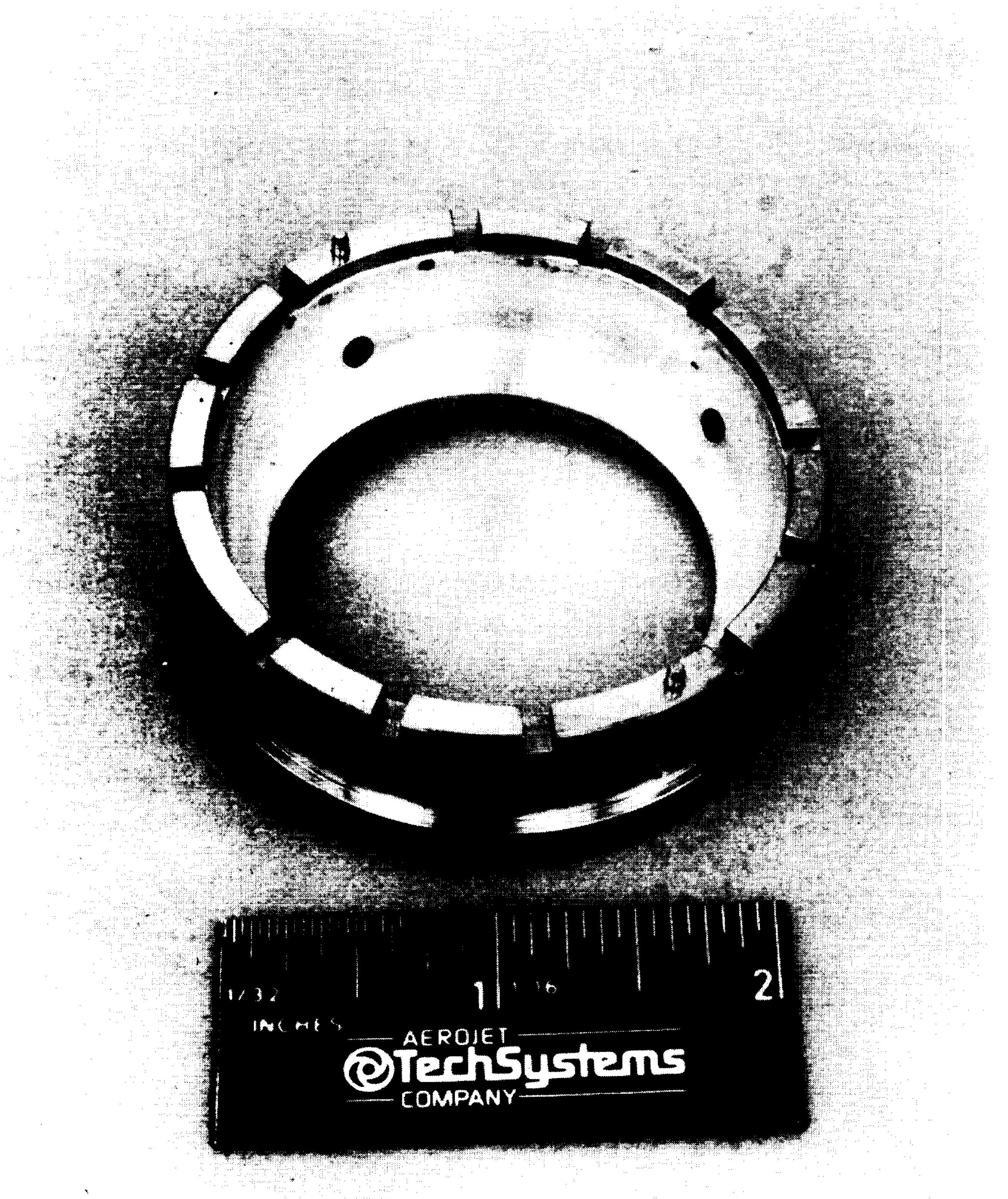

Figure 3.5-19. Pump Bearing Housing ATC Photo #C0489 1872

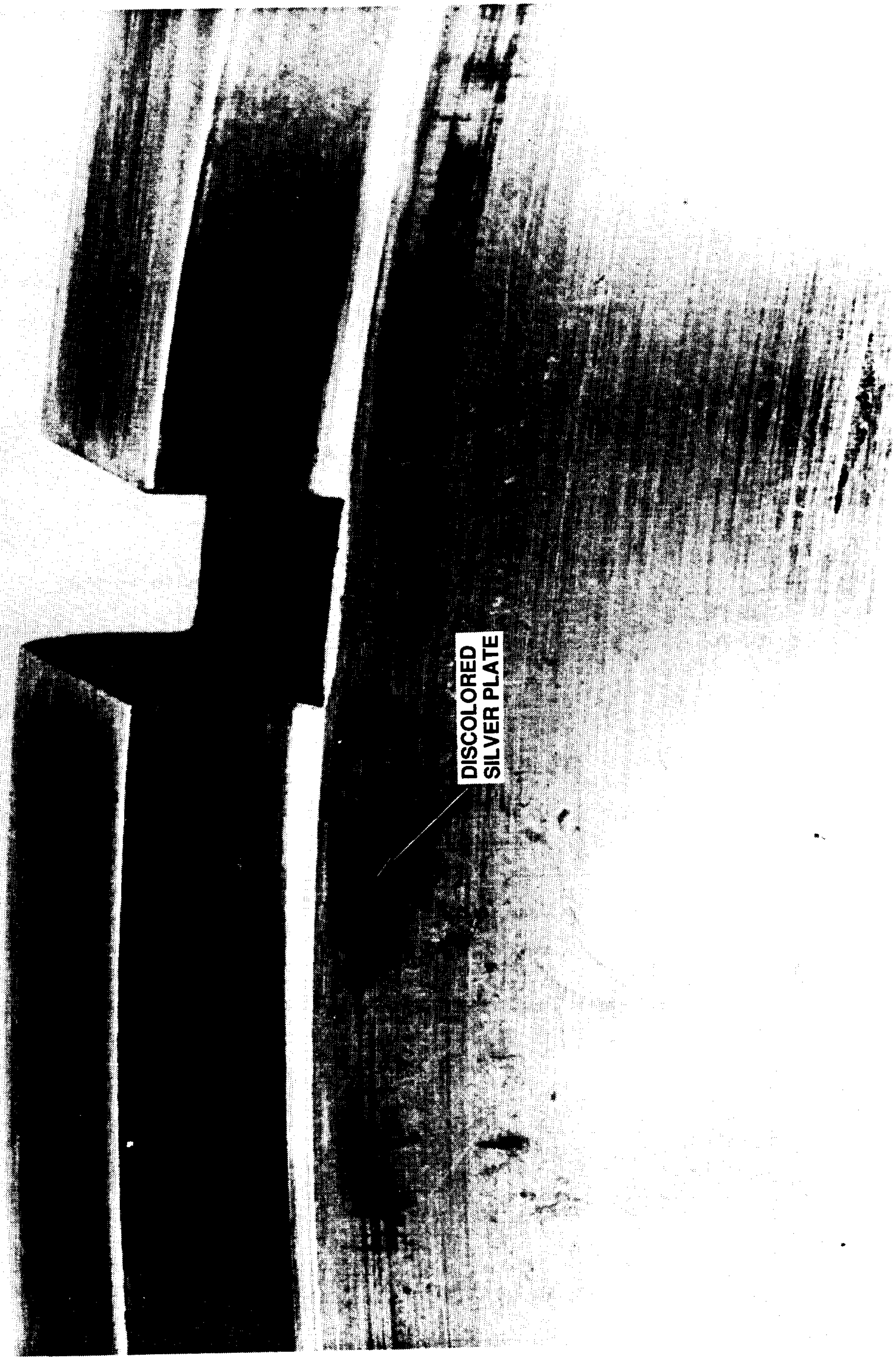

ATC Photo #C0489 1868

Figure 3.5-20. Pump Bearing Housing Cup Silver Surface

ORIGINAL PAGE
BLACK AND WHITE PHOTOGRAPH

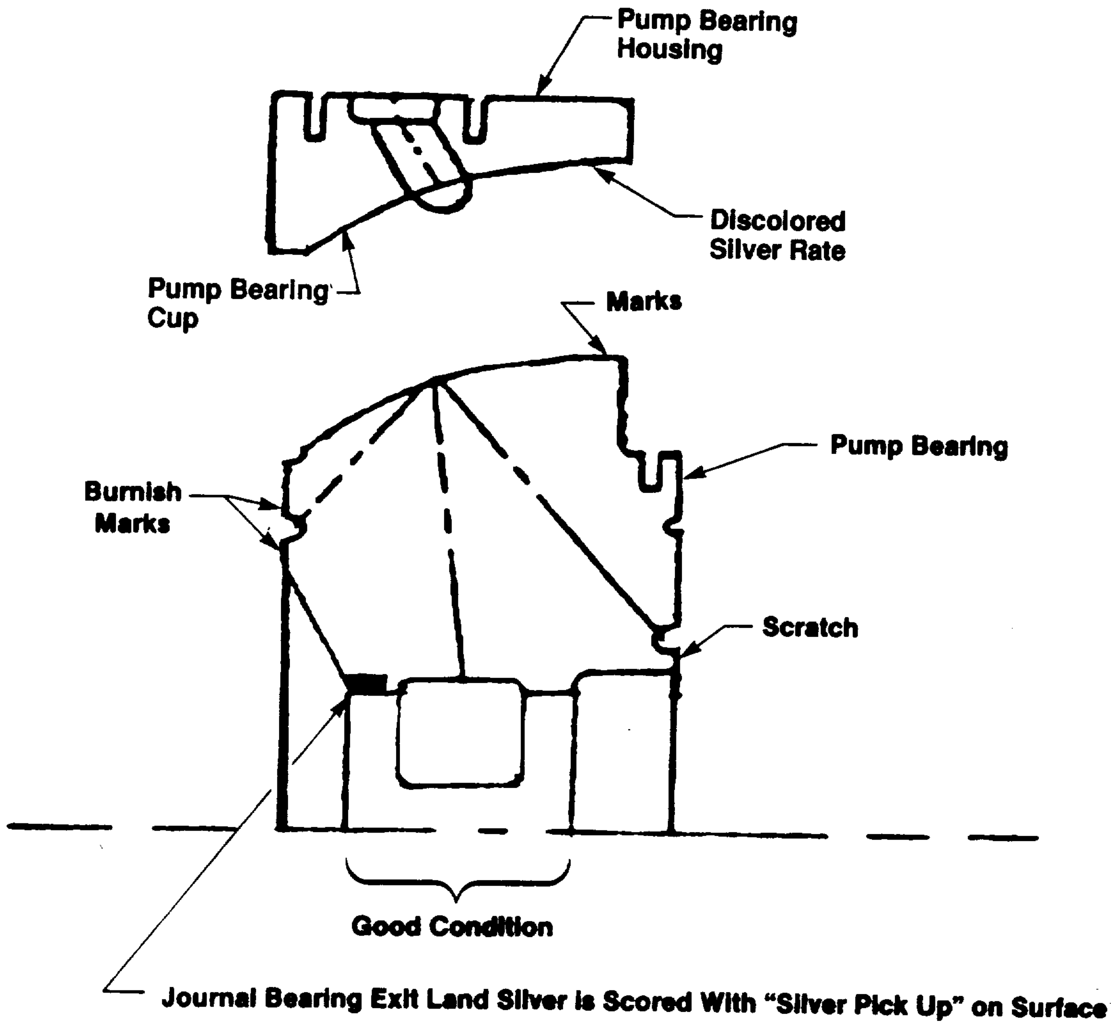

Figure 3.5-21. Contact Locations on Pump Bearing Assembly

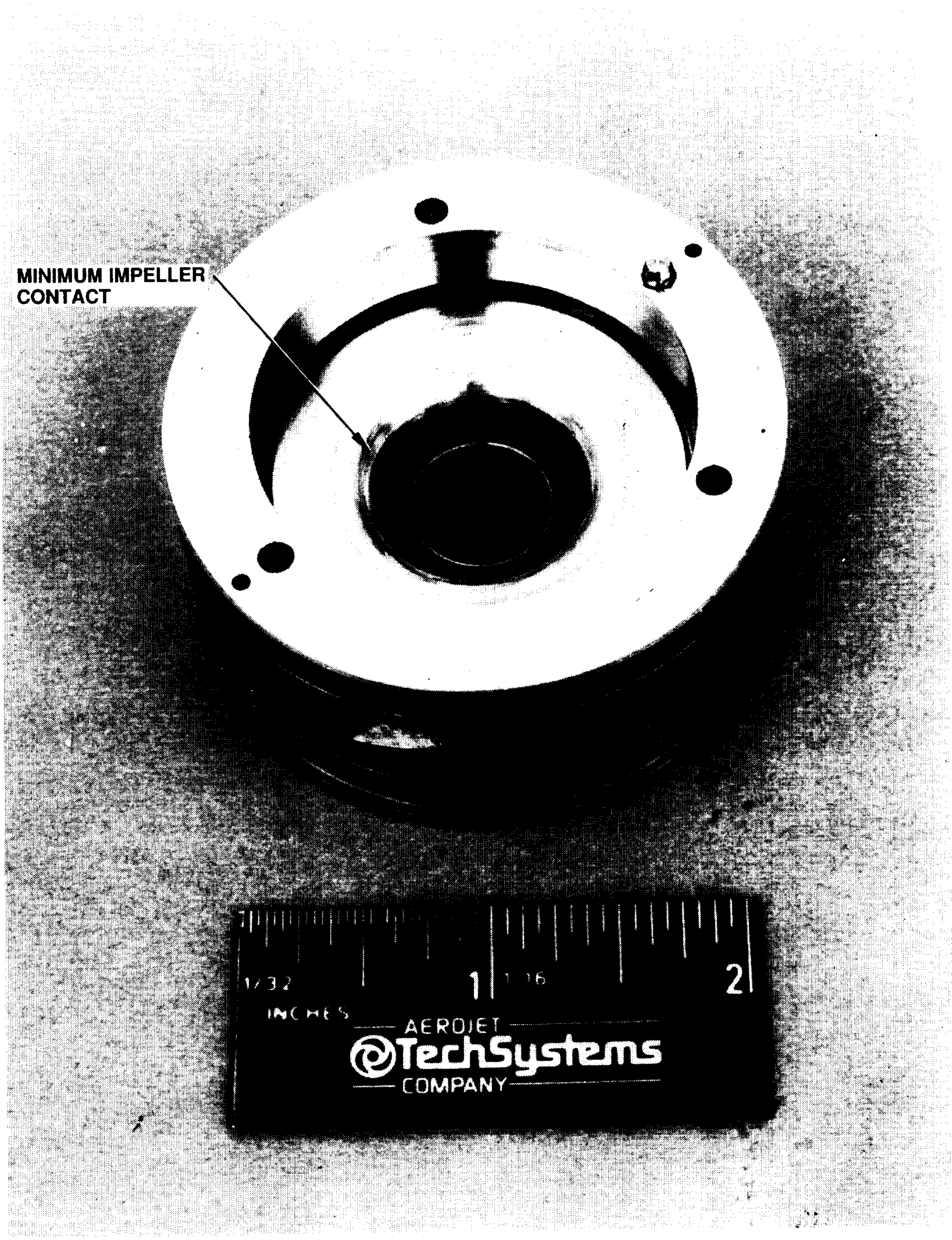

ATC Photo #C0489 1871

Figure 3.5-22. Second Stage Impeller Housing

ORIGINAL PAGE
BLACK AND WHITE PHOTOGRAPH

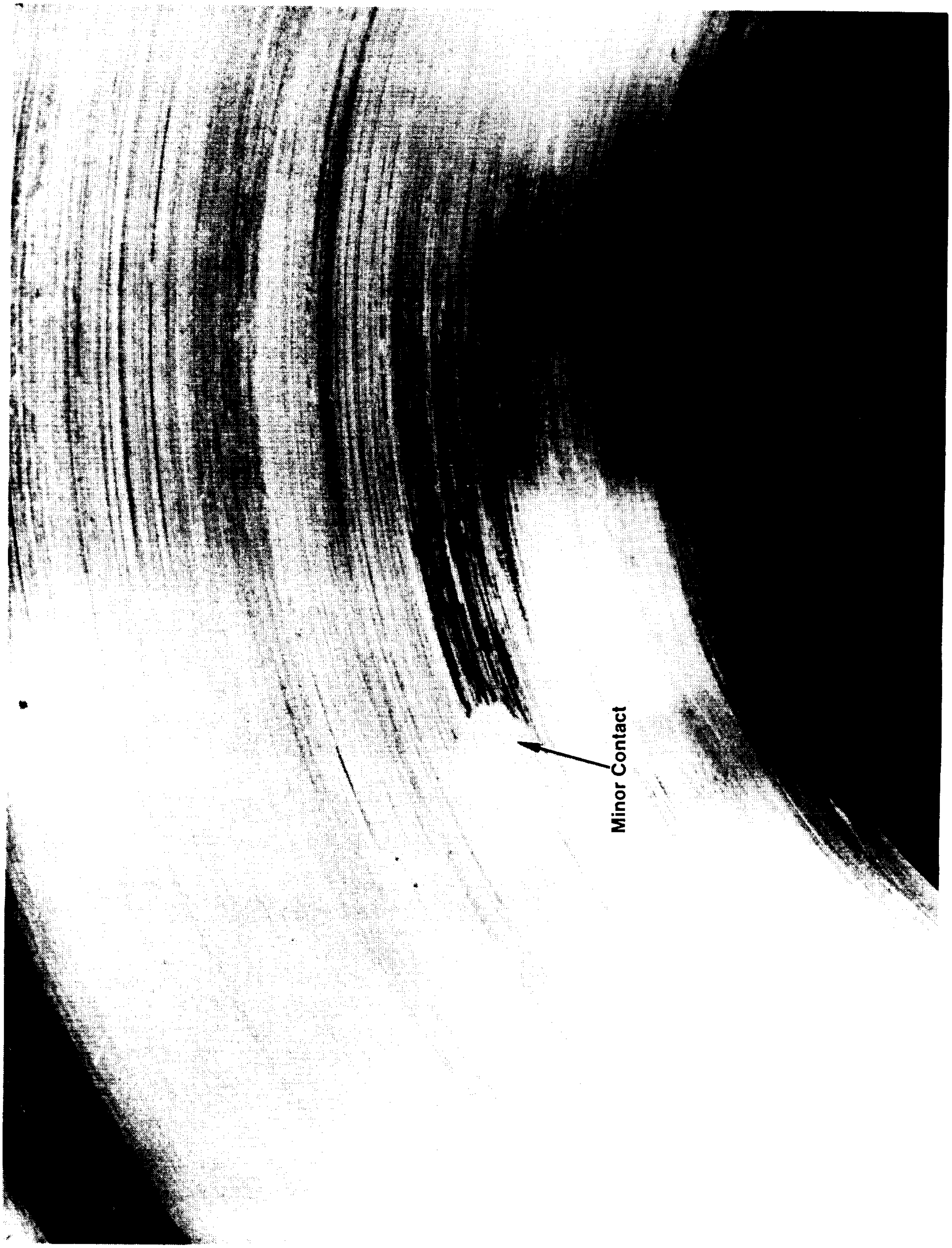

Figure 3.5-23. Second Stage Impeller Shroud Contour

ATC Photo #C0489 1869

The first stage housing impeller contour also had a local burnish mark. This contact is shown in Figure 3.5-24. On this surface the contact was light and on the radial portion of the surface near the outer diameter of the impeller. The turbopump was assembled with .002 inch axial clearance at the impeller vane tips. A small amount of silver pickup was found on two vane tips at the diameter of the contact.

The turbine disk appeared in excellent condition. There were no marks indicating any contact on the turbine blade tips and basically all original machining marks were still visible as shown in Figure 3.5-25. This is one of the key features of the design. The turbine must operating at close tip clearance without making contact in gaseous oxygen.

The turbine nozzle was in very good condition. Some difficulty was experienced with the gas piston ring seal, the location of which is identified in Figure 3.5-26. The piston ring was a two piece design, a seal ring, and an expander ring. The assembly of this ring was deep inside a blind housing and the expander ring held the seal ring out of the groove and could never be assembled. Therefore a modification was made to the end of the nozzle piece to accept a metal "V" seal. The nozzle end surface and the mating housing had about .010 inch clearance when assembled. The "V" seal was the same seal used for the turbine discharge flanges. Since the mating surfaces have clearance the seal groove depth was selected accordingly. On disassembly of the housing the seal appeared to have been offset in the groove, Figure 3.5-27. It is possible that a complete seal was not made and that some portion of the turbine flowrate bypassed the turbine through this seal. It appears that the groove O.D. was too small for the O.D. of the compressed "V" seal. It is recommended that this diameter be opened prior to the hot GOX test series at White Sands Test Facility (WSTF).

The turbine nozzle exit is shown in Figure 3.5-28. The axial clearance between the nozzle and the turbine wheel is approximately .040 inch. As expected, no evidence of contact was found in this area. Some contact indentations are seen near the outer diameter that mates with the turbine housing. This is an expected contact area.

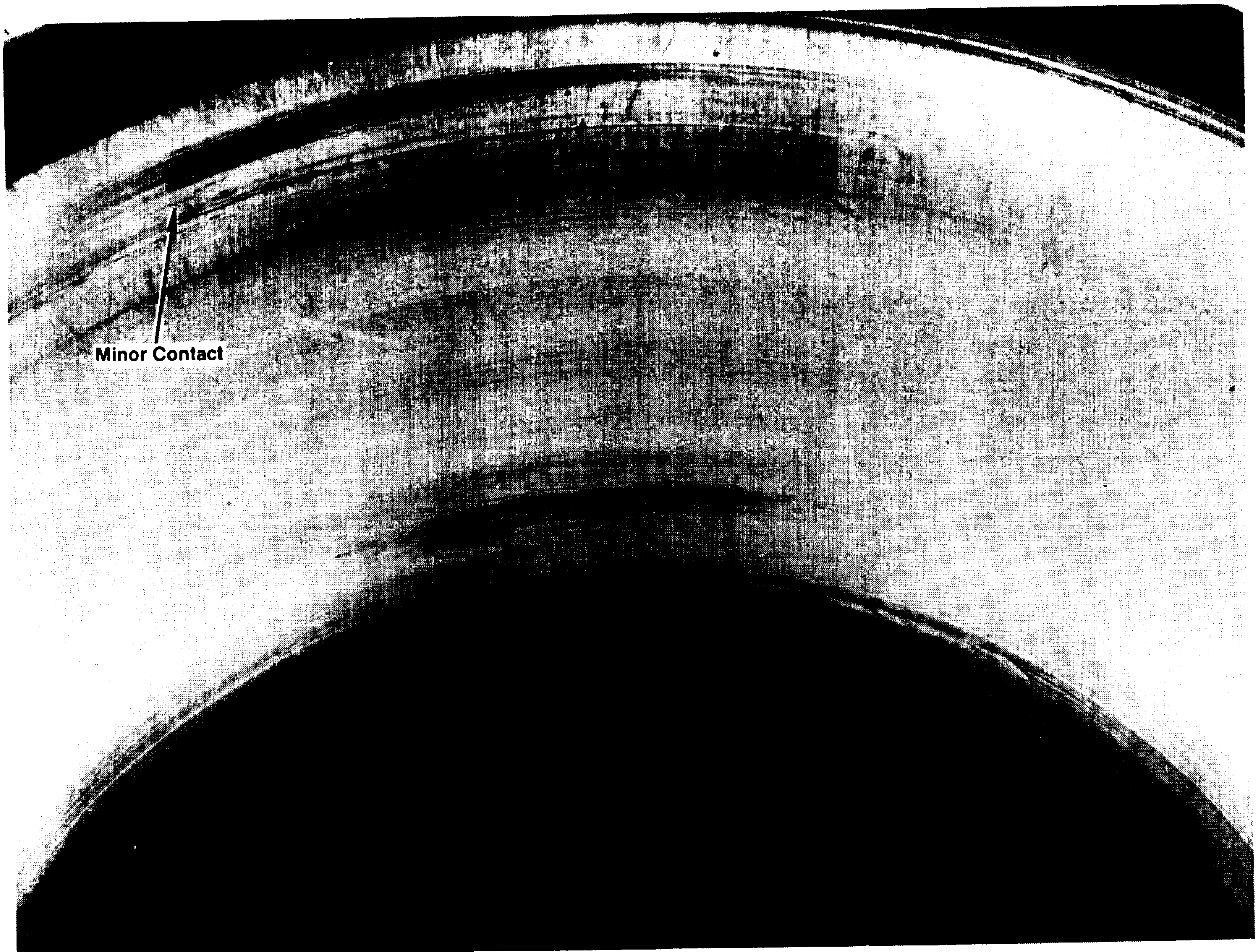

ATC Photo #C0489 1857

Figure 3.5-24. First Stage Impeller Shroud Contour

ORIGINAL PAGE
BLACK AND WHITE PHOTOGRAPH

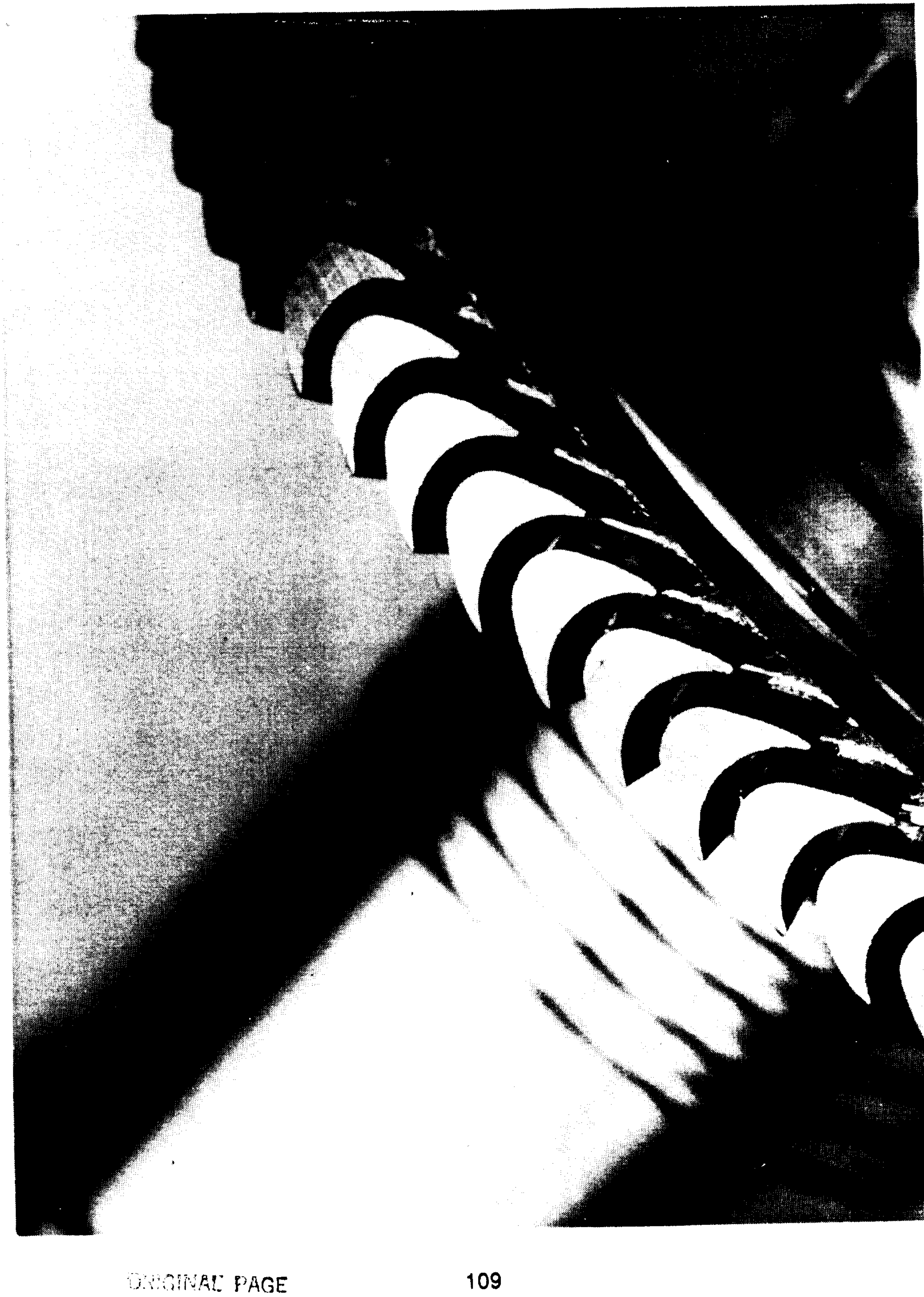

ATC Photo #C0489 1862

Figure 3.5-25. Turbine Blades

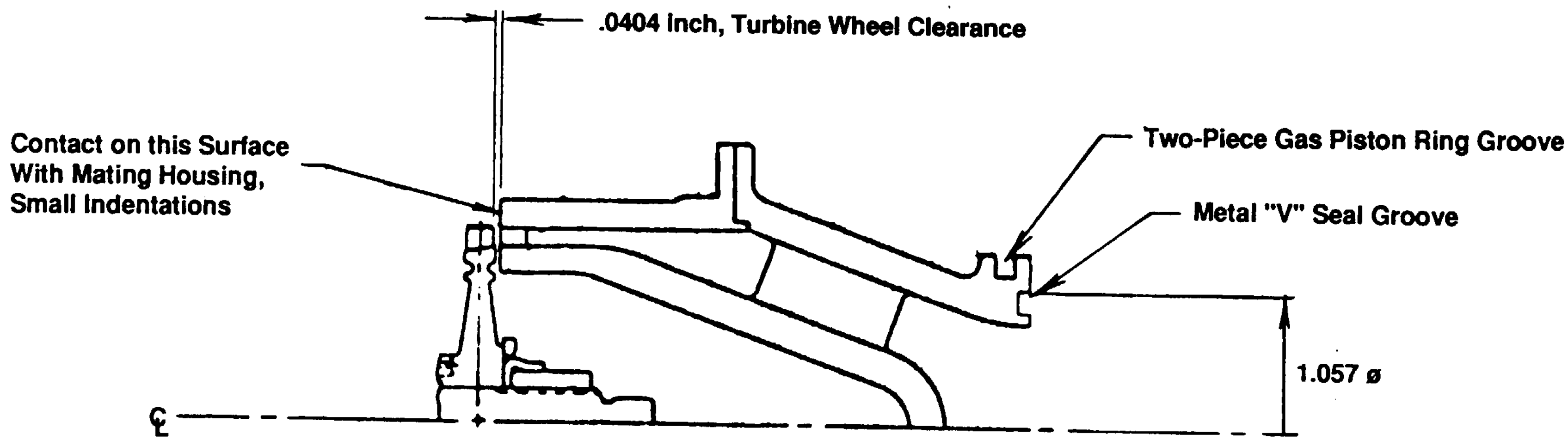

Figure 3.5-26. Turbine Nozzle Section

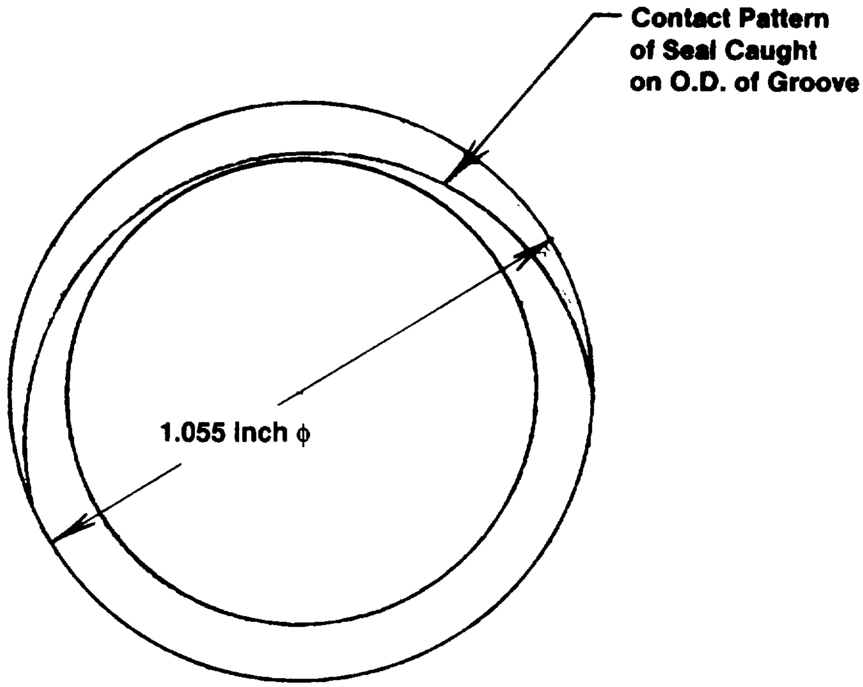

Figure 3.5-27. Turbine Nozzle "V" Seal

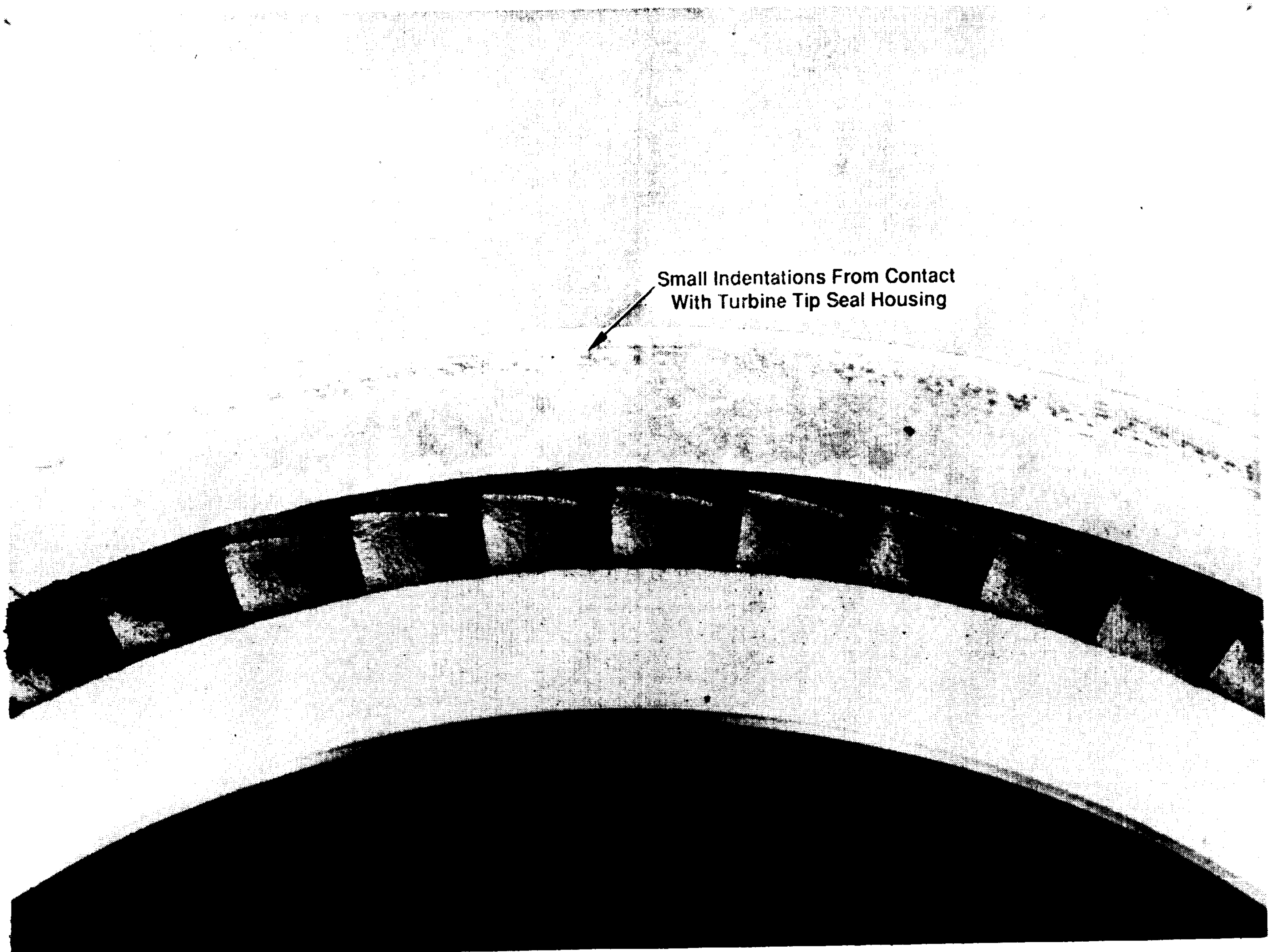

ATC Photo #C0489 1866

Figure 3.5-28. Turbine Nozzle -- Exit Side

ORIGINAL PAGE
BLACK AND WHITE PHOTOGRAPH

The mating turbine housing is shown in Figure 3.5-29 looking from the turbine inlet. This part is in excellent condition with no contact at the shaft labyrinth gold wear surface. A close up view of the turbine tip seal is shown in Figure 3.5-30. The gold tip seal surface has a small circumferential groove at the entrance to the turbine blades. Since there are no marks on the turbine blades it is possible a particle passing through the turbine made this mark. The axial scratches seen on the gold seal surface are from the shim material used for determining the installed turbine tip clearance.

An anomaly noted on disassembly on the pump interstage crossover lines was that the welded flange ends were offset approximately .010 inch from the tube. This offset is shown in Figure 3.5-31. All four ends had similar offsets. This offset will adversely affect the pump efficiency and is undesirable to have sharp corners and edges in oxygen from an ignition consideration. Therefore these offsets will be corrected before the next test series.

3.6 CONCLUSIONS

A liquid oxygen turbopump with 860°R gaseous oxygen turbine drive was designed for a 3750 lb thrust dual expander cycle rocket engine. This turbopump which requires no interpropellant seals or purges, features a 156 hp, single stage full admission impulse turbine, axial flow inducer, a two stage centrifugal pump with unshrouded impellers, long-life LOX lubricated, self-aligning, hydrostatic bearings, and a subcritical rotor design. It is constructed of Monel, a nickel-copper alloy, which has low ignition potential in oxygen. The pump was designed to deliver 34.7 gpm of liquid oxygen at a discharge pressure of 4655 psia and a shaft speed of 75,000 rpm. Completion of test series "C_1", "C_2", "D", "E_1", and "E_2" has successfully demonstrated several of the critical performance characteristics of this unique GOX-driven LOX-turbopump. Critical characteristics demonstrated are listed below.

1. Turbopump demonstrated in LO_2
2. High discharge pressure demonstrated/achieved
3. High speed demonstrated

ATC Photo #C0489 1870

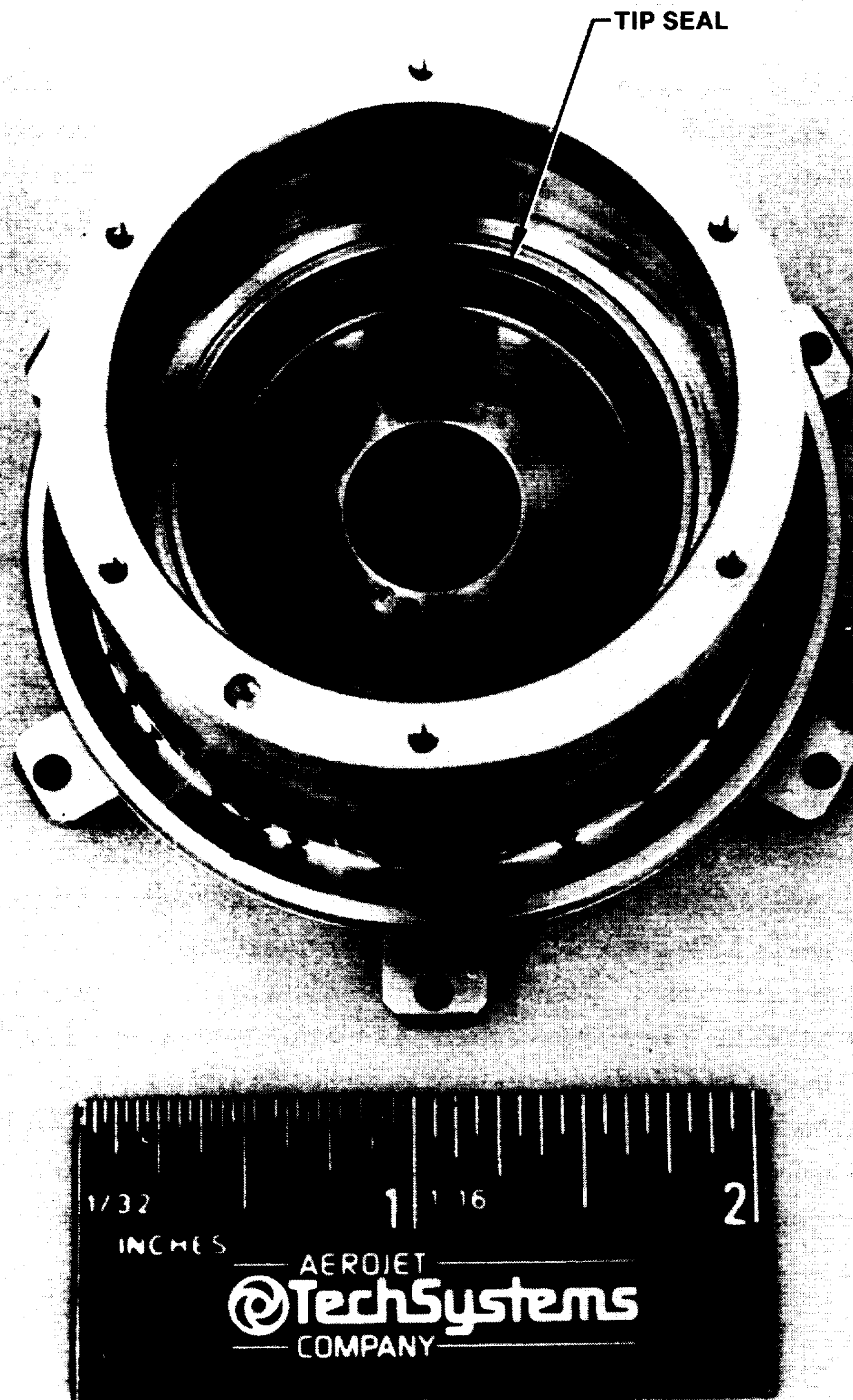

Figure 3.5-29. Turbine Tip Seal and Turbine Housing Post-Test

ORIGINAL PAGE
BLACK AND WHITE PHOTOGRAPH

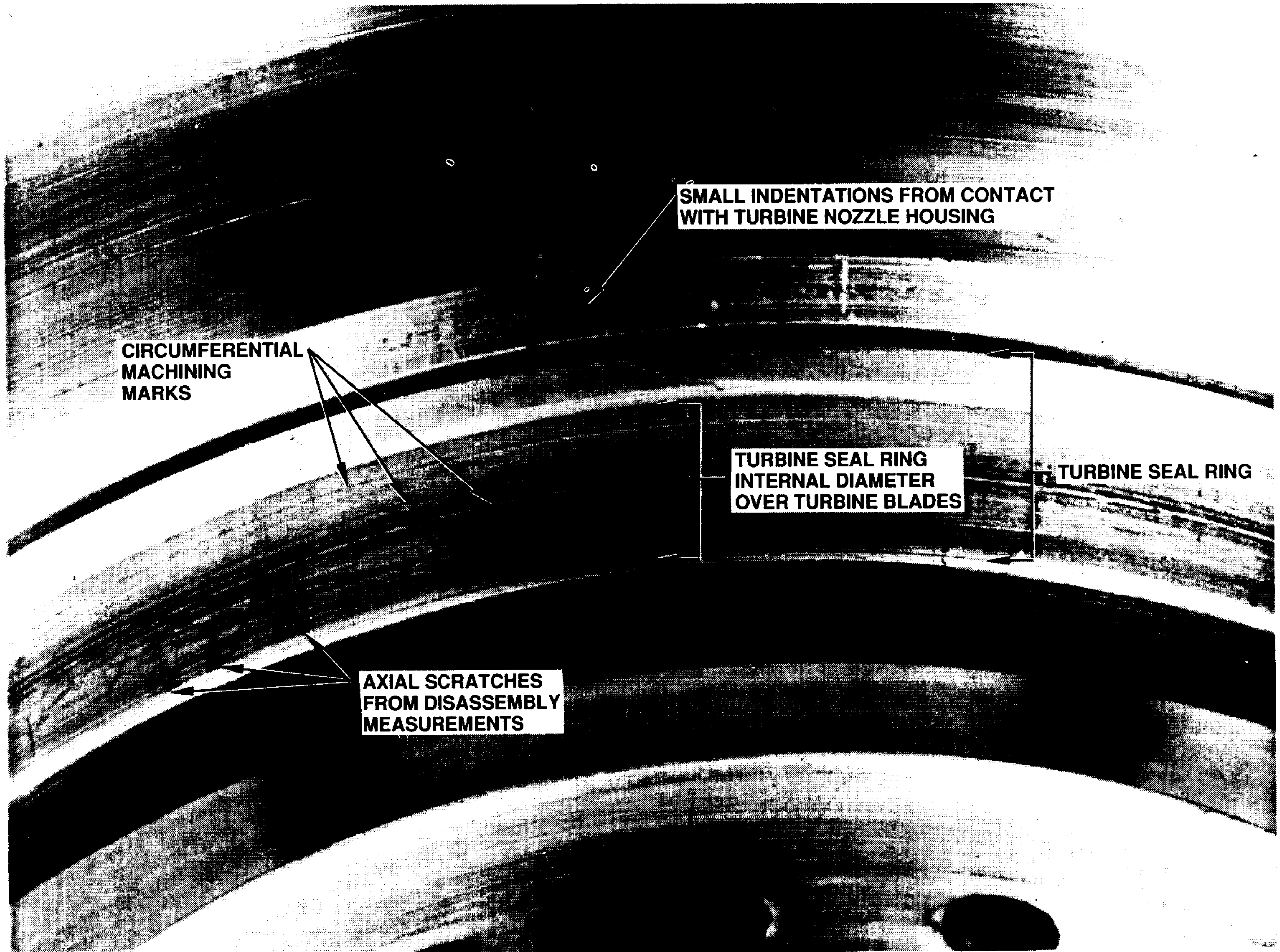

ATC Photo #C0489 1867

Figure 3.5-30. Turbine Tip Seal Post-Test

ATC Photo #C0489 1856

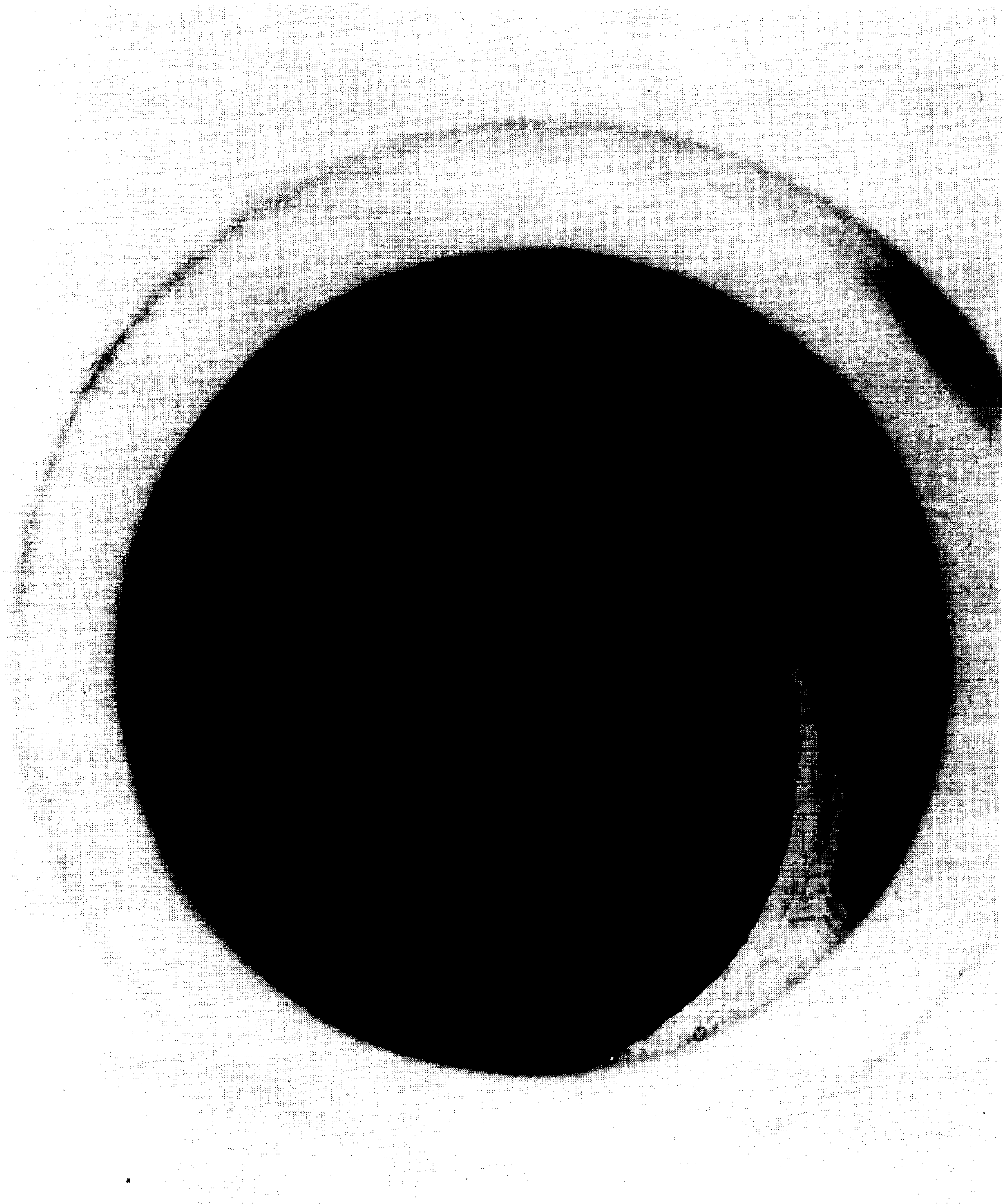

Figure 3.5-31. Pump Cross Over Pipe

4. High load capability hydrostatic bearing system demonstrated

5. Low burn factor materials running at close clearance and high pressures demonstrated in LO_2

6. Full hydrostatic self aligning LO_2 bearing demonstrated

7. Structurally and thermally layered turbopump mechanical design concept demonstrated

8. Pump throttled off-design performance demonstrated

9. Feasibility of close clearance open impeller design demonstrated

10. Sub-critical axial and radial rotor operation to speeds in excess of design speed demonstrated on Test 135 where an overspeed on shutdown reached 80,394 rpm

11. Low radial loads demonstrated with dual discharge

12. GOX driven turbine feasibility demonstrated

13. Tank fed bearing (assisted) start demonstrated

14. Unassisted bearing start demonstrated in LO_2 with GOX turbine drive

Although life testing and testing with warm (860R) GOX in the turbine must be conducted in the next test series, results of the testing to date indicate a GOX driven LOX turbopump is feasible.

3.7 RECOMMENDATIONS

Some improvement should be made to the bearing feed system to reduce excess leakage. The outer cylinder piston ring total circumferential length is 74.6 in. and the inner cylinder piston ring total length is 45.2 in. In a flight type turbopump design the outer cylinder set of piston rings would be eliminated which is equivalent to 62% of the piston ring leakage area. As a point of reference the total circumferential length of the bearing exit flow area is 10.99 in., approximately 25% of the total piston ring length.

Prior to the warm GOX drive test series several tasks are recommended, as noted throughout the text, and are summarized below:

- Resurface journal bearings
- Refurbish distance detectors
- Rework turbine nozzle static seal
- Replace static seals at Military Standard (MS) fittings
- Analyze the shaft axial oscillation phenomenon
- Fabricate new external crossovers to eliminate flange mismatch
- Add additional instrumentation capability to new crossovers

The proximity probes or distance detectors caused considerable delay and the abort of some test runs due to a shift or loss of signal. A more thermally forgiving probe is needed to correct these problems prior to any subsequent testing. Despite the numerous test runs the available probes were never able to provide a usable shaft motion for all three axes at the same time. Most runs had only one probe operating with another intermittent. One probe must operate to give a speed indication or the run is aborted. This is critical instrumentation for both testing and turbopump health diagnosis. Better probes need to be identified and procured. If they are not available commercially, the NASA-LeRC sponsored development work on a multichannel 3 axis probe should be completed to provide a usable device. (See Reference 14.)

Additional information on the OTV engine turbopump is available in References 14 and 15. Additional OTV systems background can be found in References 16 and 17.

APPENDIX A

DATA REDUCTION EQUATIONS

a. Pump Overall Pressure Rise (DELTAPO) psid

Assumptions:

1. Measured parameter nomenclature is per Test Lab Instrument Nomenclatures, Section 2.1.2.4, Table 2.1-3 and Table 2.1-4 where not defined in this Appendix.
2. Fluid density (ç lbm/ft**3) as a function of fluid temperature at that location.

$$P_{in} = PS + \frac{\varsigma_{in}}{2*32.2*144} * \left(\frac{FMSI*0.321}{\pi/4*D_{in}**2}\right)**2,$$ where D_{in} = Pipe diameter at PS.

$$P_{outi} = PD2_i + \frac{\varsigma_{outi}}{2*32.2*144} * \left(\frac{FMPDI*0.321}{\pi/4*D_{out}**2}\right)**2,$$ where D_{out} = Pipe diameter at PD2-E and PD2-W. See u. for FMPDI.

i = 1,2 (for pump discharge locations, 2SD1 and 2SD2)

$\varsigma_{in} = f\ (TS)$

$\varsigma_{outi} = f\ (TPDI), i, I = 1,2$

P_{out} is the average of the P_{outi} at the two pump discharge locations, 2SD1 and 2SD2.

$DELTAPO = P_{out} - P_{in}$

b. Pump Overall Head Rise (DELTAHO) ft

$$DELTAHO = \frac{DELTAPO * 144}{(\varsigma_{in} + \varsigma_{out})/2}$$

c. Pump Specific Speed (NPSPT,NSI) $(rpm)(gpm)^{.5}/(ft)^{.75}$

c.1 Delivered Overall Specific Speed

$$NPSPT = \frac{NT*\sqrt{FMPDE+FMPDW}}{(DELTAHO)^{0.75}}$$

c.2 Inducer Specific Speed

$$NSI = \frac{NT*\sqrt{FMSI}}{(DELTAHI)^{.75}} \text{ where DEL TAHI} = (PBPH\text{-}PS) = 144/\varsigma_{bp}'$$

d. Pump Net Positive Suction Pressure (NPSPT,NPSPI) psid

d.1 Inducer Net Positive Suction Pressure

$NPSPI = P_{in} - P_{vi}$

d.2 Centrifugal Impeller Net Positive Suction Pressure

$NPSPT = P_{in} + DELTAPI - P_{vbp}$

where:

$P_{vi} \equiv$ inlet vapor pressure as a function of TS

$P_{vbp} \equiv$ vapor pressure at inducer discharge as a function of TBPD
Note: See line g for application

e. Pump Net Positive Suction Head (NPSHPT,NPSHI) ft

e.1 Inducer Net Positive Suction Head

$NPSHI = NPSPI*144/\varsigma_{in}$

e.2 First Stage centrifugal Pump Net Positive Suction Head

$NPSHPT = NPSPT*144/\varsigma_{bp}$

ς_{in} and ς_{bp} are function of TS and TBPD, respectively.

f. Pump Suction Specific Speed (SPT,SI) $(rpm)(gpm)^{.5}/(ft)^{.75}$

f.1 Inducer Suction Specific Speed

$$SI = \frac{NT*\sqrt{FMSI}}{(NPSHI)^{.75}}$$

f.2 First Stage Centrifugal Pump Suction Specific Speed

$$SPT = \frac{NT*\sqrt{FMSI - FMBPD}}{(NPSHPT)^{.75}}$$

g. Pump Inducer Pressure Rise (DELTAPI) psid

DELTAPI = PBPH - PS

Note: Assumes the velocity head at suction and boost pump supply housing are the same.

h. Pump Inducer Head Rise (DELTAHI) ft

$DELTAHI = DELTAPI * 144/\rho_{bp}$

i. Pump Efficiency (f) Delivered Fluid Power and Fluid Losses determined from Temperature Rise (ETAP)

ETAP = HPPT/HPSF

j. Pump Shaft Power (f) [Delivered Fluid Power + (Hydraulic Power Losses (f) Temperature Rise)]

HPSF = HPPT+HPLOSS

k. Delivered Fluid Power

$HPPT = \rho_{out} * FMPD * DELTAHO/550/448.8$, where FMPD = FMPDE + FMPDW

l. Hydraulic Power Loss based upon Temperature Rise

HPLOSS = HPHEAT + HPBLEED

Centrifugal pump friction loss (f) temperature

$= [\rho_{out} * FMPD * C_p * (TPD\text{-}TS) +$ Note: See m for FMPD definiton

Pump bearing flow work + friction loss (f) temperature

ς_{pb1} * FMPBI * C_p * (TPBE-TPBI) +

Turbine bearing flow work + friction loss (f) temperature

ς_{pb2} * FMTBI * C_p * (TPBE-TBI)] *

(3600/2545/448.8) +

Boost Pump Hydraulic Turbine fluid power

[ς_{bp} * FMBPD * DELTAHI +

Pump Bearing Exit (overboard) Flow work minus Pump Bearing Recirculated flow work

ς_{be} * (FMPBE-FMPBI) *

(DELTAHO/2)]/448.8/550

Note: Uses only 2nd stage head rise, half of DELTAHP

ς_{out} = f (TPD) where TPD = (TPD1 + TPD2)/2

ς_{pb1} = f (TPBI)

ς_{pb2} = f (TBI)

ς_{bp} = f (TBPD)

ς_{be} = f (TPBE)

C_p is the fluid specific heat as a function of local temperature. ≈0.49 Btu/lbm/R for LN_2

≈0.405 for LOX

m. Pump Weight Flow Rate (PMPD) (lbm/sec)

PMPD = (FMPDE+FMPDW)*ς_{out}/448.8

n. Pump Power (HPPT) HP

HPPT = HPSF — HPLOSS (Rearranged from line j)

p. Pump Flow Rate to Speed Ratio (QI/N, QP/N) gpm/rpm

QI/N = FMSI/NT

QP/N = FMPDE+FMPDW-FMPBI-FMTBI)/NT

q. Pump Head Rise to Speed Squared Ratio (DELH0/N2) ft/rpm**2)

DELHO/N**2 = DELTAHO/NT**2

r. DELPB = PPBI-PBE, Pump Bearing Pressure Differential, psi

s. DELTB = PTBI-PTBC, Turbine Bearing Pressure Differential, psi

t. $PD2 = \frac{PD2E + PD2W}{2}$, Average Pump Discharge Pressure, psi

v. $NRT = NT/\sqrt{TTI+460}$, Turbine Speed Parameter

u. FMPDI = FMPDE + FMPDW, Total Pump Discharge Flow, gpm

w. ETAST = ETATPA/EFFPD, Turbine Total to Static Efficiency

x. HPPUMP ≡ HPSFPD, Pump Horsepower

y. HPDIS ≡ HPPFL, Fluid Horsepower

z. HPTARE = [ς_{bp} * FMBPD * DELTAHI + ς_{out} * (FMPBI + FMTBI) * DELTAHO]*

$$\frac{1}{448.8 * 550}$$, TARE Horsepower

aa. For Pump Delivered Fluid Horsepower

HPPFL = ς_{out} * (FMPDI - FMTBI - FMPBI) * DELTAHO/550/448.8, Fluid Horsepower ab. Original Predicted Design Efficiency

$EFFPD = -0.074437 + 3809.4314 * (QP/N)$

$- 8202769.6 * (QP/N)^2$

$+ 5.65306 * 10^9 * (QP/N)^3$

ac. $HPSFPD = \frac{HPPFL}{EFFPD}$, Calculated Predicted Pump Horsepower based on Predicted Design Efficiency

HPPFL = pump delivered fluid horsepower = HPPT

ad. Overall turbopump efficiency, ETATPA

ETATPA = HPPFL * 550/(WDOT * DHI * 778),

where: WDOT = turbine gas flow rate, lb/sec

DHI = CP * (TTI + 460) * (1-(1/PRS)**

((GAM-1)/GAM))

and CP = gas specific heat at constant pressure, Btu/lb°R

GAM = gas specific heat ratio

PRS = total to static pressure ratio

TTI = turbine gas total/inlet temperature, °F

ae. Turbine Blade Mean Speed to total to static gas Spouting Velocity ratio

ucø = u/Co = turbine blade-spouting velocity ratio

where: $u = DBAR * NT * \pi /(12 * 60)$

DBAR = 1.333/12 = 0.11108 ft.

$\pi = 3.14159$

Co = (2 * 32.174 * 778 * DHI)**0.5

af. Turbine flow parameter

$$WRTP = WDOT*SQRT\ (R*(TTI + 460))/PTI, \qquad \frac{\left(\frac{lbm}{sec}\right)\sqrt{ft}}{\frac{lbf}{in.^2}}$$

Floppy diskettes, plots and performance calculations were recorded for the following selected tests:

Test 154, 156, 164, 165, 167, 169, 171, 172, 173, 174, 175, 176, 177, 178, 179, 180, 181, 182, 183, 185, 186, 187, 188, 189, and 190.

NT was defined as NT-Z for calculating performance in all tests except for the following: Test 154, 169, 181, 186. NT-X was used as NT in these cases for performance calculation purposes.

APPENDIX B

TEST DATA PLOTS FROM HIGH PRESSURE
HIGH SPEED LOX/GOX TEST NO. 2459-D02-OP-183

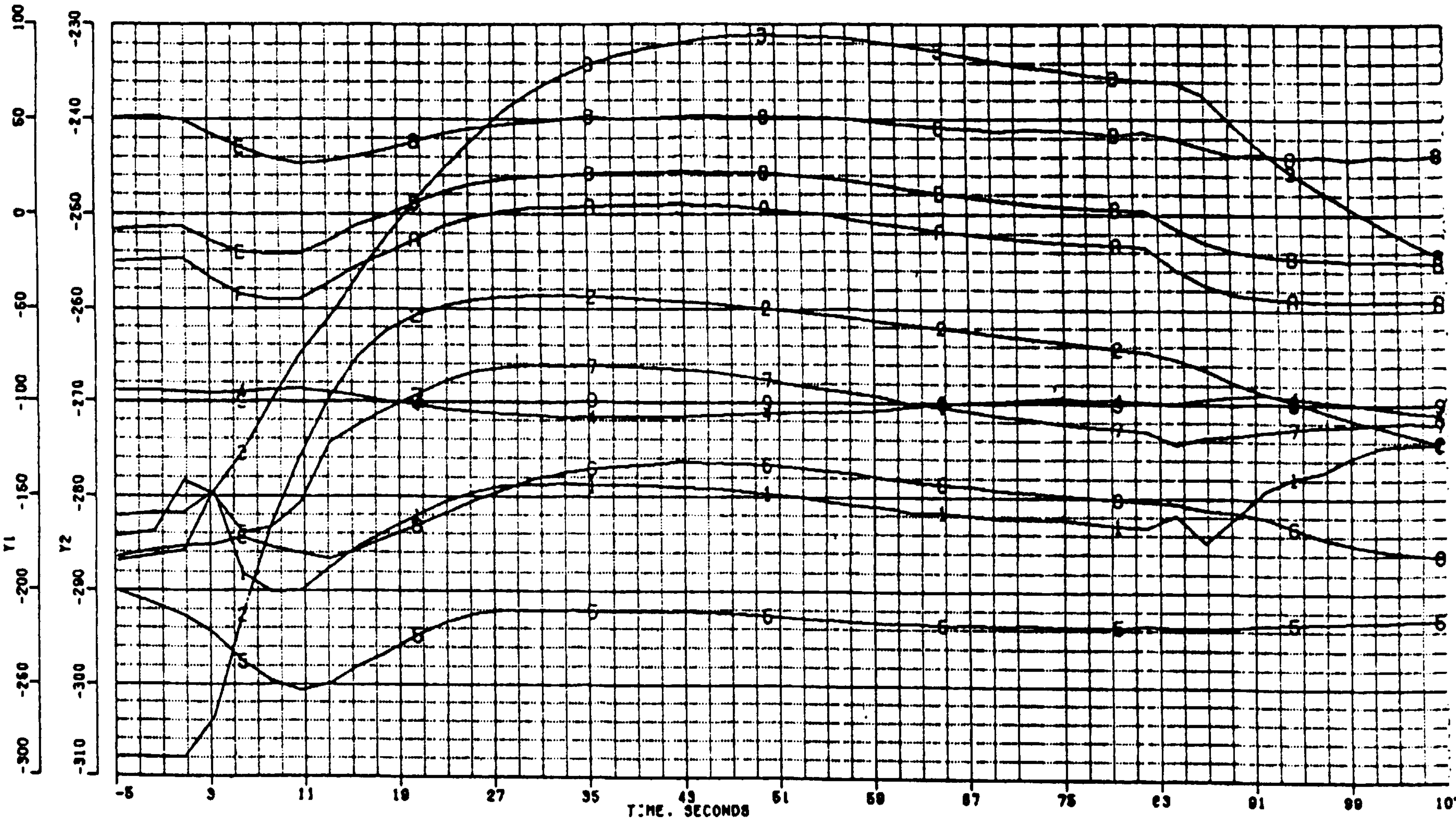

1 TBI	DEG F.Y2	8 TPD1	DEG F.Y2
2 TTM7	DEG F.Y1	9 TPD2	DEG F.Y2
3 TTBH8	DEG F.Y2	A TPD2-E	DEG F.Y2
4 TTIPM10	DEG F.Y2	B TPD2-W	DEG F.Y2
5 T5	DEG F.Y2		
6 TMX9	DEG F.Y2		
7 TPBE	DEG F.Y2		

OTV OXYGEN TPA 03-20-89 2459-D02-OP-183
PLOT 1. FLUID AND HOUSING EXTERIOR
TEST TIME 1913 82.181 SECOND DURATION

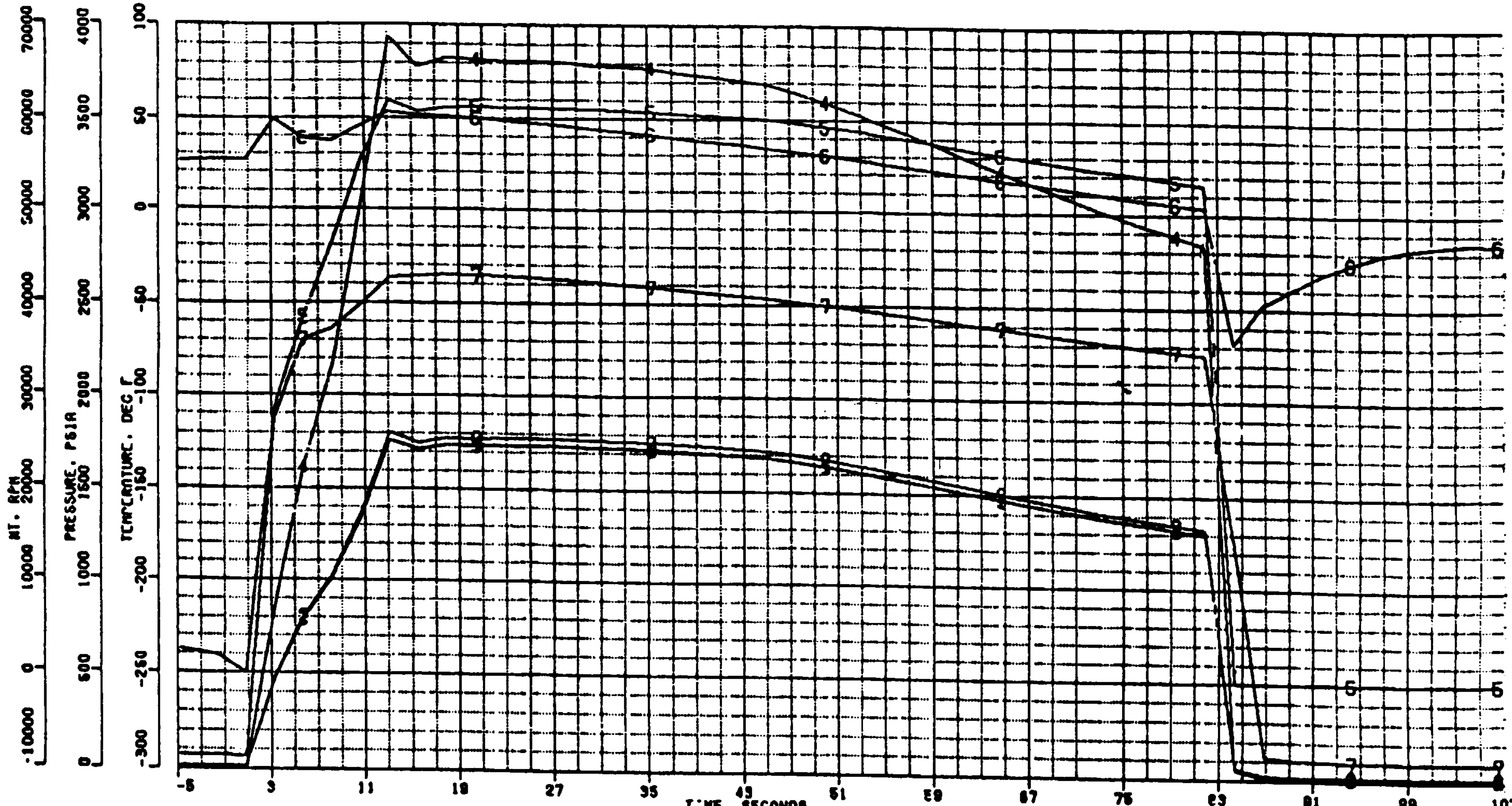

1 PTD-W PSIA
2 PTDM PSIA
3 PTD-E PSIA
4 PTI PSIA
5 NT-Z RPM
6 TTI DEG F
7 TTDM DEG F

OTV OXYGEN TPA 03-20-89 2459-D02-OP-183
PLOT 2. TEMP/PRES/FLOW VS TIME -TURBINE
TEST TIME 1913 82.161 SECOND DURATION

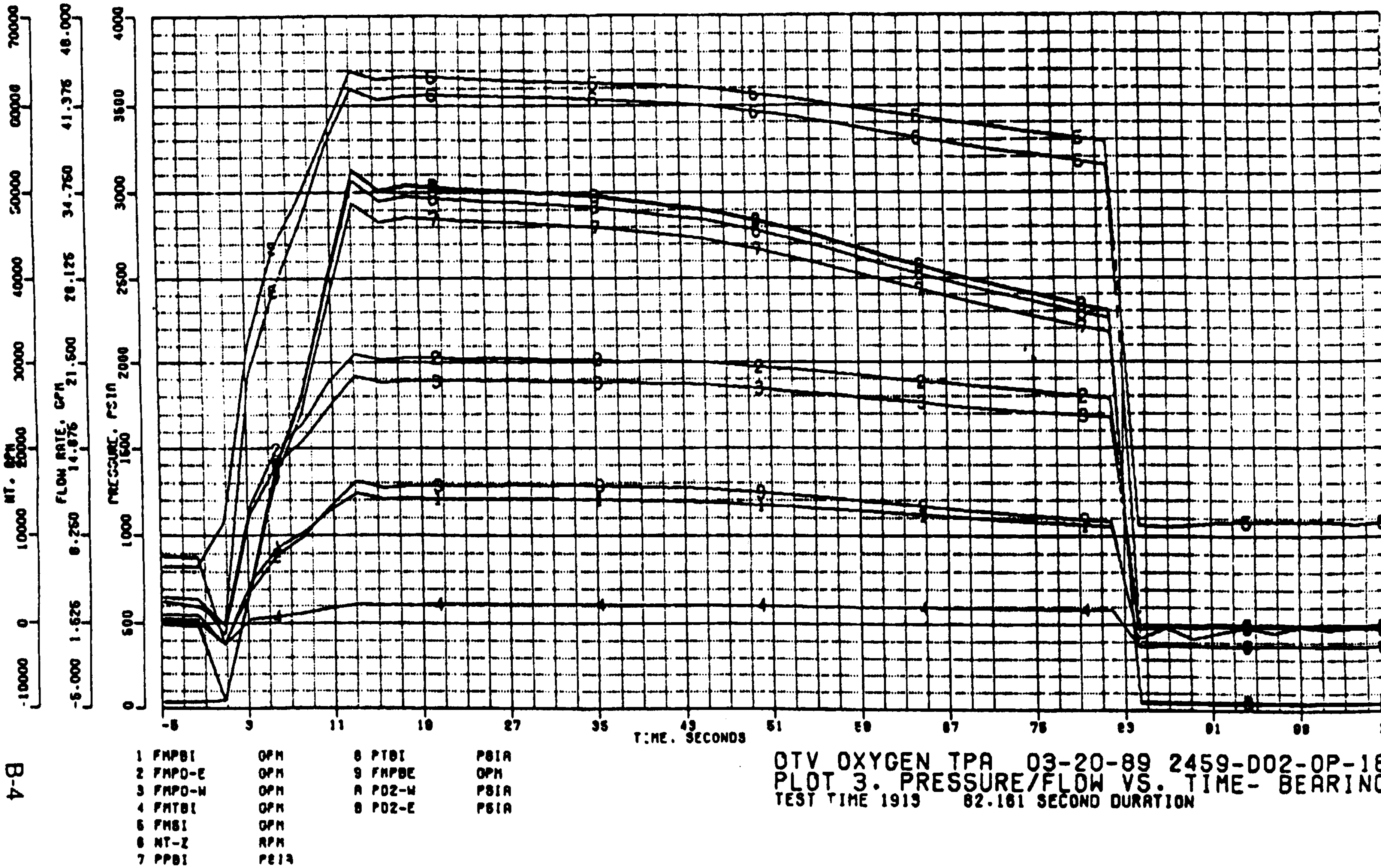

OTV OXYGEN TPA 03-20-89 2459-D02-OP-183
PLOT 3. PRESSURE/FLOW VS. TIME- BEARINGS
TEST TIME 1919 82.161 SECOND DURATION

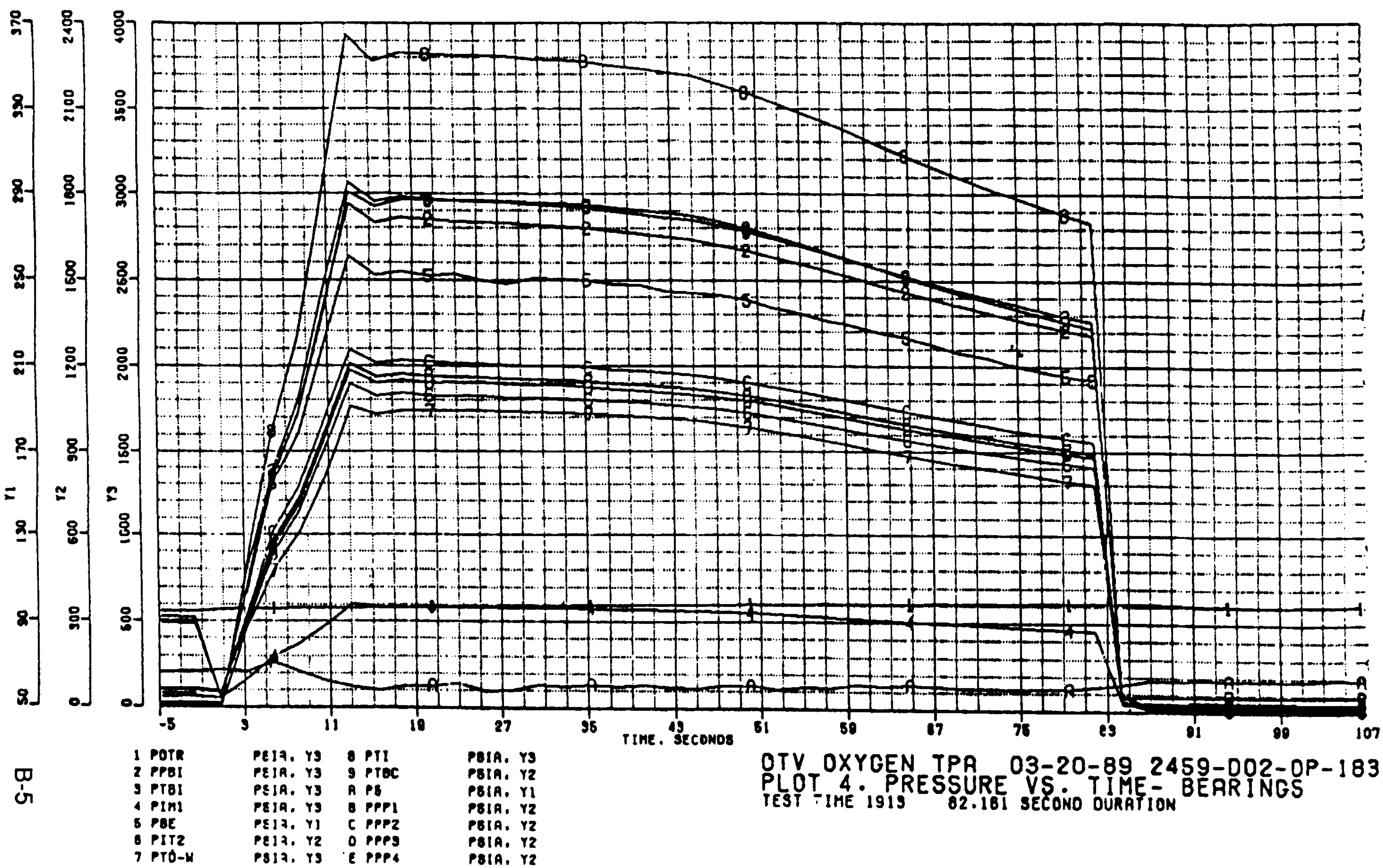

OTV OXYGEN TPA 03-20-89 2459-D02-OP-183
PLOT 4. PRESSURE VS. TIME- BEARINGS
TEST TIME 1913 82.181 SECOND DURATION

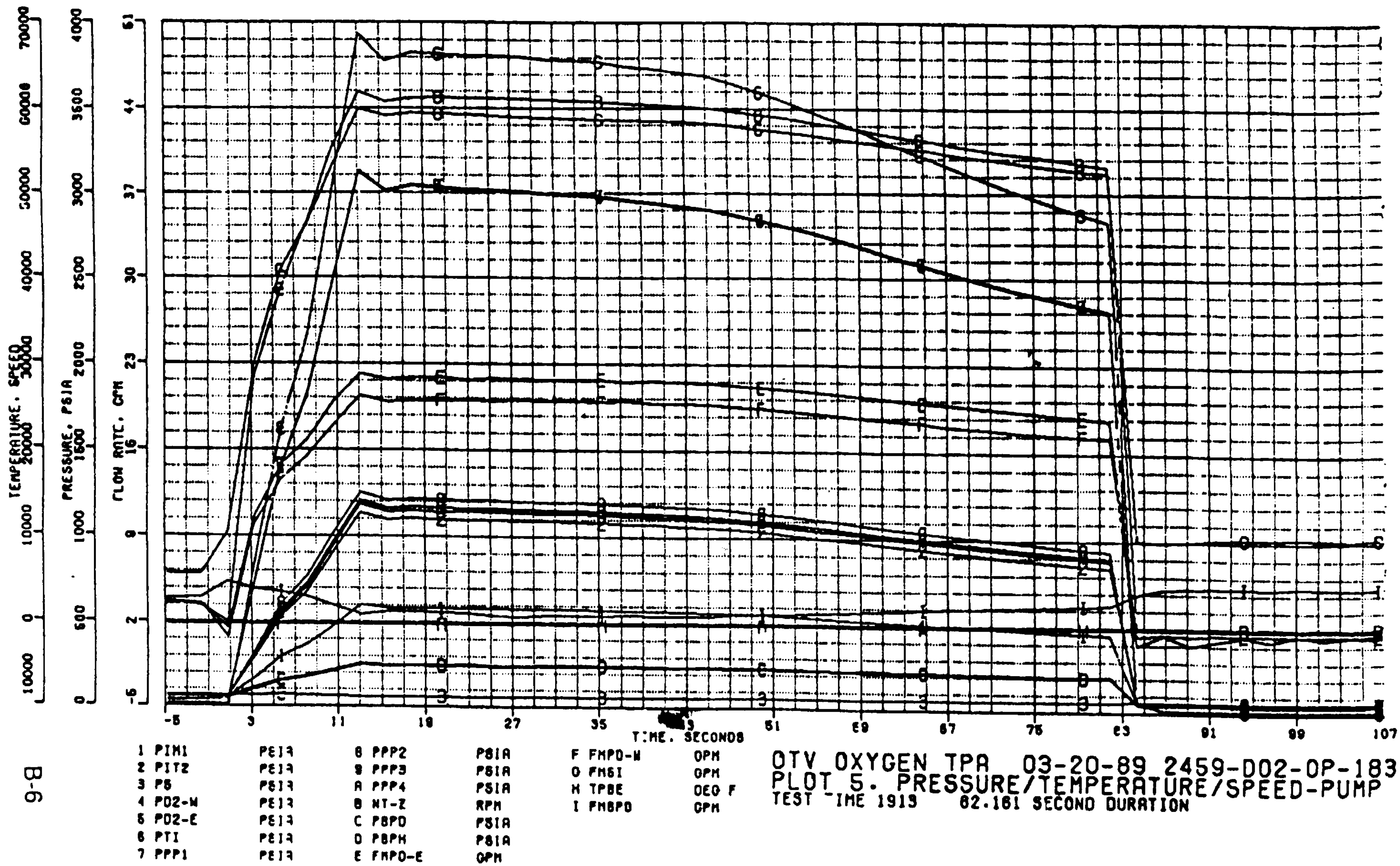

OTV OXYGEN TPA 03-20-89 2459-D02-OP-183
PLOT 5. PRESSURE/TEMPERATURE/SPEED-PUMP
TEST TIME 1913 62.161 SECOND DURATION

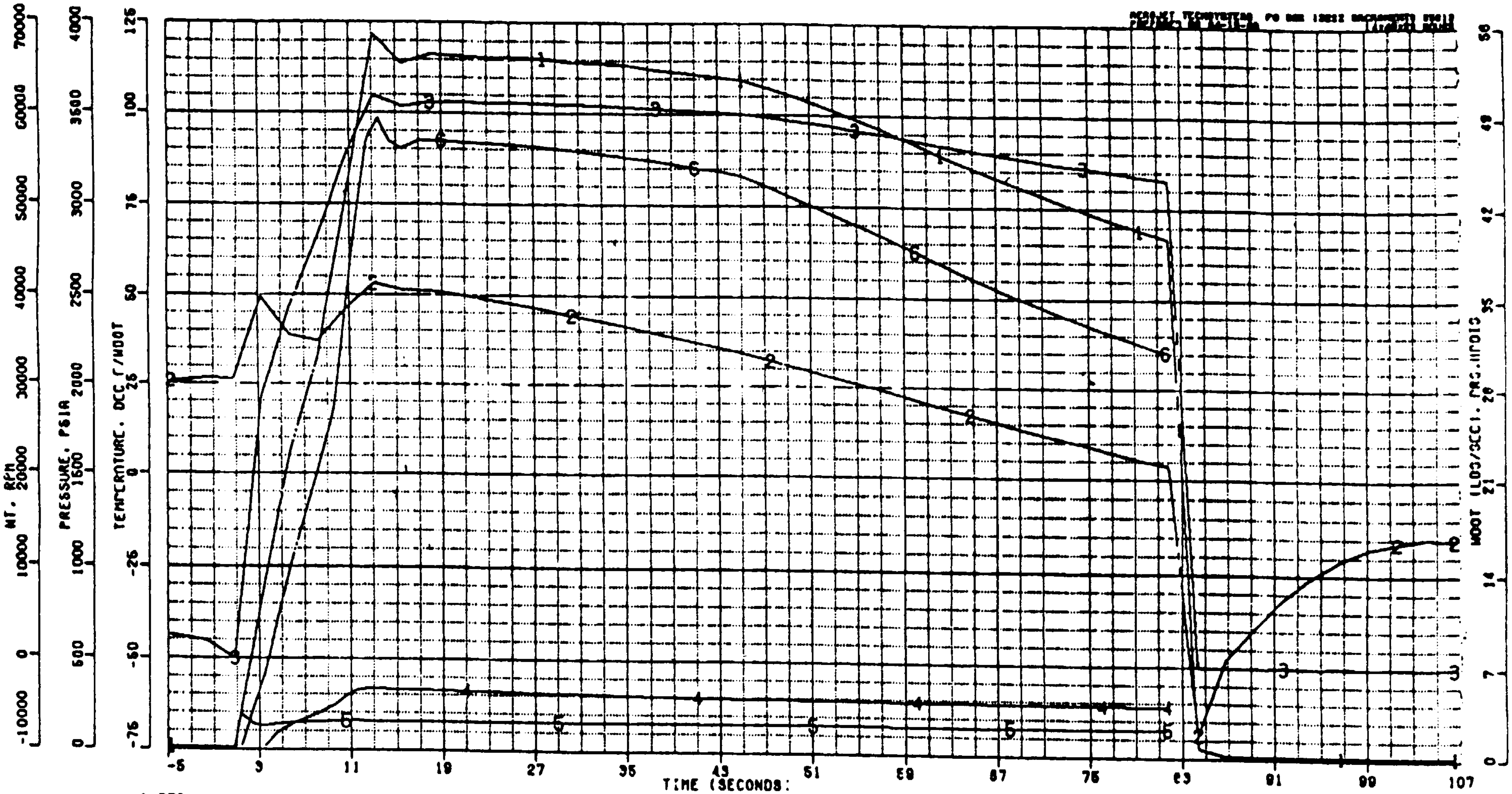

1	PTI	PSIA
2	TTI	DEG F
3	NT-Z	RPM
4	WDOT	LB/SEC
5	PRS	
6	HPDIS	HP

OTV OXYGEN TPA 03-20-89 2459-D02-OP-183

PLOT NO. 6

TEST TIME 1913 82.181 SECOND DURATION

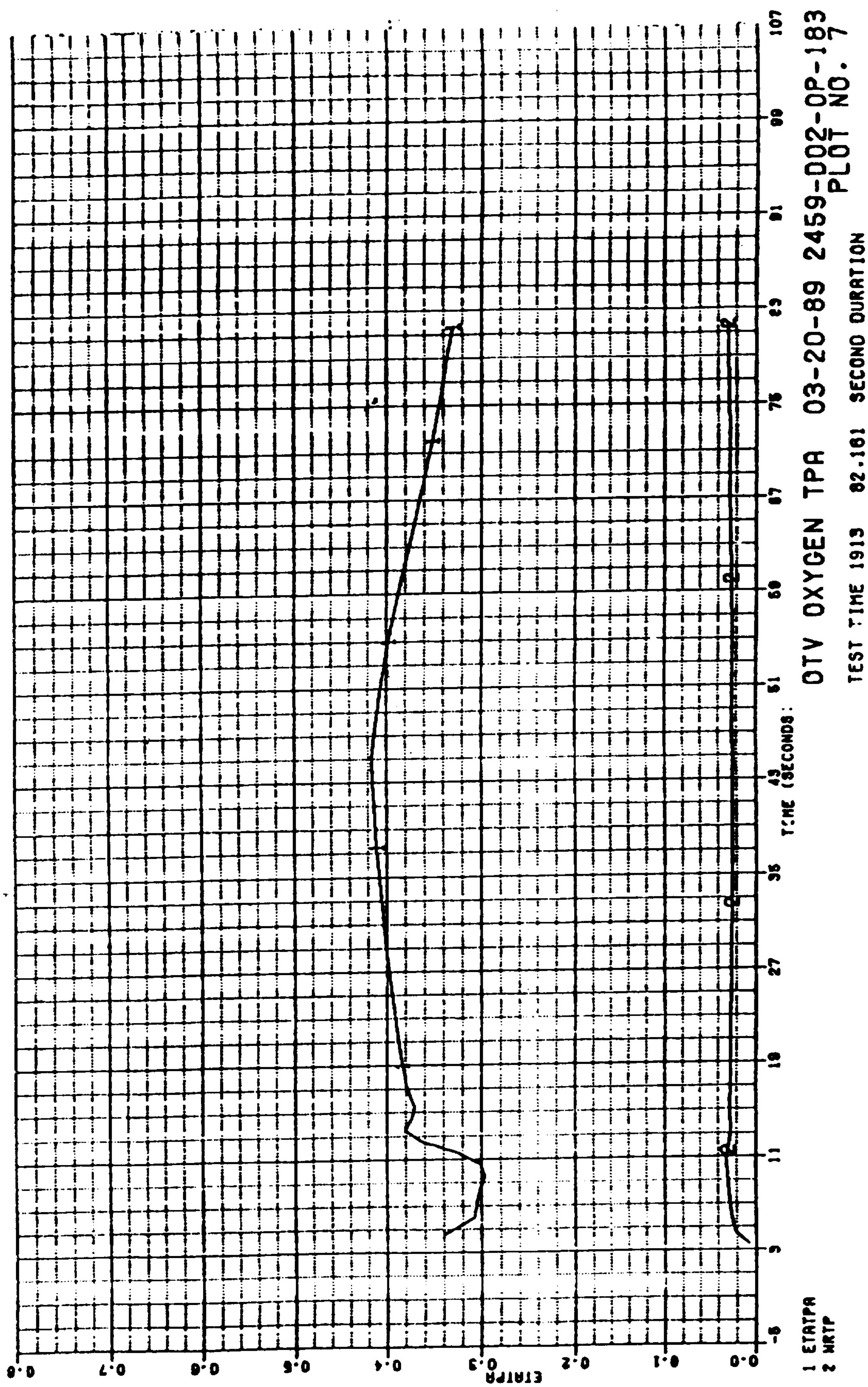
OTV OXYGEN TPA 03-20-89 2459-D02-OP-183
PLOT NO. 7
TEST TIME 1913 82.161 SECOND DURATION
TIME (SECONDS)
ETATPA
1 ETATPA
2 WRTP

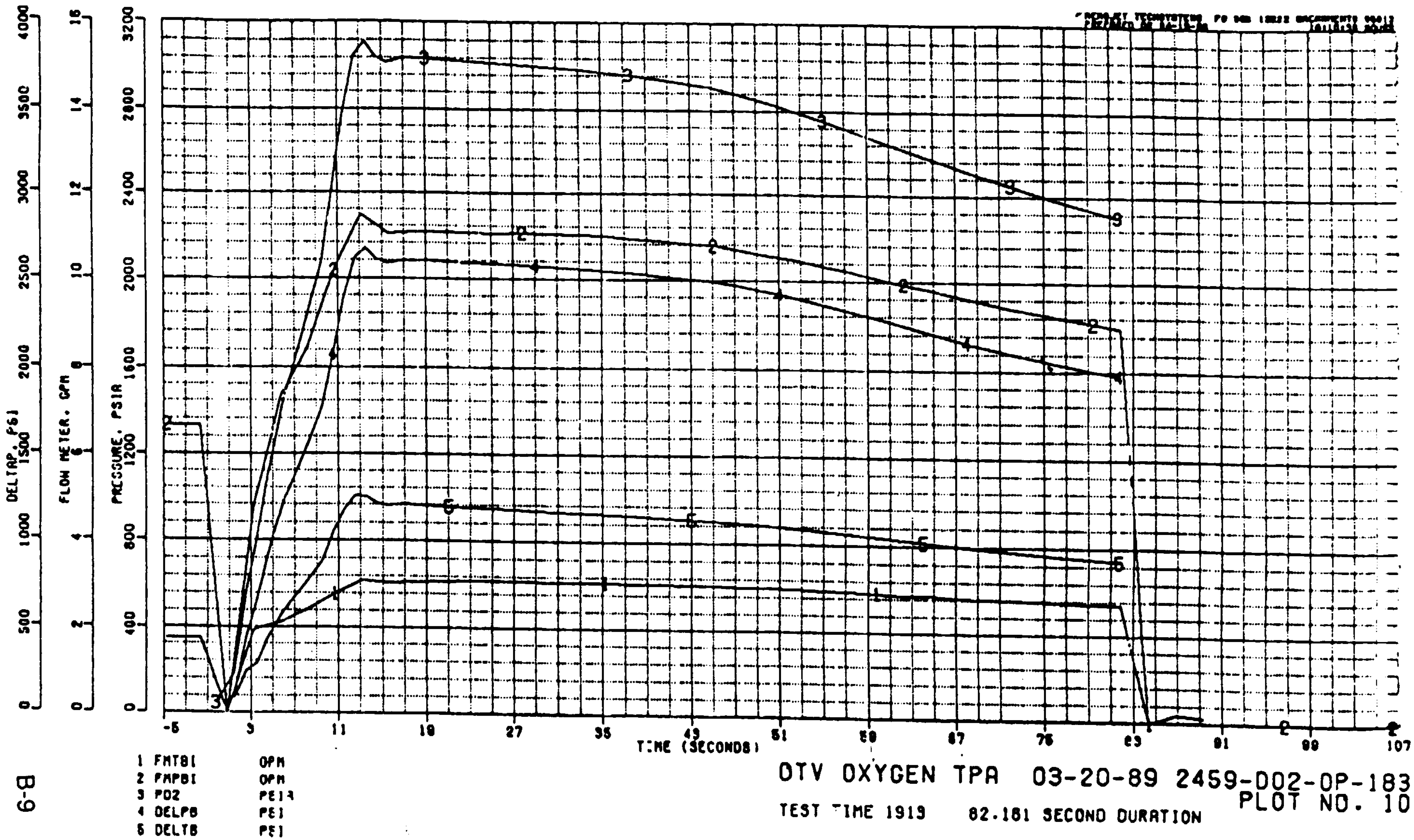

OTV OXYGEN TPA 03-20-89 2459-002-OP-183
PLOT NO. 10
TEST TIME 1919 82.181 SECOND DURATION

SYMBOLS

APPENDIX B

DELPB	PSI	Delta Pressure Across Pump Bearing
DELTB	PSI	Delta Pressure Across Turbine Bearing
ETATPA	—	Efficiency Ratio - Pump Fluid Power Out/Turbine Gas Total to Static Power In
FMBPD	GPM	Flow Meter Boostpump Drive
FMPBE	GPM	Flow Meter Pump Bearing Exit
FMPBI	GPM	Flow Meter Pump Bearing Inlet
FMTBI	GPM	Flow Meter Turbine Bearing Inlet
FMPD-E	GPM	Flow Meter Pump Discharge - East
FMPD-W	GPM	Flow Meter Pump Discharge - West
FMBI	GPM	Flow Meter Suction Inlet
HPDIS	HP	Delivered Fluid Horsepower
NT-Z	RPM	Speed Turbine - Z Axis Probe
PBE	PSIA	Pressure Pump Bearing Exit 1
PBPD	PSIA	Pressure Boost Pump Turbine Drive Line
PBPH	PSIA	Pressure Boost Pump Housing Annulus
P02	PSIA	Pump Discharge Average Pressure - [(PD2-E) + (PD2-W)]/2
PD2-E	PSIA	Pressure Discharge 2nd Stage - East
PD2-W	PSIA	Pressure Discharge 2nd Stage - West
PDTR	PSIA	Pressure Drive Turbine Run Tank
PIM1	PSIA	Pressure Impeller Wall, Mid Station 330°
PIT2	PSIA	Pressure Impeller Wall, Tip Station 300°
PPBI	PSIA	Pressure Pump Bearing Inlet
PPP1	PSIA	Pressure Pump Peripheral Wall, Station 0°
PPP2	PSIA	Pressure Pump Peripheral Wall, Station 270°
PPP3	PSIA	Pressure Pump Peripheral Wall, Station 180°
PPP4	PSIA	Pressure Pump Peripheral Wall, Station 90°
PRS	—	Turbine Pressure Ratio - Total to Static
PS	PSIA	Pressure Suction Line
PTBC	PSIA	Pressure Turbine Bearing Cavity

PTBI	PSIA	Pressure Turbine Bearing Inlet
PTD-E	PSIA	Pressure Turbine Discharge - East (TD2)
PTDH	PSIA	Pressure Turbine Discharge Housing
PTD-W	PSIA	Pressure Turbine Discharge - West (TD1)
PTI	PSIA	Pressure Turbine Inlet
TBI	DEG F	Temperature Bearing Inlet
THX9	DEG F	Temperature Housing Exterior No. 9
TPBE	DEG F	Temperature Pump Bearing Exit
TS	DEG F	Temperature Suction Line
TTBH8	DEG F	Temperature on Turbine Bearing Housing Exterior No. 8
TTDM	DEG F	Temperature on Turbine Discharge Housing Exterior
TTH7	DEG F	Temperature on Turbine Housing Exterior No. 7
TTI	DEG F	Temperature Turbine Inlet Gas
TTIPHIO	DEG F	Temperature on Pump Housing Exterior No. 10
WDOT	LB/SEC	Turbine Weight Flow Rate
WRTP	(LBM/SEC)(°R**0.5)/(LBF/IN**2)	Turbine Flow Parameter

APPENDIX C

SYMBOLS AND ACRONYMS

SYMBOLS AND ACRONYMS

Symbol	Meaning	Dimensions
A	Actual flow area	inches squared
Btu	British thermal unit	778.98 (ft-lbs)
C_d	Ratio of empirical to "blueprint" nozzle area	—
C_o	Gas spouting velocity as a function of total to static pressure ratio	ft/sec
C_p	Specific heat at constant pressure	Btu/(lb x °R)
cpm	Cycles per minute	1/min.
D, DIA	Diameter	inches
F	Force	lbs
°F	Degrees Fahrenheit	°F
ft	Feet	feet
G	Earth gravitational constant	32.17 ft/sec^2
GAL.	Gallon	gallon
GHe	Gaseous helium	—
GN_2	Gaseous nitrogen	—
GO_2	Gaseous oxygen	—
gpm	Volumetric flow rate	gal/min.
h	Enthalpy	Btu/lbm
H	Head of fluid flowing; Head rise	feet
hp, HP	Horsepower	33,000 ft. lb/min.
Hz	Cycles per second	1/sec
H_2	Hydrogen	—
in.	Inch	in.
KHz	One thousand cycles per second	1000/sec
Kpsia	One thousand pounds per square inch	1000 lb/in.^{2}
L	Length	feet; inch
lb	Pound	lb
lbf	Pound force	lbf
lbm	Pound mass	lbm
min, MIN.	Minute	min.
N	Angular speed	rev/min.
NT	Turbine angular speed	rev/min.
P,p	Pressure	lb/in^2
psia, PSIA	Absolute pressure	lb/in.^{2}

Symbols and Acronyms, (cont.)

Symbol	Meaning	Dimensions
psid, PSID	Differential pressure rise	$lb/in.^2$
psig, PSIG	Gage pressure (pressure above atmospheric)	$lb/in.^2$
Q	Volume flowrate	gal./min.
R	Gas constant	(ft)(lbf)/(°R)(lbm)
R	Radius	inches
°R	Temperature in Degrees Rankine	°R
rho	Specific weight	lbm/ft^3
rpm,RPM	Angular speed	rev./min.
S	Entropy	Btu/(lbm x °R)
sec, SEC	Time	sec.
shp	Shaft power	hp
T	Temperature	°F, °R
U	Liner velocity	ft./sec.
$\dot{\omega}$	Weight flow rate	lbm/sec
ς	Specific weight average from entrance to exit	$lbm/ft.^3$

SUBSCRIPTS

AX	Axial
d	Design
ex	Exhaust
F,f	Force
in	At entrance location
m	Mass
N	Unitless number
o	Initial state condition
PDI	Pump bearing Inlet
R	Reynolds number
1s	First Stage
2	At exit location, number of atoms

ACRONYMS

Aerojet	Aerojet TechSystems
Boeing	The Boeing Company
C/A	Thermocouple material chromel-alumel
dsk	Disk
EFF, eff	Efficiency - delivered power/input power
F	Fuel
F.S.2	Fire Switch (number 2) at the end of engine firing
GOX, GO_2	Gaseous oxygen
GN_2	Gaseous nitrogen
H, H_2	Hydrogen
hyd	Hydraulic
I.D.	Inside diameter
JSC	Joint Spacecraft Committee
K	Temperature, Kelvin
LERc	Lewis Research Center
LN_2	Liquid nitrogen
LO_2	Liquid oxygen
LOX	Liquid oxygen
MSFC	Marshall Spaceflight Center
N	Number, dimensionaless
NASA	National Aeronautics and Space Administration
O, O_2	Oxygen
OAST	Office of Astronautics and Space Transportation

O.D.	Outside diameter
OTV	Orbit Transfer vehicle
OTPA	Oxygen Turbopump Assembly
P	Pressure rise
PBE	Pump Bearing exit
PBI	Pump Bearing inlet
PV	Pressure times velocity
RL-10	Pratt and Whitney Aircraft Company liquid oxygen/liquid hydrogen fueled rocket engine
TBD	To Be Determined
TPA	Turbopump Assembly
X	Distance detector centerline inclination from the vertical at 120° and normal to the shaft centerline
Y	Distance detector centerline inclination from the vertical at 210° and normal to the shaft centerline
Z	Distance detector centerline is horizontal and parallel to the shaft centerline
ϕ	Diameter

APPENDIX D

REFERENCES

REFERENCES

1. Buckmann, P.S., Hayden, W.R., Lorenc, S.A., Sabiers, R.L., Shimp, N.R., "Orbital Transfer Vehicle, Oxygen Turbopump Technology, Design Fabrication and Series A and B Testing, Final Report, Vol. I," Aerojet Report No. 2459-54-2, Contract NAS 3-23772, NASA CR 185175, August 1989.

2. Schoenman, L., Stoltzfus, J. and Kazaroff, B., "Friction Induced Ignition of Metals In High Pressure Oxygen," Appendix B, Orbit Transfer Rocket Engine Technology Program, Monthly Report 238772-M048, May 1987.

3. Schoenman, L., "Oxygen TPA Material Ignition Study," Aerojet TechSystems Company Report 23772-M-42, November 1986.

4. Schoenman, L., "Friction Rubbing Test Results of Dissimilar Materials in High-Pressure Oxygen," Aerojet TechSystems Report 23772-M-32, appendix A, January 1986.

5. Schoenman, L., "Advanced Cryogenic OTV Engine Technology," AIAA/ASME/ASEE 21st Joint Propulsion Conference Paper No. AIAA-85-1341, July 8-10, 1985.

6. Schoenman, L., "Selection of Burn-resistant Materials for Oxygen-Driven Turbopumps," AIAA/ASME/SAE 20th Joint Propulsion Conference Paper No. AIAA-84-1287, June 11-13, 1984.

7. Brannam, R.J., "ATC Test Plan for Orbit Transfer Vehicle (OTV) LOX Turbopump Testing," 10 January 1989.

8. McCarthy, R.D., "Interactive FORTRAN Programs for Micro Computers to Calculate the Thermophysical Properties of Twelve Fluids (MIPROPS)," National Bureau of Standards, May 1986.

9. Shimp, N.R., "GO_2 Driven Turbopump for OTV (LOX TPA) Preliminary Pump Hydrodynamic Design," 25 July 1984.

10. Lorenc, S.A., "OTV Oxygen TPA Design Point Selection and Aerodynamic Design of Turbine," ATC Memo 6973:D-099:SAL:ag, 20 July 1984.

11. Glassman, A.J., ed., "Turbine Design and Application," NASA SP-290, 1972.

12. "Flow of Fluids Through Valves, Fittings, and Pipe," Crane Technical Paper No. 410, Engineering Division, Crane Co., 1980.

13. Collamore, F.N., "Integrated Control and Health Monitoring Capacitive Displacement Sensor Development Task," Final Report Orbital Transfer Rocket Engine Technology Program, NASA CR 182279, July 1989.

References, (cont.)

14. Buckmann, P.S., Hayden, W.R., and Sabiers, R.L., "Orbital Transfer Vehicle Engine Turbopump Oxygen Series A and B Test Report, " Interim Report ATC 2459-54-1, Contract/Task Order NAS 3-23772-B.4, April 1988.

15. Buckmann, P.S., "Freon Hydrostatic Bearing Test Report," Contract (NASP) August 1986.

16. Cooper, L.P., "Advanced Propulsion Concepts for Orbital Transfer Vehicles," AIAA Paper 83-1243, June 1983.

17. Cooper, L.P. and Scheer, D.D., "Status of Advanced Propulsion for Space Based Orbital Transfer Vehicle," NASA TM 88848, October 1986.

Report Documentation Page

National Aeronautics and Space Administration

1. Report No. NASA CR-185262	2. Government Accession No.	3. Recipient's Catalog No.
4. Title and Subtitle Orbital Transfer Vehicle Oxygen Turbopump Technology Final Report, Volume II Nitrogen and Ambient Oxygen Testing		5. Report Date December 1990 6. Performing Organization Code
7. Author(s) R.J. Brannam, P.S. Buckmann, B.H. Chen, S.J. Church, and R.L. Sabiers		8. Performing Organization Report No. Aerojet 2459-56-1 10. Work Unit No. 591-41-11
9. Performing Organization Name and Address GENCORP Aerojet TechSystems Aerojet Propulsion Division P.O. Box 13222 Sacramento, California 95813-6000		11. Contract or Grant No. NAS3-23772 13. Type of Report and Period Covered Contractor Report Final
12. Sponsoring Agency Name and Address National Aeronautics and Space Administration Lewis Research Center Cleveland, Ohio 44135-3191		14. Sponsoring Agency Code

15. Supplementary Notes

Project Manager, Margaret Proctor, Space Propulsion Technology Division, NASA Lewis Research Center.

16. Abstract

This report covers the testing of a rocket engine oxygen turbopump using high pressure ambient temperature nitrogen and oxygen as the turbine drive gas in separate test series. The pumped fluid was liquid nitrogen or liquid oxygen. The turbopump (TPA) is designed to operate with 400 °F oxygen turbine drive gas which will be demonstrated in a subsequent test series. The TPA Hydrostatic Bearing System was demonstrated in tests documented in the first volume of this report. Following bearing tests the TPA was finish machined (impeller blading and inlet/outlet ports). Testing started on 15 February 1989 and was successfully concluded on 21 March 1989. Testing started using nitrogen to reduce the ignition hazard during initial TPA checkout. The Hydrostatic Bearing System requires a Bearing Pressurization System. Initial testing used a separate bearing supply to prevent a rubbing start. Two test series were successfully completed with the bearing assist supplied only by the pump second stage output which entailed a rubbing start until pump pressure builds up. The final test series used ambient oxygen drive and no external bearing assist. Total operating time was 2268 seconds. There were 14 starts without bearing assist and operating speeds up to 80,000 rpm were logged. Teardown examination showed some smearing of silverplated bearing surfaces but no exposure of the underlying monel material. There was no evidence of melting or oxidation due to the oxygen exposure. The articulating, self-centering hydrostatic bearing exhibited no bearing load or stability problems. The only anomaly was higher than predicted flow losses which were attributed to a faulty ring seal. The TPA will be refurbished prior to the 400 °F oxygen test series but its condition is acceptable, as is, for continued operating. This was a highly successful test program.

17. Key Words (Suggested by Author(s))	18. Distribution Statement
Oxygen turbopump; Hydrostatic bearings; Expander cycle engine; Cryogenic propellant pumping	Unclassified – Unlimited Subject Category 20

19. Security Classif. (of this report)	20. Security Classif. (of this page)	21. No. of pages	22. Price*
Unclassified	Unclassified	154	A08

NASA FORM 1626 OCT 86

*For sale by the National Technical Information Service, Springfield, Virginia 22161